AD_____

Award Number: DAMD17-99-1-9268

TITLE: Breast Reconstruction Using Tissue Engineering

PRINCIPAL INVESTIGATOR: Charles W. Patrick, Jr., Ph.D.

CONTRACTING ORGANIZATION: The University of Texas
M. D. Anderson Cancer Center
Houston, Texas 77030

REPORT DATE: September 2002

TYPE OF REPORT: Final

PREPARED FOR: U.S. Army Medical Research and Materiel Command
Fort Detrick, Maryland 21702-5012

DISTRIBUTION STATEMENT: Approved for Public Release;
Distribution Unlimited

REPORT DOCUMENTATION PAGE

Form Approved
OMB No. 074-0188

1. AGENCY USE ONLY (Leave blank)	2. REPORT DATE	3. REPORT TYPE AND DATES COVERED
	September 2002	Final (1 Sep 99 - 31 Aug 02)

4. TITLE AND SUBTITLE
Breast Reconstruction Using Tissue Engineering

5. FUNDING NUMBERS
DAMD17-99-1-9268

6. AUTHOR(S):
Charles W. Patrick, Jr., Ph.D.

7. PERFORMING ORGANIZATION NAME(S) AND ADDRESS(ES)
The University of Texas
M. D. Anderson Cancer Center
Houston, Texas 77030
E-Mail: cpatrick@mdanderson.org

8. PERFORMING ORGANIZATION REPORT NUMBER

9. SPONSORING / MONITORING AGENCY NAME(S) AND ADDRESS(ES)
U.S. Army Medical Research and Materiel Command
Fort Detrick, Maryland 21702-5012

10. SPONSORING / MONITORING AGENCY REPORT NUMBER

11. SUPPLEMENTARY NOTES
report contains color

12a. DISTRIBUTION / AVAILABILITY STATEMENT
Approved for Public Release; Distribution Unlimited

12b. DISTRIBUTION CODE

13. Abstract ***(Maximum 200 Words)*** *(abstract should contain no proprietary or confidential information)*
This is the final report for the initial development of tissue engineering strategies for breast reconstruction following tumor resection.

14. SUBJECT TERMS
breast cancer

15. NUMBER OF PAGES
84

16. PRICE CODE

17. SECURITY CLASSIFICATION OF REPORT	18. SECURITY CLASSIFICATION OF THIS PAGE	19. SECURITY CLASSIFICATION OF ABSTRACT	20. LIMITATION OF ABSTRACT
Unclassified	Unclassified	Unclassified	Unlimited

Table of Contents

INTRODUCTION

The cure for breast cancer is a long-term clinical realization. In the meantime, patients continue to undergo mastectomies as a preventative measure against breast cancer or as a means to surgically resect an existing breast cancer. Conventional procedures for reconstructing breast, or other soft tissue defects requiring adipose tissue, involve "robbing Peter to pay Paul". That is, tissue from a donor site on the patient is used to reconstruct the breast mound. Ideally, the reconstructive goal would be to completely avoid using functional tissues, such as muscle, for soft tissue reconstruction. Considering the fact that the general cost of reconstruction is high, in both the monetary and the physical sense, a need exists to reduce costs and develop innovative reconstruction methodologies. The multidisciplinary efforts of bioengineering and materials science, cell biology, and surgical science can interact through the field of tissue engineering to help produce viable adipose tissue solutions for presently limited reconstructive applications in soft tissue augmentation and, ultimately, for incorporation into compound flap tissue for clinical use to increase soft tissue bulk and help create or repair appropriate superficial body contour and shape where well-vascularized soft tissue is needed. Figure 1 depicts the overall strategy.

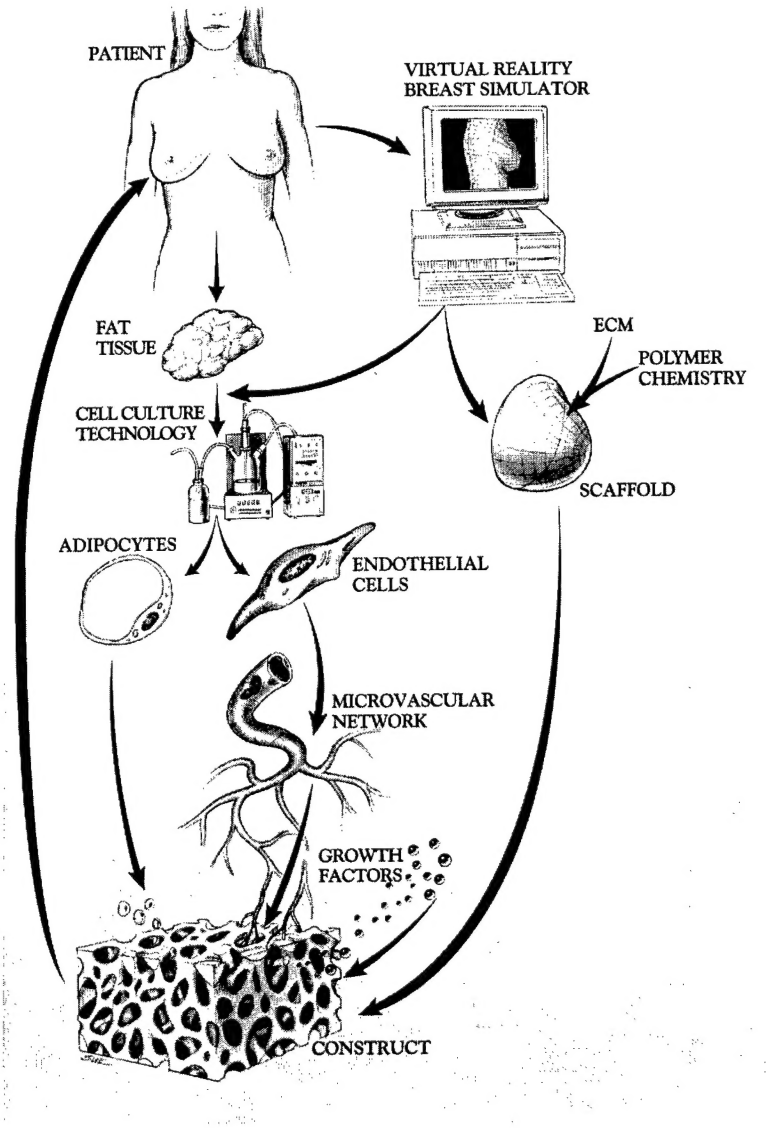

Figure 1. Overall adipose tissue engineering strategy. This grant focuses on the adipose and polymer aspects of the plan. Other grants cover the vascularization issues.

BODY

The specific tasks of the project as originally stated are to:

1. Assess *in vivo* adipose formation in PLGA polymer scaffolds seeded with primary rat preadipocytes and implanted subcutaneously for three and six months. Adipose formation will be assessed histologically using OsO_4 staining.

2. Fabricate breast-shaped PLGA polymer scaffolds using a vacuum-assisted particulate-leaching process and assess polymer architecture. A hemisphere will be used as an initial model breast shape. Pore size distribution, number of pores, and global architecture will be assessed using Hg infusion porosimetry and SEM.

3. Assess feasibility of transferring preadipocyte-seeded, breast-shaped polymer scaffolds as flaps based on an omental vascular pedicle. Conventional tissue transfer and microvascular surgery techniques will be applied to carry out this aim.

Each Task will be addressed separately below. **All three tasks were completed**, although Task 3 was modified due to data obtained in Tasks 1 & 2. In addition, each task required more time to complete than anticipated since all analysis techniques had to be concomitantly developed (i.e., since tissue engineering is such a young field, many assessment "tools" have to be developed at the same time as the research). Additional complementary studies were also conducted to answer questions raised during investigation of the tasks. Each task item is discussed and denoted with reportable outcomes for that item. General outcomes attributable to all items collectively (e.g., overview presentations and book chapters) are not included.

Task 1

Item	Reportable Outcomes
A short-term (2-5 weeks) and long-term (1-12 months) in vivo study was conducted by placing PLGA disks preseeded with autologous preadipocytes subcutaneously in rats. A quantitative histomorphometric image analysis technique was developed to measure the percent adipose tissue observed in histological slides of harvested samples. Results demonstrated that de novo adipose tissue was able to successfully form in increasing amounts from 2 weeks to 2 months, than began to resorb completely by 5 months. Thus, results were extremely encouraging and the resorption limitation is more than likely due to the fact that (a) the PLGA polymer (the cells' support) biodegraded completely by 4 months or (b) a small animal/subcutaneous model was used in a manner that physiologically does not support large amounts of fat (the subcutaneous fat layer of a rat is typically very thin). Both of these issues will require assessment in a large animal model (see Task 3).	C1-C7, D3, F1-F2, F7

As an aside, we investigated the potential of de novo adipose tissue generation in six proprietary Johnson & Johnson biomaterials ranging from polymer foams to nonwoven fibers. All materials elicited adipose tissue formation at 2-5 weeks, but did not supersede the positive results observed with PLGA. This is more than likely due to pore size issues; that is, the space in which a cell has to migrate and grow. The pore size of the Johnson & Johnson materials (~30-50 μm) was significantly lower than that of the PLGA we utilized (300-500 μm).	F4
In addition, a key transplantation constraint, namely O_2 levels, was investigated. It was determined using a quantitative Live/Dead stain and a lab-built hypoxia chamber that preadipocytes are very sensitive to levels of O_2 (markedly more than endothelial cells). The LD_{50} for preadipocyte viability under anoxic conditions is 2.3 hours. This highlights the need to have a well-developed vascular supply concomitant with the process of adipogenesis.	D2, D4, F5, F8
A prototype of a preadipocyte isolation device has been designed and built and is in the process of being tested. In addition, an invention disclosure report is being generated for patent purposes. The device will permit the large scale and effective isolation of preadipocytes from either fat biopsies or liposuction aspirates.	B1

Task 2

Item	Reportable Outcomes
This task was addressed from two different directions-biomaterials development and patient-specific scaffold modeling. Various polymer chemistries possessing different microarchitecture and degradation properties have been investigated and characterized, including polymer foams, nonwoven fibers, and photopolymerizable hydrogels. All these materials permit cell seeding with preadipocytes. Injectable, photopolymerizable hydrogels appear to be the best candidate for small soft tissue defects (e.g., lumpectomy) and polymer foams the best candidate for large soft tissue defects. Current work has focused on methods with which to derivatize the surface of polymer scaffolds with preadipocyte-specific adhesion molecules. Our results have shown that preadipocytes prefer to bind to the ECM protein laminin and that the integrin molecule $\alpha_1\beta_1$ is specifically involved in preadipocyte adhesion to and migration on laminin substrata. This information is being used to derivatize polymers with laminin peptide sequences (e.g., YIGSR) to enhance preadipocyte binding and promote migration, both of which will assist in long-term tissue formation and integration.	C8, D6, F13-F14, G1, G8, G13

A virtual reality model of patient-specific breast scaffolds has been developed in collaboration with an investigator from the University of Houston (I. Kakadiaris). Briefly, a patient's breast is scanned using a 3D laser surface scanner and the resulting range data is used as input into a geometric-based virtual simulation of the breast. The output is the desired 3D volume of a breast scaffold required to restore the breast mound to its original proportions. The virtual model can then be used as input into a CAD/CAM device to mill a physical polymer scaffold.	D1, D5, F3, F6, F9-F10

Task 3

Item	Reportable Outcomes
The focus of this task was changed slightly based on the need to develop a large animal model. A large animal model does not currently exist for testing clinically translatable adipose tissue engineering strategies for breast reconstruction prior to proceeding to clinical trials in humans. One cannot scale up from small animal models to human studies. Small animal models possess two predominant limitations. One, small animal models cannot be carried out long enough to assess the robustness and persistence of breast restoration strategies. Assessing the maintenance of *de novo* tissue is critical for determining whether tissue is remodeled and resorbed, reaches desired homeostasis, or continues to grow unchecked (i.e., tumor). Second, small animal models do not permit assessment of clinically sized tissue volumes. Tissue regeneration strategies in small animal models are necessarily limited to small volumes that can survive by diffusion and transient neovascularization. This is not the case in humans and large animal models. That is, mass transport issues (i.e., blood supply) are chief design constraints for tissue engineering strategies involving large tissue volumes. We have elected to use Yucatan MicroPigs as a large animal model as they satisfy the criteria for an adipose tissue engineering large animal model listed in Table 1. MicroPigs, specifically, offer the advantages of being a pure breed (less *in vivo* variation), hairless, gentle and tractable, used extensively as a wound healing and cardiovascular models, and have a slow, defined growth rate and desirable size (14-20 kg at sexual maturity/5-6 months and 40-60 kg at adult/12-14 months). Moreover, preadipocytes have been successfully cultured from swine in a manner similar to how we have cultured rat preadipocytes. In collaboration with a plastic surgeon (E. Beahm), we have conducted preliminary studies of transplanting constructs based on a	F11-F12

conducted preliminary studies of transplanting constructs based on a host blood supply and assessing whether mature constructs can be transferred as a free flap using conventional microsurgical techniques. The epigastric and mammary vessels of male MicroPigs were assessed. The mammary vessels proved to be ideal candidates for construct placement and transfer. A DOD renewal has been submitted to continue developing the large animal model and testing preadipocyte-seeded polymer constructs.

Table 1: Design criteria for large animal model

Blood vessels must be of sufficient diameter to permit anastamosis using standard microsurgery techniques.
Animal size must be large enough to reflect convection- and diffusion- dependent mass transport.
Animal's tissue structure must permit the harvest, isolation, and culture of preadipocytes.
Animal's anatomy must permit placement of constructs without impairing the animal's mobility or quality of life, and provide protection from mechanical damage due to animal's lifestyle.
Animal's growth rate must permit long-term studies in that the animal must not become too large or reach the end of its natural life expectancy.
Animal's soft tissue and cardiovascular physiology should be similar to human.

KEY RESEARCH ACCOMPLISHMENTS

Key accomplishments include:

- First laboratory to demonstrate de novo adipose tissue engineering.
- First laboratory to conduct a long-term small animal model.
- Transplantation constraints have been defined.
- Through its research, the laboratory has defined the key adipogenesis limitations that need to be investigated and have disseminated this knowledge to the scientific community.
- A method for fabricating patient-specific scaffolds has been developed.
- Several polymer scaffolds have been investigated and candidate scaffolds determined.
- Preadipocyte harvest, isolation, culture, and adhesion and migration processes have been determined.
- Large animal model development has begun.
- Five undergraduate and two graduate students have been trained and mentored in the laboratory under the auspices of this grant.

REPORTABLE OUTCOMES

During the course of the grant, the PI was promoted to Associate Professor and received the 2001 Faculty Scholar Award for Research from the University of Texas M.D. Anderson Cancer Center. In addition, he serves as Associate Director of the newly created University of Texas Center for Biomedical Engineering (www.txcbme.org). He continues to hold active adjunct positions at three academic institutions. Other academic metrics of importance follow:

(A) Other grant support obtained based in initial Army support (*pending grant):

1. Hydrogel-based adipose tissue engineering, Cancer Fighters of Houston, Principal Investigator, 01/00-12/01, total $20,000.

2. Assessment of preadipocyte-seeded biomaterials for adipose tissue engineering: Short-term study, Johnson & Johnson/Ethicon-EndoSurgery, Principal Investigator, 06/00-06/01, total $20,000.

3. Soft tissue repair using cell-seeded, factor-loaded microparticles, Plastic Surgery Education Foundation, Principal Investigator, 07/99-06/01, total $5,000.

4. A cell-free method to induce adipogenesis for soft tissue augmentation, Plastic Surgery Education Foundation, Co-Investigator (P. Chevray, Principal Investigator), 08/01-07/02, total $5,000.

5. *Novel adipogenic hydrogel for soft tissue restoration, Culpeper Foundation, Principal Investigator, total $25,000.

6. *In vivo porcine test bed for restoring the postmastectomy breast through tissue engineering, U.S. Army Medical Research & Material Command DOD Breast Cancer Research Grant, Principal Investigator, total $450,000. [Competing renewal of this proposal]

7. *Test bed system for adipose tissue engineering, NASA, Principal Investigator, $1,011,332.

(B) Patents/Invention Disclosures

1. Invention Disclosure, Adipose-derived cell isolation device: Adipolator, prototype complete and application in preparation.

(C) Manuscripts

1. **Patrick Jr., C.W.**, Chauvin, P.B., Reece, G.P Preadipocyte seeded PLGA scaffolds for adipose tissue engineering. *Tissue Engineering* 5:139-151, 1999.

2. **Patrick Jr., C.W.,** Tissue engineering of fat. *Seminars in Surgical Oncology,* 19:302-311,2000.

3. Brey, E., **Patrick Jr., C.W.** Tissue engineering applied to reconstructive surgery. *IEEE Engineering in Medicine and Biology* 19:122-125, 2000.

4. Miller, M.J., Loftin, B., **Patrick Jr., C.W.**, Rosen, J.M., Siemionow, M., Face to face: A

maxillofacial forum: New technologies, *Maxillofacial News* 15(3):5-10, 2000.

5. **Patrick Jr., C.W.,** Emerging technology for the new millennium: Tissue engineering. *Maxillofacial News* 15(3):1-13, 2000.

6. **Patrick Jr., C.W.,** Tissue engineering strategies for soft tissue repair. *Anatomical Record*, 263:361-366, 2001.

7. **Patrick Jr., C.W.,** Zheng, B., Johnston, C., Reece, G.P. Long-term implantation of preadipocyte seeded PLGA scaffolds. *Tissue Engineering* 8:283-293, 2002.

8. **Patrick Jr., C.W.,** Wu, X. Integrin-mediated preadipocyte adhesion and migration dynamics on laminin-1, *Annals of Biomedical Engineering*, submitted.

(D) Abstracts in Peer-Reviewed Journals

1. Kakadiaris, I., Chen, D., Miller, M.J., Loftin, B., and **Patrick Jr., C.W.** Simulation-base determination of breast tissue engineering design parameters. *Tissue Engineering* 6:662, 2000.

2. Wu, X. and **Patrick Jr., C.W.** Comparison of preadipocyte and mature adipocyte hypoxia tolerance. *Tissue Engineering* 6:691, 2000.

3. **Patrick Jr., C.W.,** Reece, G., Johnston, C. Long-term implantation of preadipocyte-seeded PLGA scaffolds. *Annals of Biomedical Engineering* 29 (supp):150, 2001.

4. **Patrick Jr., C.W.,** Frye, C., Dempsey, K., Wu, X. Transplantation constraints for adipose tissue engineering. *Annals of Biomedical Engineering* 29 (supp):155, 2001.

5. Sarh, K., Kakadiaris, I.A., Ravi-Chandar, K., Miller, M., **Patrick Jr., C.W.** Towards a biomechanical model of the breast: A simulation-based study. *Annals of Biomedical Engineering* 29 (supp):S34, 2001.

6. Patel, P., and **Patrick Jr., C.W.** Cytocompatibility of preadipocytes in diacrylated polyethylene glycol cross-linked with various UV light photoinitiating systems. *Annals of Biomedical Engineering* in press, 2002.

7. Parul Patel, Robb, G.L., **Patrick Jr., C.W.** Soft tissue restoration using tissue engineering. *Seminars in Plastic Surgery*, in preparation (invited).

(E) Book Chapters

1. Chen, D.T., Kakadiaris, I.A., Miller, M.J., Loftin, R.B., **Patrick Jr., C.W.** Modeling for plastic and reconstructive breast surgery. In: Delp, S.L, DiGioia, A.M., Jaramaz, B. (eds)

Lecture Notes in Computer Science, pp. 1040-1050, Berlin, Springer, 2000.

2. **Patrick Jr., C.W.,** Wu, X., Johnston, C., Reece, G.P. Epithelial cell culture: Breast. In: Atala, A., Lanza, R. (eds) Methods of Tissue Engineering, pp. 143-154, San Diego, Academic Press, 2001.

3. Robb, G.L., Miller, M.J., **Patrick Jr., C.W.** Breast reconstruction. In: Atala, A., Lanza, R. (eds) Methods of Tissue Engineering, pp. 881-889, San Diego, Academic Press, 2001.

4. **Patrick Jr., C.W.** Tissue engineered adipose tissue. In: Clinics of Plastic Surgery. In preparation (invited).

(F) Presentations at National Conferences

1. **Patrick Jr., C.W.,** Elbjerami, W., Chauvin, P.B., Reece, G.P. Adipose tissue engineering. Summer Bioengineering Conference, Big Sky, Montana, 06/99.

2. **Patrick Jr., C.W.,** Tissue engineering, South Texas Society of Plastic Surgery, Austin, Texas, 10/99.

3. Kakadiaris, I., Chen, D., Miller, M.J., Loftin, B., and **Patrick Jr., C.W.** Simulation-based determination of breast tissue engineering design parameters. Tissue Engineering Society, Orlando, Florida, 11/00-12/00.

4. Roweton, S., Freeman, L., **Patrick Jr., C.W.,** Dempsey K., Zimmerman, M. Preadipocyte-seeded absorbable matrices. Johnson & Johnson Excellence in Science Symposium, New Jersey, 11/00.

5. Wu, X. and **Patrick Jr., C.W.** Comparison of preadipocyte and mature adipocyte hypoxia tolerance. Tissue Engineering Society, Orlando, Florida, 11/00-12/00.

6. Parker, T., Miller, M.J., **Patrick Jr., C.W.,** King, T.W., Ames, F.C., Robb, G.L. Aesthetic refinements in autologous breast reconstruction: Tailored breast skin envelope by the wise pattern. American Society for Reconstructive Microsurgery, San Diego, California, 01/01.

7. **Patrick Jr., C.W.,** Reece, G., Johnston, C. Long-term implantation of preadipocyte-seeded PLGA scaffolds. Biomedical Engineering Society, Durham, North Carolina, 10/01.

8. **Patrick Jr., C.W.,** Frye, C., Dempsey, K., Wu, X. Transplantation constraints for adipose tissue engineering. Biomedical Engineering Society, Durham, North Carolina, 10/01.

9. Sarh, K., Kakadiaris, I.A., Ravi-Chandar, K., Miller, M., **Patrick Jr., C.W.** Towards a

biomechanical model of the breast: A simulation-based study. Biomedical Engineering Society, Durham, North Carolina, 10/01.

10. Sarh, K., Kakadiaris, I.A., Ravi-Chandar, K., Miller, M., **Patrick Jr., C.W.** Towards a biomechanical model of the breast: A simulation-based study. Advances in Bioengineering, American Society of Mechanical Engineering, New York, New York, 11/01.

11. **Patrick Jr., C.W.** Restoring the breast with tissue engineering. Era of Hope 2002 DOD Breast Cancer Research Program Meeting, Orlando, Florida, 9/02

12. **Patrick Jr., C.W.**, Reece, G.P., Beahm, E., Wu, X., Johnson, C. Restoring the breast following mastectomy via tissue engineering strategies. Era of Hope 2002 DOD Breast Cancer Research Program Meeting, Orlando, Florida, 9/02. (poster)

13. Wu, X. and **Patrick Jr., C.W.** Preadipocyte adherence to and migration on extracellular matrix substrata. IEEE Engineering in Medicine and Biology Society and Biomedical Engineering Society, Houston, Texas, 10/02.

14. Patel, P., and **Patrick Jr., C.W.** Cytocompatibility of preadipocytes in diacrylated polyethylene glycol cross-linked with various UV light photoinitiating systems. IEEE Engineering in Medicine and Biology Society and Biomedical Engineering Society, Houston, Texas, 10/02.

(G) Presentations at Universities/Companies

1. **Patrick Jr., C.W.,** Robb, G.L, Miller, M.J. Hydrogel-based adipose tissue engineering, Cancer Fighters of Houston Committee, The University of Texas M.D. Anderson Cancer Center, Houston, Texas, 10/99.

2. **Patrick Jr., C.W.** Tissue engineering indications for reconstructive surgery at UTMDACC, Board of Visitors, The University of Texas M.D. Anderson Cancer Center, Houston, Texas, 11/99.

3. **Patrick Jr., C.W.** Tissue engineering applied to reconstructive surgery, Johnson & Johnson Corporate Biomaterials Center, Somerville, New Jersey, 11/99.

4. **Patrick Jr., C.W.**, Morrison, S., Robb, G.L. Plastic Surgery Program, Presented to UTMDACC's Clinical Research Council, The University of Texas M.D. Anderson Cancer Center, Houston, Texas, 03/00.

5. **Patrick Jr., C.W.** Boob in a box? Rationale and state-of-the-art of breast tissue engineering, Integrative Graduate Education and Research Training lecture, The University of Texas at Austin, Austin, Texas, 9/00.

6. **Patrick Jr., C.W.** Engineering approach to breast reconstruction, University of Maryland Baltimore County, Baltimore, Maryland, 10/00.

7. **Patrick Jr., C.W.** Advances in reconstructive breast surgery, South Texas Society of Plastic Surgery, Irving, Texas, 11/00.

8. Wu, X., Dempsey, K., and **Patrick Jr., C.W.** Preadipocyte cell adhesion to ECM proteins optimized for adipose tissue engineering, 1st Annual Biomedical Engineering Center & Department Retreat, The University of Texas at Austin, Austin, Texas, 12/00.

9. **Patrick Jr., C.W.** Advances in reconstructive surgery, Chancellor's Council, The University of Texas M.D. Anderson Cancer Center, Houston, Texas, 2/01.

10. **Patrick Jr., C.W.** UT Center for Biomedical Engineering: Tissue Engineering, Advances in Oncology Institutional Grand Rounds, The University of Texas M.D. Anderson Cancer Center, Houston, TX, 03/01.

11. **Patrick Jr., C.W.** Plastic surgery and tissue engineering, 1st Annual Biomedical Engineering Center & Department Retreat, The University of Texas at Austin, Austin, Texas, 12/00.

12. **Patrick Jr., C.W.** Tissue engineering, Department of Head Neck Surgery Conference Series, The University of Texas M.D. Anderson Cancer Center, Houston, TX, 01/02.

13. Wu, X., Dempsey, K., and **Patrick Jr., C.W.** Preadipocyte cell adhesion to ECM proteins optimized for adipose tissue engineering, 1st Annual Biomedical Engineering Center & Department Retreat, The University of Texas at Austin, Austin, Texas, 9/02.

(H) Media Coverage

1. Potential for stem cell research, *Cancer Newsline* (distributed to 170 national TV stations), 4/01.

2. Spotlight of faculty, *Biomedical Engineering Center News* 1:3, 2001.

3. Tissue engineering, *Cancer Newsline* (distributed to 170 national TV stations), 6/01.

4. Growing tissue for breast reconstruction, *Cancer Newsline* (distributed to 170 national TV stations), 11/01.

5. New biomedical engineering program created, *Texas Medical Center News* 23:20, 2002.

(I) Training of Young Investigators

Summer Undergraduate Internships

Shannon Scott	Dept. Bioengineering, Rice University	6/00-8/00, 6/01-8/01
Jeff Reitsema	Dept. Bioengineering, Rice University	6/01-8/01
Samit Soni	Dept. Biomedical Engineering University of Texas at Austin	6/02-8/02
Bob Cooley	Dept. Biomedical Engineering University of Texas at Austin	5/02-8/02
David Kroll	Yale University	6/02-8/02

Graduate Students

Parul Patel	Dept. Chemical Engineering Rice University	6/00-present
Angela Papagiorgiou	University of Texas Graduate School of Biomedical Sciences	6/01-5/02

Technical Staff

May Wu	Research Assistant
Cindy Frye	Laboratory Coordinator
Carol Johnston	Research Histologist

CONCLUSIONS

The results of this grant have been successful in both a young scientific field (tissue engineering) and infant application area (adipose tissue engineering). Feasibility of adipose tissue engineering has been demonstrated, knowledge has been increased, design constraints have been defined, and the next steps required to reach the ultimate goal of a clinically translatable strategy are clear. There are now laboratories in three other countries focused on the area of adipose tissue

engineering. Support from the DOD has allowed this laboratory to not only be the first laboratory to publish results but also to remain at the forefront.

REFERENCES:

See Reportable Outcomes section C-E above.

APPENDICES

1. **Patrick Jr., C.W.**, Chauvin, P.B., Reece, G.P Preadipocyte seeded PLGA scaffolds for adipose tissue engineering. *Tissue Engineering* 5:139-151, 1999.

2. Chen, D.T., Kakadiaris, I.A., Miller, M.J., Loftin, R.B., **Patrick Jr., C.W.** Modeling for plastic and reconstructive breast surgery. In: Delp, S.L, DiGioia, A.M., Jaramaz, B. (eds) Lecture Notes in Computer Science, pp. 1040-1050, Berlin, Springer, 2000.

3. **Patrick Jr., C.W.,** Tissue engineering of fat. *Seminars in Surgical Oncology,* 19:302-311,2000.

4. **Patrick Jr., C.W.,** Tissue engineering strategies for soft tissue repair. *Anatomical Record*, 263:361-366, 2001.

5. **Patrick Jr., C.W.,** Wu, X., Johnston, C., Reece, G.P. Epithelial cell culture: Breast. In: Atala, A., Lanza, R. (eds) Methods of Tissue Engineering, pp. 143-154, San Diego, Academic Press, 2001.

6. Robb, G.L., Miller, M.J., **Patrick Jr., C.W.** Breast reconstruction. In: Atala, A., Lanza, R. (eds) Methods of Tissue Engineering, pp. 881-889, San Diego, Academic Press, 2001.

7. **Patrick Jr., C.W.,** Zheng, B., Johnston, C., Reece, G.P. Long-term implantation of preadipocyte seeded PLGA scaffolds. *Tissue Engineering* 8:283-293, 2002.

TISSUE ENGINEERING
Volume 5, Number 2, 1999
Mary Ann Liebert, Inc.

Preadipocyte Seeded PLGA Scaffolds for Adipose Tissue Engineering

C.W. PATRICK, Jr., Ph.D., P.B. CHAUVIN, B.S., J. HOBLEY, B.S., and G.P. REECE, M.D.

ABSTRACT

Adipose tissue equivalents have not been addressed as yet despite the clinical need in congenital deformities, posttraumatic repair, cancer rehabilitation, and other soft tissue defects. Preadipocytes were successfully harvested from rat epididymal fat pads of Sprague-Dawley and Lewis rats and expanded *ex vivo*. *In vitro* cultures demonstrated full differentiation of preadipocytes into mature adipocytes with normal lipogenic activity. The onset of differentiation was well-controlled by regulating preadipocyte confluency. Poly(lactic-co-glycolic) acid (PLGA) polymer disks with 90% porosity, 2.5 mm thick, 12 mm diameter, pore size range of 135–633 μm were fabricated and seeded with preadipocytes at 10^5 cells/mL. Disks *in vitro* demonstrated fully differentiated mature adipocytes within the pores of the disks. Short-term *in vivo* experiments were conducted by implanting preseeded disks subcutaneously on the flanks of rats for 2 and 5 weeks. Histologic staining of harvested disks with osmium tetroxide (OsO_4) revealed the formation of adipose tissue throughout the disks. Fluorescence labeling of preadipocytes confirmed that formed adipose tissue originated from seeded preadipocytes rather than from possible infiltrating perivascular tissue. This study demonstrates the potential of using primary preadipocytes as a cell source in cell-seeded polymer scaffolds for tissue engineering applications.

INTRODUCTION

TISSUE ENGINEERING is a broad multidisciplinary field dedicated to the advancement of the human biological environment in healing, correction of deformity, as well as overall tissue function. A natural next step for soft tissue structuring efforts lies in the area of adipose tissue. As early as 1893,[1] surgeons have attempted to transplant autologous adipose tissue with minimal success.[2–7] Conventional procedures for reconstructing breast or other soft tissue defects composed of adipose tissue involve "robbing Peter to pay Paul." That is, a section of living tissue that carries its own blood supply (donor site) is moved from one area of the body to another to repair a deficit of skin, fat, muscle, and to restore movement, or skeletal support. Often, muscle must be used for the most extensive soft tissue reconstruction requirements.[10] Composite flaps comprised of muscle, fat, and skin restore similar consistency and permit the transposition

Laboratory of Reparative Biology and Bioengineering, Department of Plastic Surgery, University of Texas M.D. Anderson Cancer Center, Houston, Texas.

of relatively large volumes of tissue for reconstruction. However, there are several problems associated with use of muscle for soft tissue reconstruction, such as loss of some function at the donor site, aberrant degree of "softness" at the recipient site, and decrease in soft tissue volume with time because of muscle atrophy (25–50%) due to noninnervation.

Adipose tissue *in vivo* is composed of mature adipocytes that are extremely fragile and do not proliferate.[8,9] Moreover, unless a blood supply is immediately incorporated with the transplanted mature adipose tissue (or fat) the tissue begins to undergo necrosis. These limitations provide challenges for developing viable fat tissue solutions for current reconstructive applications in soft tissue augmentation and, ultimately, for incorporation into composite flap tissue for clinical use to increase soft tissue bulk and help create or repair appropriate superficial body contour and shape where well-vascularized soft tissue is needed.

There are extensive indications for the use of adipose tissue equivalents, primarily for reconstructive purposes in congenital deformities (e.g., Poland's syndrome, Romberg's syndrome, and hemifacial microsomia), posttraumatic repair, and cancer rehabilitation. As a first step toward developing adipose tissue equivalents, poly(lactic-co-glycolic) acid (PLGA) polymer disks have been fabricated and seeded with preadipocytes. Preadipocytes *in vitro* and *in vivo* differentiate into mature adipocytes and exhibit lipogenic activity. Histology of seeded PLGA disks implanted subcutaneously in rats demonstrates the formation of adipose tissue throughout the disks and fluorescence labeling confirms the source of adipose tissue to be the seeded preadipocytes. This study demonstrates the potential of using primary preadipocytes as a cell source in cell-seeded polymer scaffolds for tissue engineering applications.

MATERIALS AND METHODS

Adipose Harvest and in Vitro *Culture*

Adipocyte precursors (preadipocytes) are isolated from epididymal fat pads of male, 250 g, 70–80-day-old Sprague-Dawley or Lewis rats (Harlan, Indianapolis, IN) via enzymatic digestion. Briefly, rats are euthanized with CO_2 asphyxiation and the shaved harvest site is scrubbed with Betadyne followed by alcohol wash. Within 5 min of death, epididymal adipose tissue is aseptically harvested and placed in 4°C saline solution supplemented with 500 U/ml penicillin and 500 μg/ml streptomycin (Gibco, Gaithersburg, MD). Using a dissecting microscope, connective tissues and tissue containing blood vessels are resected from the fat. This minimizes fibroblast contamination of *ex vivo* cultures. Harvested tissue is finely minced with a scalpel and enzymatically digested in Ca^{+2}/Mg^{+2}-free saline supplemented with 2% (w/v) type I collagenase (Sigma Chemical Co., St. Louis, MO) and 5% (w/v) bovine serum albumin (BSA, Sigma) for 20 min at 37°C on a shaker; 5 ml of dissociation medium are required/4 fat pads. The digested tissue is filtered through a 250-μm mesh followed by a 90-μm nylon mesh to separate undigested debris and capillary fragments from preadipocytes. The filtered cell suspension is centrifuged and the resulting pellet of preadipocytes is then plated at 10^4 cells/cm^2 onto plastic culture flasks. Preadipocytes are cultured in Dulbecco's Modified Eagle's Medium (DMEM) supplemented with 10% fetal bovine serum (FBS, Sigma), 100 U/ml penicillin, and 100 μg/ml streptomycin. During cell expansion, the preadipocytes are passed prior to confluency since contact inhibition initiates adipocyte differentiation and ceases preadipocyte proliferation. The 1° passage yields approximately 1.5×10^6 preadipocytes/fat pad.

Polymer Fabrication

Fabrication of 2.5-mm thick, 12-mm diameter, and 90% porosity polymer disks are prepared by a particulate-leaching technique (Figure 1).[12] Briefly, 5 g of solid 75:25 PLGA (Birmingham Polymers Inc., Birmingham, AL) polymer are dissolved in 80 ml of dichloromethane (Fisher Scientific, Pittsburgh, PA) to form a solution. Sieved NaCl crystals (Fisher) at a NaCl/PLGA weight fraction of 1:9 are evenly dispersed over a 150-mm Pyrex petri dish (Fisher) with a Teflon lining (Cole-Parmer Instrument Co., Vernon Hills, IL). The PLGA/dichloromethane solution is then gently poured over the NaCl crystals. Sieved NaCl crystal size distribution was measured with quantitative microscopy and found to be 135–633 μm. Dichloromethane is evaporated under vacuum, leaving a polymer/NaCl composite 2.5 mm thick. The composite is removed from the Teflon-lined petri dish, and 12-mm-diameter disks are cut using a plug cutter

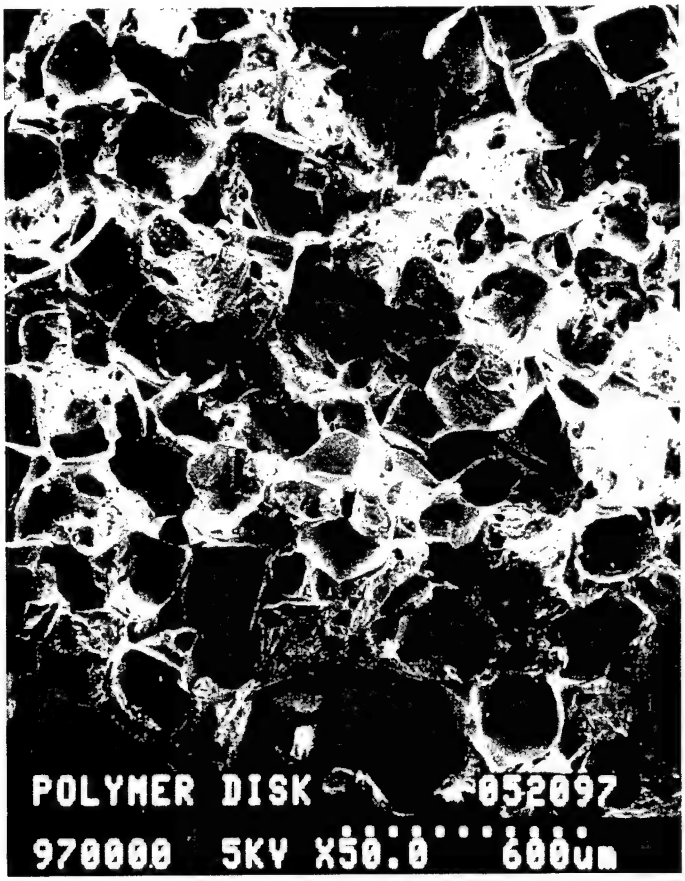

FIG. 1. SEM (×50) showing the pore structure of a PLGA disk having a pore size range of 135–633 μm, a porosity of 90%, and a 75:25 lactic-to-glycolic acid ratio. Bar = 600 μm.

and drill press. The NaCl crystals are then leached from the composite disks by immersion in 800 ml of DI water for 48 h (water changed every 8 h) to yield porous disks. Disks are lyophilized and stored in a vacuum dessicator until use. Disk diameter and thickness were chosen such that disks fit into individual wells of 24-well culture plates for *in vitro* experiments and four disks can be implanted subcutaneously in a rat for *in vivo* experiments.

Polymer Seeding

Prior to seeding, the disks are prewetted and sterilized with absolute ethanol for 30 min followed by two sterile saline washes at 20 min/wash and a DMEM wash for 20 min. A 20-μl suspension of preadipocytes (10^5 cells/ml) are injected onto each disk under sterile conditions. Prewetting permits the cell suspension to readily flow throughout the disks. Following 3 h for cell attachment, 24-well culture plates containing 1 disk/well are filled with 1.5 ml of medium/well. Medium is changed 3×/week. For *in vitro* experiments, Sprague-Dawley preadipocytes are allowed to differentiate within the disks in DMEM supplemented with 10% FBS, 100 U/ml penicillin, and 100 μg/ml streptomycin for periods of 14 days. For *in vivo* experiments, Lewis preadipocytes are seeded onto the disks and allowed to adhere to the polymer for a minimum of 3 h prior to implantation.

In Vivo *Implantation*

Seeded disks are implanted subcutaneously in Lewis rats under anesthesia (0.2 ml/100 gbw intramuscular injection of premixed solution composed of 64 mg/ml ketamine HCl, 3.6 mg/ml xylazine, and 0.07

mg/ml atropine sulfate). An isogenic strain is required to avoid an immune response to seeded preadipocytes. The University of Texas M.D. Anderson Cancer Center Animal Care and Use Committee has approved the implantation of adipocyte seeded disks. After shaving the back, two longitudinal incisions (~2 cm each) are made through the skin of the dorsal midline. Individual "pockets" for each disk are prepared in the subcutaneous space of both flanks by careful dissection. Disks are inserted into each pocket and sutured in place with 5-0 suture (Ethicon), as shown in Figure 2A. Two disks are placed on each side of the incision (4 disks/rat) and the incisions closed with 4-0 suture (Ethicon; Figure 2B). Animals were housed individually and fed standard rat chow. The disks are left *in vivo* 2 and 5 weeks. After the elapsed time, the rats are euthanized with CO_2 and the disks harvested. Immediately after harvest, the disks are placed in 10% neutral buffered formalin (Fisher) for future histology.

For this study, a total of 10 rats are used at 5 rats/time period. Each rat is implanted with 4 disks. Three disks are seeded with preadipocytes, and 1 disk is implanted without seeding to serve as an acellular control. A total of 30 seeded and 10 acellular disks were used in this study. Preadipocytes seeded in two rats

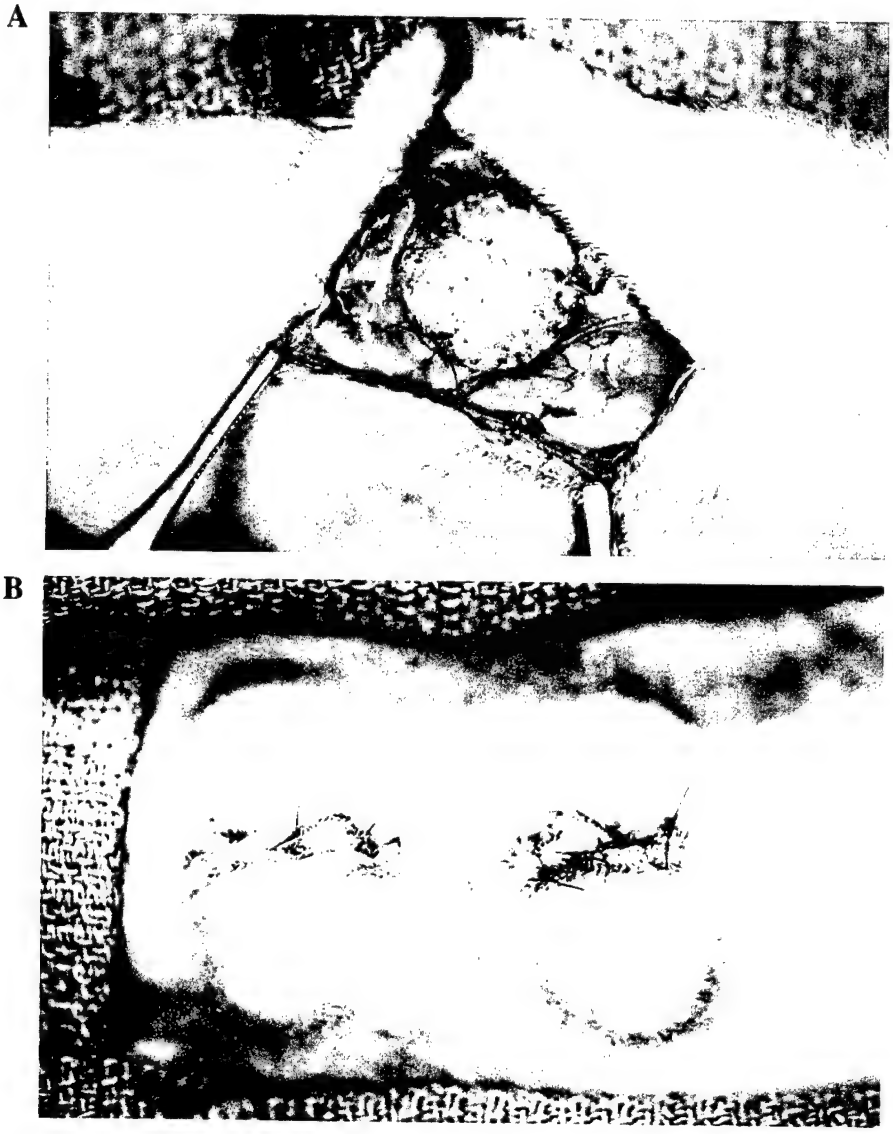

FIG. 2. Implantation of preadipocyte-seeded PLGA disks. **(A)** Disk sutured subcutaneously within prepared pouch. **(B)** Rat closed with all four disks implanted.

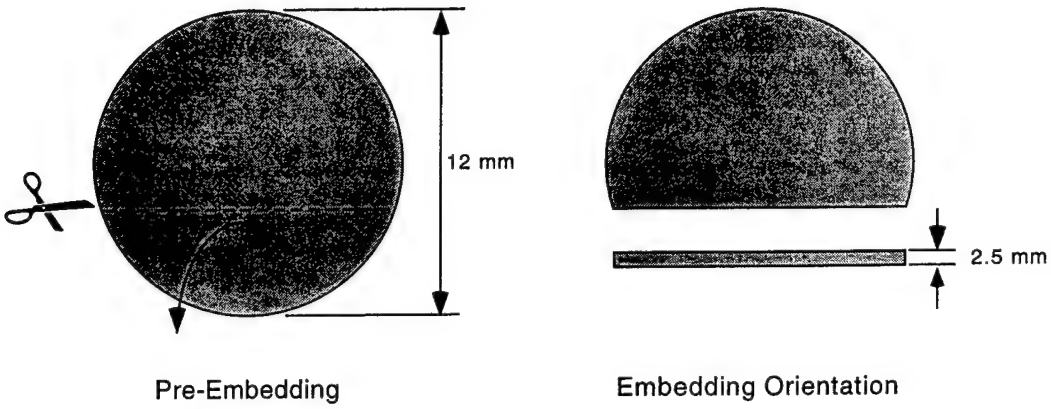

FIG. 3. Orientation of OsO_4 fixed disks for paraffin embedding. This orientation allows a face and cross-sectional cut to be made at the same time.

were prelabeled with 25 μM Hoechst 33342 (Molecular Probes, Eugene, OR) to determine if adipose formation in the disks originated from seeded cells or from surrounding perivascular tissue.

Microscopy and Digital Imaging

Cell cultures are visualized using an inverted microscope (IX 70, Olympus, Tokyo, Japan) with phase, polarized, and brightfield optics and either a B/W charged-coupled device (CCD) camera (BP500, Panasonic, Ft. Worth, TX) for gray scale images, a color CCD camera (WV-E550, Panasonic) for histology images, or a cooled CCD camera (Princeton Instruments, Trenton, NJ) for fluorescence images. The video signal from the B/W and color cameras is fed to a 24-bit, 640 × 480 pixel frame grabber (CG-7, Scion Corp., Frederick, MD) housed in a PowerTower Pro 225 computer (Power Computing Corp., Round Rock, TX) for digitization. A high-resolution monitor (SMPTE-C, JVC, Elmwood Park, NJ) and CPU monitor (20″ Multi-Scan, Apple Computer, Cupertino, CA) allow real-time visualization of the digitized images. IPLab Spectrum software (Scanalytics, Fairfax, VA) orchestrates the entire acquisition process, providing complete automation, as well as postprocessing and analyses of acquired images.

Histology

An osmium tetroxide (OsO_4) paraffin procedure was used to demonstrate fat within harvested *in vivo* disks.[13] Routine staining outlines only "ghost" cells since histological processing with organic solvents and alcohols extract lipid from cells. OsO_4 chemically combines with fat, blackening it in the process. Fat that combines OsO_4 is insoluble in alcohol and xylene and the tissue can be processed for paraffin embedding and counterstained. Small fat droplets and individual cells are well demonstrated via this method, whereas gross amounts of fat are not fixed. After staining with OsO_4, disks are processed for paraffin embedding using standard procedures, except that hemo-D (Fisher) is substituted for xylene. Infiltrated disks are cut and oriented in embedding cassettes as shown in Figure 3. Sections 6 μm thick are cut with a microtome (Leica, Wetzlar, Germany), placed on slides, and coverslipped. Sections are analyzed using brightfield and polarized microscopy. The later allows demarcation of fibrovascular tissue and PLGA by virtue of the fact that oriented collagen fibers in fibrovascular tissue appears high contrast when compared to polymer and void space.

Adipocyte differentiation *in vitro* is routinely monitored using Oil Red O staining for intracellular lipid pools or phase contrast microscopy (lipid appears as phase bright).

Scanning Electron Microscope

Samples of adipocyte-seeded polymer disks, excised epididymal adipose tissue, and disk architecture are treated with a fixative containing 3% glutaraldehyde and 2% paraformaldehyde in 0.1 M cacodylate buffer,

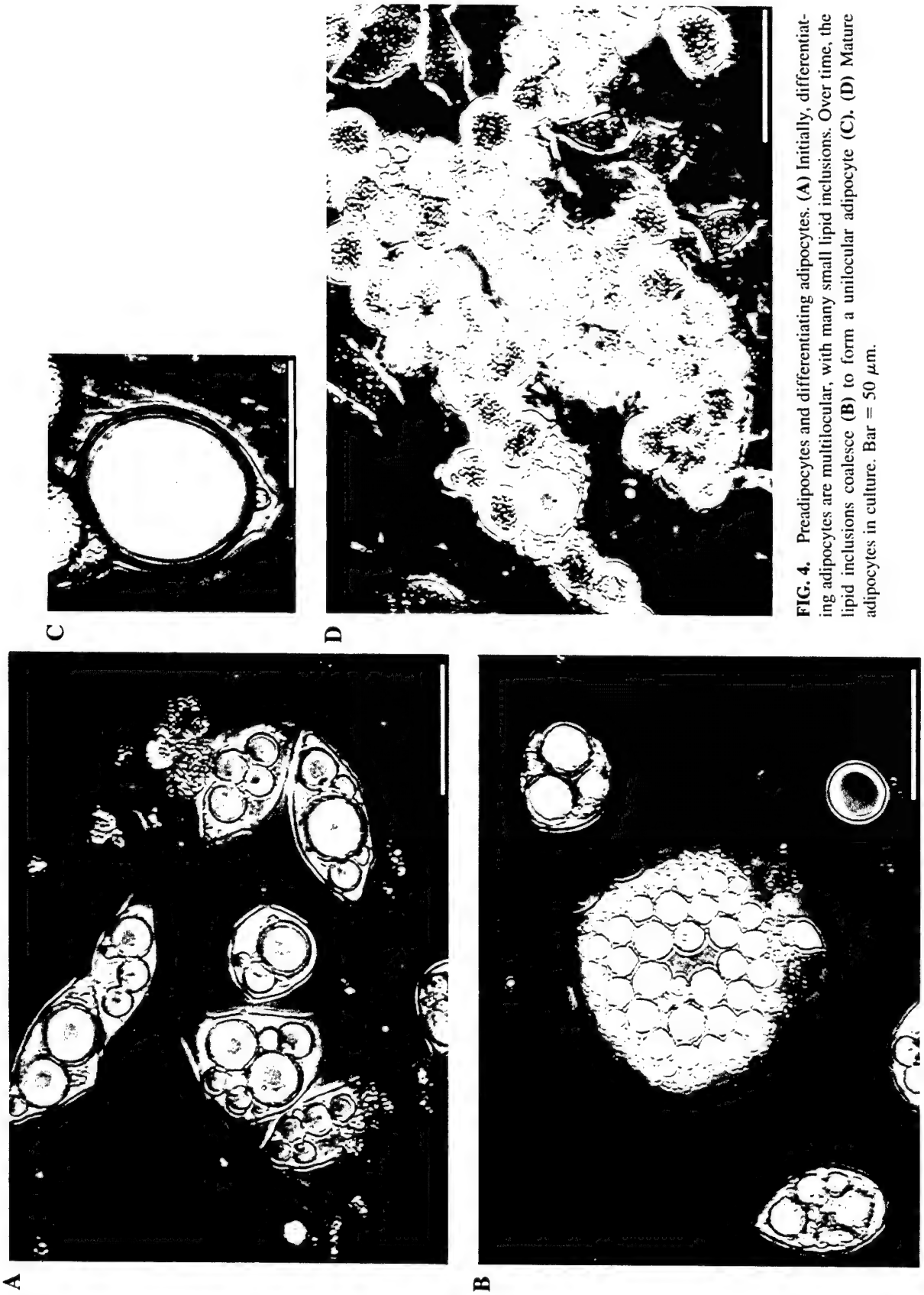

FIG. 4. Preadipocytes and differentiating adipocytes. **(A)** Initially, differentiating adipocytes are multilocular, with many small lipid inclusions. Over time, the lipid inclusions coalesce **(B)** to form a unilocular adipocyte **(C)**. **(D)** Mature adipocytes in culture. Bar = 50 μm.

pH 7.2 for 1 h at room temperature. The samples are rinsed in 0.1 M cacodylate buffer 3× for 5 min/wash and subsequently fixed in cacodylate buffered 1% OsO_4 for 1 h. The samples are then washed in DI water 3× for 5 min/wash and transferred to 1% (aq) thiocarbohydrazide for 10 min. Next, the samples are washed in DI water and transferred to 1% OsO_4 for 10 min and then washed in DI water 3× for 5 min/wash. The samples are dehydrated in a graded series of ethanol, followed by three changes of absolute ethanol, and transferred to 1,1,1,3,3,3-hexamethyldisilazanc (Eastman Kodak Co., Rochester, NY) for 5 min, air dried for 2 h, and vacuum evaporated with Pt/Pd alloy in Balzers MED 010 evaporator (Bal-Tec Products Inc., Middlebury, CT). Samples are examined in a Hitachi S520 SEM operating at an accelerating voltage of 5 kV. Micrographs are recorded on Polaroid 55 P/N film.

RESULTS

In Vitro *Culture and Differentiation*

Primary preadipocytes differentiate from a fibroblast-like spindle morphology with small lipid inclusions, to a multilocular stage with numerous large inclusions, and finally to a state of a single, large lipid inclusion. As lipid accumulates, the plasma membrane shows several micropinocytotic vesicular areas, and the external laminae elaborates. Figure 4 depicts an early preadipocyte with many lipid inclusions, a preadipocyte with a single, large lipid inclusion, and mature adipocytes. Although smaller, the mature adipocytes closely resemble *in vivo* mature adipocytes (Figure 5). It typically required 7–10 days postplating for adipocytes to differentiate into a state typified by Figure 4D. The primary source of lipid for the differentiating adipocytes was 10% FBS. Culturing with 20% and 1% markedly caused an FBS-dependent increase and decrease, respectively, in lipid accumulation (data not shown). Hence, primary preadipocytes were successfully harvested, expanded, and differentiated. In addition, the cells were responsive to changes in lipid loading.

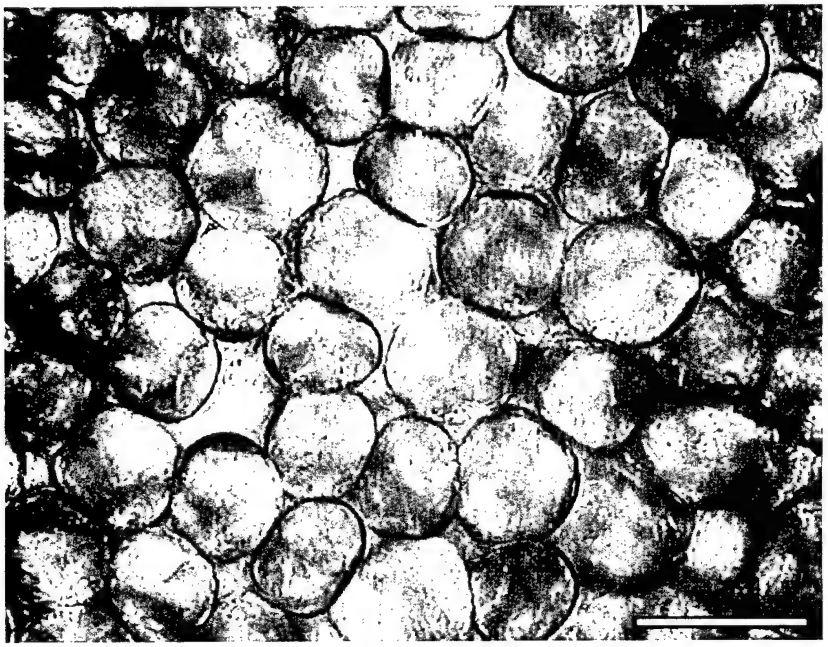

FIG. 5. Mature adipose tissue from rat epididymal fat pads. The tissue is a loose association of lipid filled adipocytes innervated with capillaries and held together with collagen fibers. Bar = 50 μm.

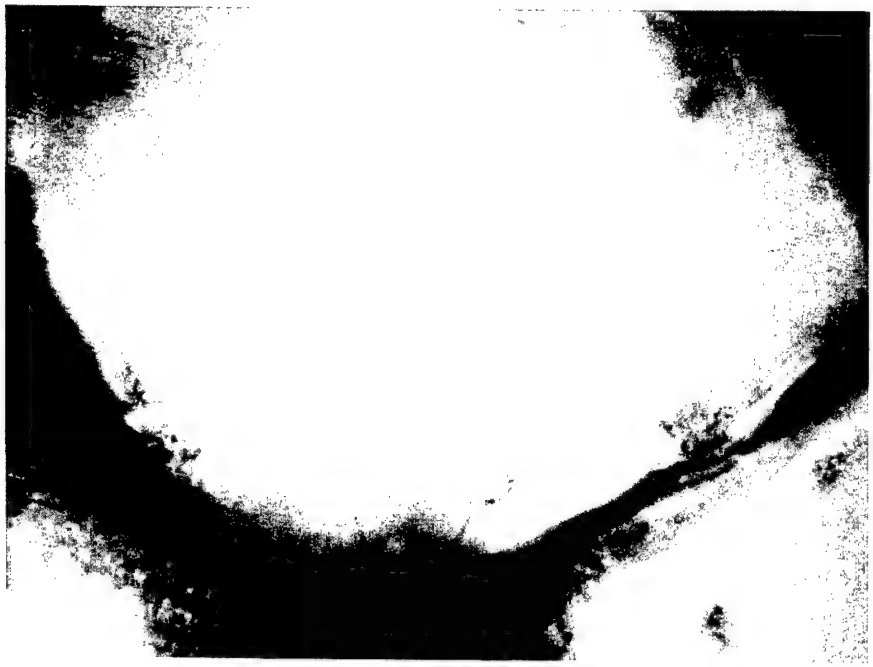

FIG. 6. Differentiated adipocytes observed within the pore of an *in vitro* PLGA disk 11 days postseeding.

In Vitro *Polymer Seeding*

Preadipocytes were cultured, removed from culture flasks, and seeded in PLGA disks to determine the feasibility of cell differentiation within the architecture of a polymer foam. Figure 6 shows differentiated adipocytes adhered to the side of a pore within a PLGA disk 11 days postseeding. This is illustrative of all disks tested. SEMs of preadipocyte-seeded disks reveal that preadipocytes use the pores of the polymer as a scaffold and fill the pores (Figure 7A). It is known that extracellular matrix fibers (predominantly colla-

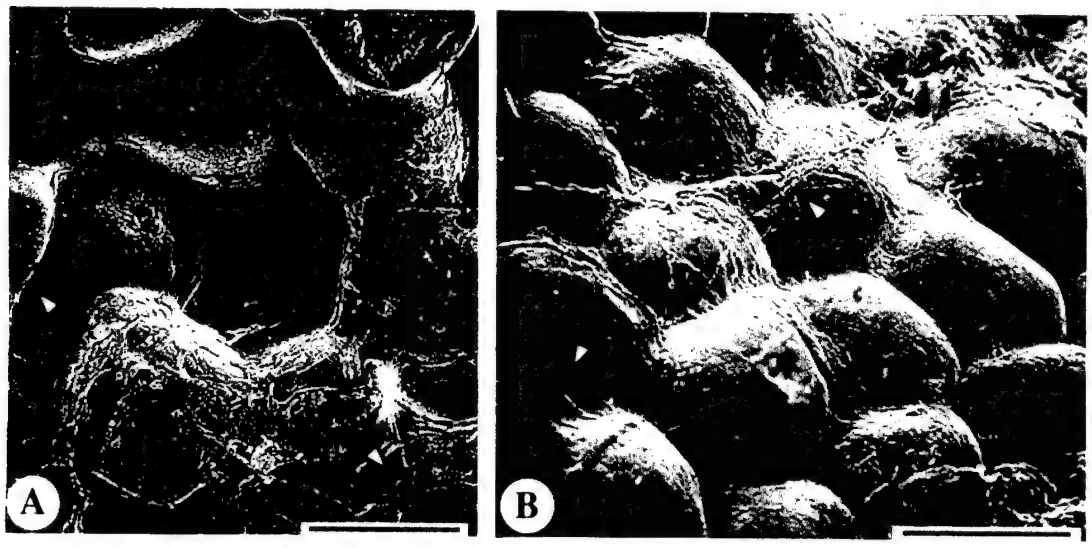

FIG. 7. **(A)** SEM (×100) of preadipocyte-seeded PLGA disks. Adipocytes have adhered to and filled the polymer pores. Arrows denote extracellular matrix fibers and the bar represents 300 μm. **(B)** SEM (×500) of epididymal adipose tissue. Arrows denote extracellular matrix fibers. Bar = 60 μm.

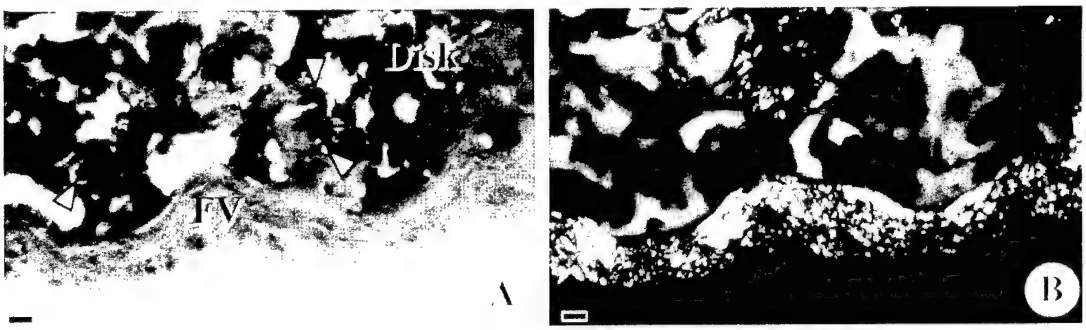

FIG. 8. Use of polarized light **(A)** in conjunction with brightfield optics **(B)** to distinguish polymer boundaries and fibrovascular tissue (FV). Arrows denote black stained adipocytes within the polymer. Bar = 50 μm.

gen I) hold mature adipocytes together.[14] These fibers are present within the preadipocyte-seeded disks (Figure 7A). The adipocyte morphology and extracellular matrix fibers are reminiscent of those observed in epididymal adipose tissue (Figure 7B). Again, as observed in culture flasks, adipocytes in seeded PLGA disks are smaller than those in epididymal adipose tissue.

In Vivo *Polymer Seeding*

Preadipocyte-seeded and acellular disks (control) were implanted in rats for 2 and 5 weeks. The rats were mobile and their range of motion unimpeded by the four disks during the duration of implantation. Harvest of 40 disks revealed a thin layer of fibrovascular tissue around each (mild inflammatory foreign body reaction), but no signs of infection as evidenced by lack of neutrophils. To accurately distinguish between the PLGA disk borders and the fibrovascular tissue under brightfield optics, polarized microscopy was utilized. Collagen organized within the fibrovascular tissue appears brighter than the PLGA under polarized

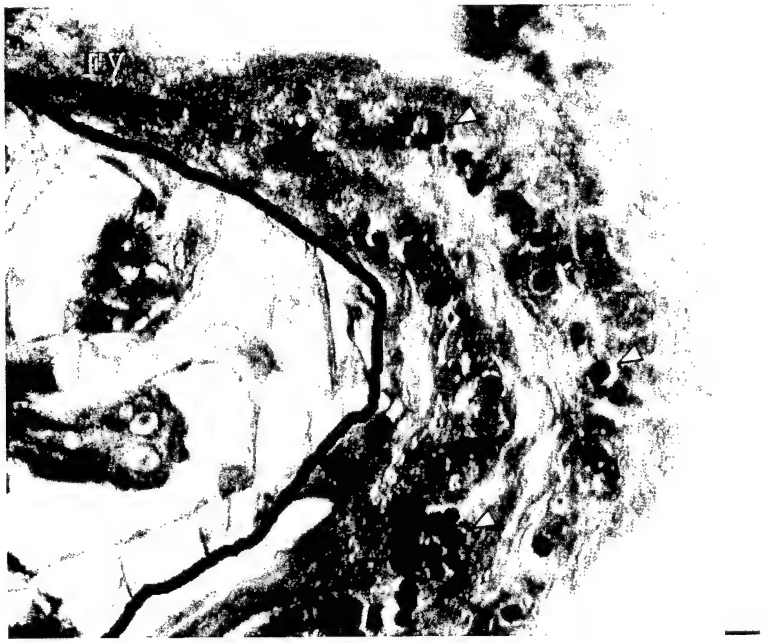

FIG. 9. OsO_4 staining of acellular (control) PLGA disks harvested after 5 weeks. Adipocytes (black round structures denoted by arrows) are only present within the fibrovascular tissue (FV). The border between the PLGA disk and the fibrovascular tissue is denoted by a heavy black line. Bar = 50 μm.

FIG. 10. **(A–C)** OsO_4 staining of preadipocyte-seeded PLGA disks harvested after 5 weeks. **(A,B)** Face cut sections of disks. **(C)** Cross-section of disk. Adipocytes present within the PLGA disks are denoted by arrows. Stars in A denote gross amounts of fat (unstained), and double arrow in C denotes "host" adipocyte. The border between the PLGA disk and fibrovascular tissue (FV) is denoted by a heavy black line. Bar = 50 μm.

light (Figure 8). No adipocytes were observed within all 10 acellular control disks. Clusters of adipocytes were, however, present in the surrounding fibrovascular tissue as expected (Figure 9). Simple agglomerations of fat cells in connective tissue are known as perivascular fat and differs from adipose tissue by virtue of their blood supply.[7]

All preadipocyte-seeded disks demonstrated the presence of differentiated, mature adipocytes throughout. Figure 10 illustrates representative OsO_4 stained sections of preadipocyte-seeded PLGA disks. In Figure 10A, numerous adipocytes are stained black throughout the entire area of the disk. Since OsO_4 only renders individual adipocytes or lipid droplets insoluble, gross amounts of adipose appear as "ghost" cells (☆ regions in Figure 10A) as it normally appears in conventional histological processing. Importantly, mature adipocytes are present in the center region of the disk as well as the edges. Similarly, Figure 10B illustrates that stained adipocytes are observed within the disk. A cross section through the central region of a PLGA disk is shown in Figure 10C. Differentiated adipocytes are demonstrated throughout the entire thickness of the disk. In addition, Figures 9 and 10 demonstrate that void area is still present after 2 and 5 weeks for preadipocyte expansion (i.e., fibrovascular tissue has not completely filled the disk).

Adipocytes present in the disks do not originate from surrounding fibrovascular tissue, as evidenced by Hoechst labeling of preadipocytes. Labeled preadipocytes were present in seeded disks (Figure 11) and not in acellular disks. Moreover, no labeled preadipocyte was observed to migrate out of the disks into the surrounding perivascular tissue.

FIG. 11. Hoechst labeling of preadipocytes. Fluorescently labeled adipocyte nuclei (blue) overlying a brightfield image of a disk.

DISCUSSION

Previous investigators have isolated preadipocytes from rats[15–19] and humans[20–23] and have demonstrated *in vitro* differentiation. In agreement, primary preadipocytes in this study were initially fusiform and proliferated *in vitro*. Once contact inhibited, the cells accumulated lipid inclusions, became rounder, and acquired an eccentric nucleus. In addition, this study has demonstrated for the first time the attachment, proliferation, and differentiation of preadipocytes within a polymer scaffold, both *in vitro* and *in vivo*. Others have shown that preadipocytes placed *in vivo* (but not in scaffolds) differentiate to mature adipocytes.[19,24] Preseeded PLGA disks implanted in rats demonstrated mature adipocytes throughout the disks at both 2 and 5 weeks.

Admittedly, this study is an initial attempt at adipose tissue engineering and many variables (e.g., cell seeding density, duration of implantation, cell state at implantation time, and polymer architecture) need to be addressed in future experiments. However, there appears to be great potential for using primary preadipocytes as a cell source in cell–seeded polymer scaffolds for soft tissue engineering applications. Preadipocytes have several advantages over mature adipose tissue from a design standpoint. Past investigators have shown that adipose tissue transplants and seeding of mature adipocytes do not result in adequate clinical results or cosmesis for repair of soft tissue defects.[2–7] Mature adipocytes are too fragile,[8,9] do not tolerate hypoxic environments well, and, being fully differentiated, do not proliferate. Because of their undifferentiated state, preadipocytes can be expanded *ex vivo*. Moreover, the initiation of differentiation after expansion is well controlled by simply regulating preadipocyte confluency. Unlike mature adipocytes which are ~90% lipid, preadipocytes are mechanically stable[25] and can be injected into polymers (i.e., they do not "liquefy" during handling or aspiration through a needle). Moreover, preadipocytes are able to tolerate extreme environments (e.g., the hypothesized hypoxic center of the PLGA disks) more easily than fully differentiated cells.

As with research in any new area, the initial data acquired raise many questions. This is compounded greatly in adipose tissue engineering by the fact that the biology of adipose tissue has not been explored in depth, with the exception of how adipocytes relate to obesity. The molecular mechanisms of adipocyte differentiation are just beginning to be explored.[26–30] From a surgical context, adipose grafting, transplantation, and healing remain poorly understood. In addition, very little is known on the basic characterization of fat cells, the features of the cytoplasm and cell membrane receptors, the expression of growth factors, or cell lineage from mesenchymal stem cells. To be sure, the development of clinically translatable adipose tissue equivalents remain challenging and unfulfilled, but results from this study are progressive steps toward realization.

REFERENCES

1. Neuber, G.A. Fettransplantation. Dtsch. Gesellschaft Chir. **22,** 66, 1893.
2. Ersek, R.A. Transplantation of purified autologous fat: a 3-year follow-up disappointing. Plast. Reconstr. Surg. **87,** 219, 1991.
3. Fagrell, D., Eneström, S., Berggren, A., and Kniola, B. Fat cylinder transplantation: an experimental comparative study of three different kinds of fat transplants. Plast. Reconstr. Surg. **98,** 90, 1996.
4. Peer, L.A. The neglected "free fat graft," its behavior and clinical use. Plast. Reconstr. Surg. **11,** 40, 1956.
5. Peer, L.A. Transplantation of fat. In: Converse, J.M., ed. Reconstructive Plastic Surgery: Principles and Procedures in Correction, Reconstruction, and Transplantation. Philadelphia: Saunders, 1977, p. 251.
6. Smahel, J. Failure of adipose tissue to heal in the capsule preformed by a silicone implant. Chir. Plast. **8,** 109, 1985.
7. Smahel, J. Experimental implantation of adipose tissue fragments. Br. J. Plast. Surg. **42,** 207, 1989.
8. Kotonas, T.C., Bucky, L.P., Hurley, C., and May Jr., J.W. The fate of suctioned and surgically removed fat after reimplantation for soft-tissue augmentation: a volumetric and histologic study in the rabbit. Plast. Reconstr. Surg. **91,** 763, 1993.
9. Nguyen, A., Pasyk, K.A., Bouvier, T.N., Hassett, C.A., and Argenta, L.C. Comparative study of survival of autologous adipose tissue taken and transplanted by different techniques. Plast. Reconstr. Surg. **85,** 378, 1990.
10. Mathes, S.J. Clinical Applications for Muscle and Musculocutaneous Flaps. St. Louis, MO: Mosby–Year Book, 1982.

11. American Society of Plastic and Reconstructive Surgeons and Plastic Surgery Education Foundation.
12. Wake, M.C., Patrick, Jr., C.W., and Mikos, A.G. Pore morphology effects on the fibrivascular tissue growth in porous polymer substrates. Cell Transplant. **3,** 339, 1994.
13. Carson, F.L. Osmium tetroxide paraffin procedure. In: Carson, F.L., ed. Histotechnology: A Self-Instructional Text. Chicago: ASCP Press, 1997, p. 153.
14. Wertheimer, E., and Shapiro, B. The physiology of adipose tissue. Physiol. Rev. **28,** 451, 1948.
15. Björntorp, P., Karlsson, M., Pertoft, H., Pettersson, P., Sjöström, L., and Smith, U. Isolation and characterization of cells from rat adipose tissue developing into adipocytes. J. Lipid Res. **19,** 316, 1978.
16. Carraro, R., Lu, Z., Li, Z.H., Johnson, Jr., J.E., and Gregerman, R.I. Adipose tissue islets: tissue culture of a potential source of fat cells in the adult rat. F.A.S.E.B. J. **4,** 201, 1990.
17. Novakofski, J.E. Primary cell culture of adipose tissue. In: Hausman, G.J., and Martin, R.J., eds. Biology of the Adipocyte: Research Approaches. New York: Van Nostrand Reinhold, 1987, pp. 160–197.
18. Van, R.L.R., and Roncari, D.A.K. Isolation of fat cell precursors from adult rat adipose tissue. Cell Tissue Res. **181,** 197, 1977.
19. Van, R.L.R., and Roncari, D.A.K. Complete differentiation *in vivo* of implanted cultured adipocyte precursors from adult rats. Cell Tissue Res. **225,** 557, 1982.
20. Entenmann, G., and Hauner, H. Relationship between replication and differentiation in cultured human adipocyte precursor cells. Am. J. Physiol. **270,** C1011, 1996.
21. Hauner, H., Entenmann, G., Wabitsch, M., et al. Promoting effect of gluctosteroids on the differentiation of human adipocyte precursor cells cultured in a chemically defined medium. J. Clin. Invest. **84,** 1663, 1989.
22. Poznanski, W.J., Waheed, I., and Van, R. Human fat cell precursors: morphologic and metabolic differentiation in culture. Lab. Invest. **29,** 570, 1973.
23. Strutt, B., Khalil, W., and Killinger, D. Growth and differentiation of human adipose stromal cells in culture. In: Jones, G.E., ed. Methods in Molecular Medicine: Human Cell Culture Protocols. Totowa, NJ: Humana Press, 1996, pp. 41–51.
24. Greene, H., and Kehinde, O. Formation of normally differentiated subcutaneous fat pads in an established preadipocyte cell line. J. Cell. Physiol. **101,** 169, 1979.
25. Billings, Jr., E., and May, Jr., J.W. Historical review and present status of free fat graft autotransplantation in plastic and reconstructive surgery. Plast. Reconstr. Surg. **83,** 368, 1989.
26. Brun, R.P., Kim, J.B., Altiok, S., and Spiegelman, B.M. Adipocyte differentiation: a transcriptional regulatory cascade. Curr. Opin. Cell Biol. **8,** 826, 1996.
27. Butterworth, S.C. Molecular events in adipocyte development. Pharmac. Ther. **61,** 399, 1994.
28. Cornelius, P., MacDougald, O.A., and Lane, M.D. Regulation of adipocyte development. Annu. Rev. Nutr. **14,** 99, 1994.
29. MacDougald, O.A., and Lane, M.D. Transcriptional regulation of gene expression during adipocyte differentiation. Annu. Rev. Biochem. **64,** 345, 1995.
30. Smas, C.M., and Sul, H.S. Control of adipocyte differentiation. Biochem. J. **309,** 697, 1995.

Address reprint requests to:
C.W. Patrick, Jr.
Laboratory of Reparative Biology and Bioengineering
Department of Plastic Surgery
University of Texas M.D. Anderson Cancer Center
1515 Holcombe Blvd., Box 62
Houston, TX 77030

cpatrick@notes.mdacc.tmc.edu

Modeling for Plastic and Reconstructive Breast Surgery

David T. Chen[1], Ioannis A. Kakadiaris[1], Michael J. Miller[2],
R. Bowen Loftin[1], Charles Patrick[2]

[1] Virtual Environments Research Institute and Department of Computer Science
University of Houston, Houston, TX 77204, USA
{davechen,ioannisk,bowen}@uh.edu
[2] Laboratory for Reparative Biology & Bioengineering, Dept. of Plastic Surgery
UT M.D. Anderson Cancer Center Houston, TX 77030, USA
{mmiller,cpatrick}@mail.mdanderson.org

Abstract. In this paper, we present the modeling and estimation aspects of a virtual reality system for plastic and reconstructive breast surgery. Our system has two modes, a *model creation* mode and a *model fitting* mode. The model creation mode allows a surgeon to interactively adjust the shape of a virtual breast by varying key shape variables, analogous to the aesthetic and structural elements surgeons inherently vary manually during breast reconstruction. Our contribution is a set of global deformations with very intuitive parameters that a surgeon can apply to a generic geometric primitive in order to model the breast of his/her patient for pre-operative planning purposes and for communicating this plan to the patient. The model fitting mode allows the system to automatically fit a generic deformable model to patient specific three-dimensional breast surface measurements using a physically-based framework. We have tested the accuracy of our technique using both synthetic and real input data with very encouraging results.

1 Introduction

Virtual reality (VR) has revolutionized many scientific disciplines by providing novel methods to visualize complex data structures and by offering the means to manipulate this data in real-time in a natural way. The most promising fields for the application of VR systems include engineering, education, entertainment, military simulations and medicine. With VR-based systems surgeons are able to: navigate through the anatomy, practice established procedures, practice new procedures, learn how to use new surgical tools, and assess their progress. In particular, the application domain of existing VR applications in surgery can be broadly classified in three categories: a) education and training, b) pre-operative planning, and c) intra-operative assistance. In pre-operative planning the aim is to study patient data before surgery and to plan the best way to carry out that procedure. We are currently developing a VR system that will allow a surgeon to plan and rehearse a plastic and reconstructive breast surgery based on patient specific data.

In this paper, we present the modeling and estimation aspects of a virtual reality system for plastic and reconstructive breast surgery. Our system has two

modes, a *model creation* mode and a *model fitting* mode. The model creation mode allows a surgeon to interactively adjust the shape of the breast by varying key shape variables, analogous to the aesthetic and structural elements surgeons inherently vary manually during breast reconstruction. Our contribution is a set of global deformations with very intuitive parameters that a doctor can apply to a generic geometric primitive in order to model the breast of his/her patient for pre-operative planning purposes and for communicating this plan to the patient. The model fitting mode allows the system to automatically fit a generic deformable model to patient specific three-dimensional breast surface measurements using a physically-based framework [4, 6].

The remainder of this paper is organized as follows. In Section 2 we present the motivation behind our work, and in Section 3 we present the theoretical framework of our research. In particular, in Section 3.1 we describe the basic geometric primitive employed for modeling a breast, in Section 3.2 we formulate the deformations that we have developed, and in Section 3.3 we present the methods employed for fitting a generic virtual breast model to patient-specific breast surface measurements. Finally, in Section 4 we present very encouraging results related to the adequacy of our modeling method and the accuracy of our fitting method using both synthetic and real input data.

2 Motivation

Breast size and shape are a significant part of female body image and sense of femininity. Breast deformities can occur due to cancer, congenital and traumatic causes, or the natural changes associated with aging. The psychological impact varies, but some breast deformities are a major cause of morbidity.

Breast deformities. The shape and size of the human female breast is determined by physical characteristics such as tissue volume, skin dimensions, and chest wall circumference. It is a dynamic structure that is soft and easily deformed by position, gravity, and external pressure. The configuration of the mature breast in each individual changes in response to physiologic alterations (e.g., pregnancy, menstrual cycle, etc.) and with advancing age. In addition to these natural changes, deformities can occur as a result of congenital causes, trauma, and cancer treatment.

- **Congenital breast deformities:** These include both disorders of excessively large breasts (hypermastia), small breasts (hypomastia), and breast asymmetries. Because these disorders generally appear at the time of puberty, they can cause significant emotional problems in teenagers and young adults.
- **Postpartum breast deformities:** After multiple episodes of breast-feeding, the breast atrophies and becomes ptotic in the late 30's and 40's. This is the most common reason for aesthetic breast surgery to modify the shape and nipple position.
- **Traumatic breast deformities:** These are uncommon but include sharp injuries and burns.

- **Cancer-related breast deformities:** Breast cancer is the most common cancer in women with an incidence of 11%. Deformities related to cancer treatment are the most common type. They range from complete absence of the breast to more limited contour problems resulting from breast conservation treatment (i.e., lumpectomy and radiation). Radiation can cause progressive changes in the breast over many years, making it firmer, rounded, and contracted in areas of scar.

Breast deformities can result in significant emotional and psychological morbidity. As a result, a variety of procedures have been devised to modify the shape and size of the breast.

Plastic surgery for the breast. Plastic surgery is surgery that alters the shape of tissues. Many operations have been devised to alter the female breast. Some enlarge or reduce the size the entire breast. Some alter not the size but only the shape and location of the nipple-areolar complex. Breast reconstruction recreates the entire breast (e.g., after mastectomy) using breast implants or tissue transferred from other parts of the body. Some procedures are a combination of each of these.

Specific techniques for these operations include various skin incisions and methods for removing tissue, adding tissue, inserting prosthetic devises, and fashioning the nipple/areolar complex. It is difficult to predict exactly how the breast will be changed by a specific procedure in any particular patient. How long should incisions be and where should they be placed? What size of breast implant will yield the best results? Is there enough tissue to recreate a breast that would meet the expectations of the patient? What does the patient want her breast to look like? Answering these questions is required for pre-operative planning. There is a certain amount of "trial and error" in the process. The exact result depends heavily on the experience, training, and personal artistic and surgical skills of the individual practitioner. Currently, these procedures are learned by surgeons by operating on actual patients, initially under the instruction of more senior surgeons, then later by independent experience. The patient will not know the final result until after the operation. She must trust the judgment of the surgeon to understand her needs and make many decisions without consulting her. Under these circumstances, the possibility is increased for undesirable outcomes.

Modeling and estimation. The uncertainties associated with breast surgery may be reduced by applying modeling and simulation. A virtual breast simulator may enhance the practice of breast surgery at multiple points. It enables the patient to communicate her expectations more clearly to the surgeon. It allows the surgeon to educate the patient with more accurate explanations of what can be accomplished, and after the patient encounter, it helps the surgeon plan specific aspects of the procedure to achieve the agreed upon goals. Finally, it facilitates surgical training by allowing trainees to design procedures and understand the results prior to actually performing surgery on the patient. In this paper, we limit our discussion in the modeling and estimation aspect of our VR system.

3 Theoretical Framework

In this section, the theoretical framework that will allow the analysis of a model's deformations is presented. We begin by reviewing the notation for deformable models and then we formulate the global deformations that we developed for modeling the shape of a breast.

3.1 Deformable Models: Modeling Geometry

The models used in this work are three-dimensional surface shape models. The material coordinates $\mathbf{u} = (u, v)$ of a point on these models are specified over a domain Ω. The three-dimensional position of a point w.r.t. a world coordinate system is the result of the translation and rotation of its position with respect to a non-inertial, model-centered coordinate frame ϕ. Therefore, the position of a point (with material coordinates $\mathbf{u}$) on a deformable model i at time t with respect to an inertial frame of reference Φ is given by the formula:

$$^{\Phi}\mathbf{x}_i(\mathbf{u}, t) = {}^{\Phi}\mathbf{t}_i(t) + {}^{\Phi}_{\phi}\mathbf{R}_i(t)\,{}^{\phi}\mathbf{p}_i(\mathbf{u}, t) \ , \tag{1}$$

where ${}^{\Phi}\mathbf{t}_i$ is the position of the origin O_i of the model frame ϕ_i with respect to the frame Φ (the model's translation), and ${}^{\Phi}_{\phi_i}\mathbf{R}_i$ is the matrix that encapsulates the orientation of ϕ_i with respect to Φ [4, 7]. ${}^{\phi_i}\mathbf{p}(\mathbf{u}, t)$ is the position of a model point with material coordinates $\mathbf{u}$ w.r.t. the model frame i and can be expressed as the sum of a reference shape ${}^{\phi_i}\mathbf{s}(\mathbf{u}, t)$ and a local displacement ${}^{\phi_i}\mathbf{d}(\mathbf{u}, t)$ as given by the formula: ${}^{\phi_i}\mathbf{p}(\mathbf{u}, t) = {}^{\phi_i}\mathbf{s}(\mathbf{u}, t) + {}^{\phi_i}\mathbf{d}(\mathbf{u}, t)$. The reference shape captures the salient shape features of the model and it is the result of applying global deformations $\mathbf{T}$ to a geometric primitive $\mathbf{e} = [e_x, e_y, e_z]^{\mathsf{T}}$. The geometric primitive $\mathbf{e}$ is defined parametrically in $\mathbf{u} \in \Omega$ and has global shape parameters $\mathbf{q_e}$. For the purposes of this research, we employ a superquadric $\mathbf{e}(u, v)$:$[-\frac{\pi}{2}, \frac{\pi}{2}) x [-\pi, \pi) \rightarrow \mathbb{R}^3$, whose global shape parameters are $\mathbf{q_e} = [a_1, a_2, a_3, \epsilon_1, \epsilon_2]^{\mathsf{T}}$. A superquadric surface is defined by a vector sweeping a closed surface in space by varying the material coordinates u and v. The parametric equation of a superquadric is given by the formula [2, 1]:

$$\mathbf{e}(\mathbf{u}) = [a_1 C_u{}^{\epsilon_1} C_v{}^{\epsilon_2}, a_2 C_u{}^{\epsilon_1} S_v{}^{\epsilon_2}, a_3 S_u{}^{\epsilon_1}]^{\mathsf{T}}, \tag{2}$$

where $-\frac{\pi}{2} \leq u \leq \frac{\pi}{2}$, $-\pi \leq v \leq \pi$, $a_1, a_2, a_3 \geq 0$ are the parameters that define the superquadric size, and ϵ_1 and ϵ_2 are the "squareness" parameters in the latitude and longitude plane, respectively. To model the shape of a breast, we only need half of the (u, v) space, therefore in our case $0 \leq u \leq \frac{\pi}{2}$. In addition, in order to be able to vary the sizes of different halves of the superquadric, we employ an asymmetric superquadric with the following parameters: $\mathbf{q_e} = [a_{1b}, a_{1t}, a_{2l}, a_{2r}, a_3, \epsilon_1, \epsilon_2]^{\mathsf{T}}$, where a_{1b} relates to the bottom half of the superquadric ($|v| \geq \frac{\pi}{2}$), a_{1t} relates to the top half ($|v| < \frac{\pi}{2}$), a_{2l} corresponds to the left half ($v \geq 0$), and a_{2r} to the right half ($v < 0$).

The local coordinate system for our asymmetric superquadric has the x axis protruding outward through the nipple, the z axis going up, and the y axis goes to the patient's life (Fig. 1). The deformations described in this paper are all expressed in this coordinate system.

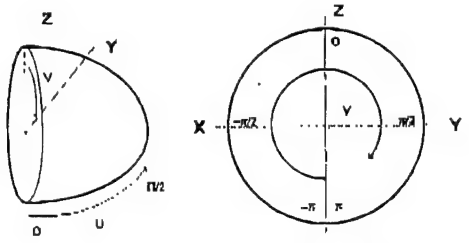

Fig. 1. Side and front views of the virtual breast model and of its associated coordinate systems.

3.2 Global Deformations

In our system, we model (using global deformations) five major features of the shape of the breast. First, the *Ptosis* deformation models the sagging that affects a breast as a subject ages. Second, the *Turn* deformation causes the breast to point towards the left or the right. Third, the *Top-Shape* deformation models the concavity/convexity of the profile of the top half of the breast. For an ideal breast shape the top half is concave, however in cases where large implants have been inserted into the breast, the top half becomes convex. Fourth, the *Flatten-Side* deformation flattens the shape of the half of the breast towards the middle of the torso. Finally, the *Turn-Top* deformation turns the top half of the breast towards the shoulder. In particular, the shape of the virtual breast model is given by $^{\phi}\mathbf{s}(\mathbf{u}, l) = [s_x, s_y, s_z]^{\mathsf{T}} = \mathbf{T}(\mathbf{c}; \mathbf{q}_{\mathbf{T}})$, where the global deformations $\mathbf{T}$ depend on the parameters $\mathbf{q}_{\mathbf{T}}$. In the following, we provide in detail the global deformations employed for modeling the breast.

Ptosis deformation. The Ptosis deformation depends on the parameters $\mathbf{q}_{\mathbf{T}} = [b_0, b_1]^{\mathsf{T}}$ and it is modeled as a quadratic function with coefficients b_0 and b_1. The deformation affects a point's vertical position (z) as a function of its depth (x). In particular, the Ptosis deformation $\mathbf{s} = \mathbf{T}_{\mathbf{p}}(\mathbf{e}; b_0, b_1)$ along a centerline parallel to the z-axis of a primitive $\mathbf{e} = [e_x, e_y, e_z]^{\mathsf{T}}$ is given by:

$$s_x = e_x, \;\; s_y = e_y, \;\; s_z = e_z - (b_0 e_x + b_1 {e_x}^2) \;\; .$$

Figure 2 depicts front and side views of a deformable breast model to which Ptosis deformation has been applied.

Turn deformation. The Turn deformation causes the shape of the breast to turn to the left or to the right. It uses a quadratic function to scale the y coordinate of a model point as a function of its x coordinate. The parameters of the deformation are $\mathbf{q}_{\mathbf{T}} = [c_0, c_1]^{\mathsf{T}}$, where c_0 controls the first order turning rate, and c_1 controls the second order turning. In particular, the Turn deformation $\mathbf{s} = \mathbf{T}_{\mathbf{t}}(\mathbf{e}; c_0, c_1)$ along a centerline parallel to the y-axis of a primitive $\mathbf{e}$ is given by:

$$s_x = e_x, \;\; s_y = e_y(c_0 e_x + c_1 {e_x}^2), \;\; s_z = e_z \;\; .$$

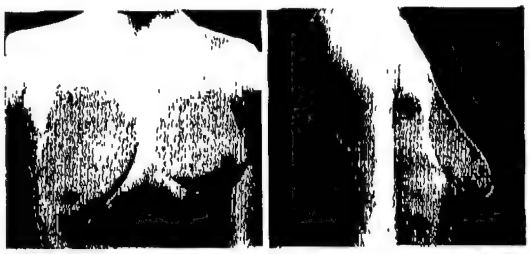

Fig. 2. Examples of Ptosis deformation with parameters $(b_0, b_1) = (0.479, -0.160)$ for the virtual patient's left breast, and $(b_0, b_1) = (0.691, 0.479)$ for the right breast.

Figure 3 depicts front and top views of a virtual patient's right breast to which turn deformation has been applied.

Top-Shape deformation. The Top-Shape deformation allows the user to modify the shape of the top half of the breast ($-\frac{\pi}{2} \leq v \leq \frac{\pi}{2}$). For such a point, we apply a polynomial that scales its z coordinate as a function of its u value (i.e., the point's longitude where the nipple is the north pole). In addition, $u' = u\frac{2}{\pi}$ and spans the range $[0, 1]$. The deformation's parameters are $\mathbf{q_T} = [s_0, t_0, s_1, t_1]^\mathsf{T}$, where s_0 is the slope for $u' = 0$, t_0 is the curvature for $u' = 0$, s_1 is the slope for $u' = 1$, and t_1 is the curvature for $u' = 1$. The slope parameters allow the user to vary the slope of the points near the torso and near the nipple. Similarly, the curvature parameters allow the user to adjust the curvatures near the torso and near the nipple. The Top-Shape deformation $\mathbf{s} = \mathbf{T_t}(\mathbf{e}; s_0, t_0, s_1, t_1)$ is formulated as:

$$s_x = e_x, \quad s_y = e_y, \quad s_z = e_z \mathbf{f}_1(u') \ .$$

In determining the order of the polynomial and its coefficients, we seek to adhere to the following constraints. The positions of the points where the breast merges with the torso and of the nipple must stay fixed, thus $\mathbf{f}_1(0) = 1$ and $\mathbf{f}_1(1) = 1$. The following equalities must hold for the slope parameters: $\mathbf{f}_1'(0) = s_0$ and $\mathbf{f}_1'(1) = s_1$. Finally, curvature parameters should satisfy the following

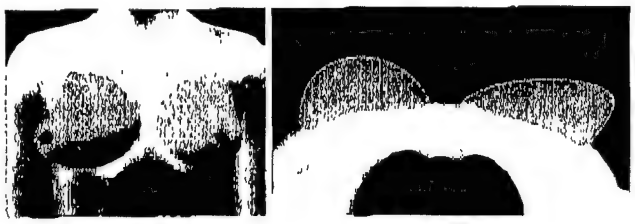

Fig. 3. Examples of Turn deformation with parameters $(c_0, c_1) = (-0.053, 0)$ for the virtual patient's left breast, and $(c_0, c_1) = (0.798, 0.213)$ for the patient's right breast.

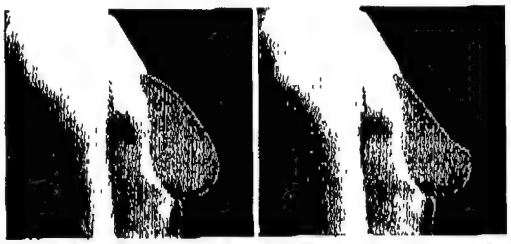

(a) (b)

Fig. 4. Examples of Top-Shape deformation with parameters $(s_0, t_0, s_1, t_1) = (.904, -7.979, 0, 0)$ (left image) and $(s_0, t_0, s_1, t_1) = (-1.543, -6.915, 2.287, -1.064)$ (right image).

equalities: $\mathbf{f}_1''(0) = t_0$ and $\mathbf{f}_1''(1) = t_1$. With this six constraints our polynomial is a quintic with coefficients A through F as follows:

$$\mathbf{f}_1(u') = Au'^5 + Bu'^4 + Cu'^3 + Du'^2 + Eu' + F \ ,$$

where $A = -\frac{1}{2}t_0 - 3s_0 - 3s_1 + \frac{1}{2}t_1, B = \frac{3}{2}t_0 + 8s_0 + 7s_1 - \frac{1}{2}t_1, C = -\frac{3}{2}t_0 - 6s_0 - 4s_1 + \frac{1}{2}t_1, D = \frac{1}{2}t_0, E = s_0$, and $F = 1$. Figure 4 depicts side views of examples of the Top-Shape deformation applied to the right breast. In Fig.4(a) the slope at the torso is positive, creating a convex upper breast, while in 4(b) the slope at the nipple is negative, creating a dip near the nipple.

Flatten-Side deformation. The shape of the breast has a tendency to flatten out as it approaches the sternum. To achieve this shape, we use the Flatten-Side deformation that affects the inner half of the breast. For example, for a patient's left breast the deformation flattens the breast's right side and similarly for a patient's right breast the deformation flattens the breast's left side (as seen by the patient's point of view). The right side of the virtual breast model includes points for which $v \leq 0$, while the left side includes points for which $v > 0$.

This deformation uses a cubic function that scales a point's x coordinate as a function of its horizontal position (y). The cubic is given by:

$$\mathbf{f}_2(y') = Ay'^3 + By'^2 + Cy' + D \ ,$$

where y' is normalized to $[0, 1]$ from the middle of the breast to the sternum. The parameters of the deformation are $\mathbf{q}_T = [g_0, g_1]^T$, where g_0 controls the scaling of points towards the sternum, and g_1 controls the change in the scaling as points move towards the middle of the breast. Since the function should not affect the breast at the nipple, we apply the constraint $\mathbf{f}_2(0) = 1$ and $\mathbf{f}_2'(0) = 0$. For our parameters $\mathbf{f}_2(1) = g_0$ and $\mathbf{f}_2'(1) = g_1$. Thus, the Flatten-Side deformation $s = \mathbf{T}_2(\mathbf{e}; g_0, g_1)$ is given by:

$$s_x = e_x, \ \ s_y = e_y \mathbf{f}_2(e_{y'}), \ \ s_z = e_z \ ,$$

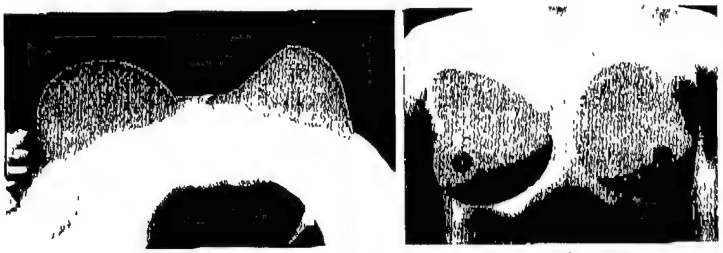

(a) (b)

Fig. 5. (a) Example of a Flatten-Side deformation with parameters $(g_0, g_1) = (1, 0)$. (b) Example of a Turn-Top deformation with parameters $(h_0, h_1) = (0.266, 0.372)$ for the virtual patient's right breast.

where $\mathbf{f}_2(y') = Ay'^3 + By'^2 + Cy' + D$, $A = g_1 + 2 - 2g_0$, $B = -g_1 - 3 + 3g_0$, $C = 0$, and $D = 1$. Figure 5(a) depicts a top-down view of a Flatten-Side deformation applied to a virtual patient's right breast.

Turn-Top deformation. The *Turn-Top* deformation changes the shape of the top half of the breast laterally. This deformation allows the top part of the virtual breast to point towards the shoulder. The deformation uses a quadratic function to adjust a point's y coordinate as a function of its normalized z coordinate, z'. Its parameters are $\mathbf{q}_T = [h_0, h_1]^T$, and it is applied to points for which $-\frac{\pi}{2} \leq v \leq \frac{\pi}{2}$. In particular, the Turn Top deformation $\mathbf{s} = \mathbf{T}_h(\mathbf{e}; h_0, h_1)$ along a centerline parallel to the y-axis of a primitive $\mathbf{e}$ is given by:

$$s_x = e_x, \quad s_y = e_y - h_0 e_z - h_1 e_z'^2, \quad s_z = e_z \ .$$

Figure 5(b) depicts a Turn-Top deformation applied to a virtual patient's right breast.

3.3 Fitting

Through the application of Lagrangian mechanics, the geometric parameters of the virtual breast deformable model, the global (parameterized) and local (free-form) deformation parameters, and the six degrees of freedom of rigid-body motion are systematically converted into generalized coordinates or dynamic degrees of freedom [7, 5]. The resulting Lagrangian equations are of the form $\dot{\mathbf{q}} + \mathbf{K}\mathbf{q} = \mathbf{f}_q$, for shape estimation tasks, where $\mathbf{K}$ is the stiffness matrix, $\mathbf{f}_q$ are the generalized external forces that act on the model, and $\mathbf{q}$ are the model's generalized coordinates. The damping and the stiffness matrices determine the viscoelastic properties of the deformable model. The elastic properties of the virtual breast model are being adapted in space and in time using the techniques described in [4, 6]. In physics-based shape estimation techniques, data points apply forces to the deformable model. These forces that the data apply to the model are converted to generalized 3D forces. Based on these forces the model will deform to minimize the discrepancy between the model and the data.

Table 1. The parameters for the virtual breast model depicted in Fig. 6(b)

Deformation	Parameter Values	
	Left Breast	**Right Breast**
Top-Shape	(−0.532, −7.447, 1.277, 0.000)	(−0.532, −6.383, 1.702, 0.000)
Ptosis	(1.0110, 0.000)	(1.0110, 0.000)
Turn	(0.106, 0.000)	(0.000, 0.000)
Flatten-Side	(1.000, 0.000)	(1.000, 0.000)
Turn-Top	(−0.160, −1.489)	(0.160, 1.489)

Table 2. The parameters for the virtual breast model depicted in Fig. 6(d)

Deformation	Parameter Values	
	Left Breast	**Right Breast**
Top-Shape	(−2.234, 8.511, 1.064, −0.532)	(−2.234, 8.511, 1.064, −0.532)
Ptosis	(0.798, 0.851)	(0.638, 0.745)
Turn	(0.000, −0.053)	(0.213, −0.053)
Flatten-Side	(0.505, 0.000)	(0.452, 0.000)
Turn-Top	(−0.106, −0.638)	(0.319, 0.638)

4 Experimental Results

In order to access the adequacy of the proposed global transformations, we have performed a number of experiments where a plastic surgeon constructs a virtual deformable model for a breast depicted in an image. The example images depicted in Figs. 6(a,c,e) have been randomly selected from [3]. Figures 6(b,d,f) depict the deformable models build by the surgeon. The parameters for these virtual breast models are detailed in Tables 1, 2, and 3, respectively.

Furthermore, in order to access the accuracy of the fitting, we have performed a number of shape estimation experiments with both synthetic and real data. Figure 6(g) depicts range data obtained from a subject using a Cyberware scanner, while Fig. 6(h) depicts the estimated model. The parameters for the estimated deformable breast model are detailed in Table 4.

5 Conclusion

In this paper, we have presented the modeling and shape estimation module of a VR system for plastic and reconstructive breast surgery. In particular, we presented the global deformations that enables us to model a female breast. We have presented several modeling examples along with very encouraging results from fitting a generic deformable breast model to three-dimensional data obtained using range scanning techniques.

Table 3. The parameters for the virtual breast model depicted in Fig. 6(f)

Deformation	Parameter Values	
	Left Breast	Right Breast
Top-Shape	$(-1.064, 7.979, 0.532, 0.000)$	$(-1.064, 7.979, 0.532, 0.000)$
Ptosis	$(0.319, 0.000)$	$(0.266, 0.106)$
Turn	$(0.266, -0.372)$	$(-0.053, 0.319)$
Flatten-Side	$(1.000, 0.000)$	$(1.000, 0.000)$
Turn-Top	$(0.319, 0.638)$	$(0, 0)$

Table 4. Parameter values for the estimated deformable model (Fig. 6(h))

Deformation	Parameter Values
Top-Shape	$(-1.543, -6.915, 1.915, -2.128)$
Ptosis	$(0.213, -0.160)$
Turn	$(0.160, 0.000)$
Flatten-Side	$(0.319, -1.489)$
Turn-Top	$(0.160, -0.372)$

References

1. A. Barr. Global and local deformations of solid primitives. *Computer Graphics*, 18(3):21–30, 1984.
2. A. H. Barr. Superquadrics and angle-preserving transformations. *IEEE Computer Graphics and Applications*, 1(1):11–23, January 1981.
3. John Bostwick III. *Plastic and Reconstructive Breast Surgery*. Quality Medical Publishing, St. Louis, Missouri, 1990.
4. I. A. Kakadiaris. *Motion-Based Part Segmentation, Shape and Motion Estimation of Multi-Part Objects: Application to Human Body Tracking*. PhD dissertation, Dept of Computer and Information Science, Univ. of Pennsylvania, Philadelphia, PA, Oct. 1996.
5. I. A. Kakadiaris and D. Metaxas. 3D Human body model acquisition from multiple views. *International Journal on Computer Vision*, 30(3):191–218, 1998.
6. D. Metaxas and I. A. Kakadiaris. Elastically adaptive deformable models. In Bernard Buxton and Roberto Cipolla, editors, *Proceedings of the Fourth European Conference on Computer Vision*, Lecture Notes in Computer Science, pages II:550–559, Cambridge, UK, April 14-18 1996.
7. D. Metaxas and D. Terzopoulos. Shape and nonrigid motion estimation through physics-based synthesis. *IEEE Transactions on Pattern Analysis and Machine Intelligence*, 15(6):580–591, June 1993.

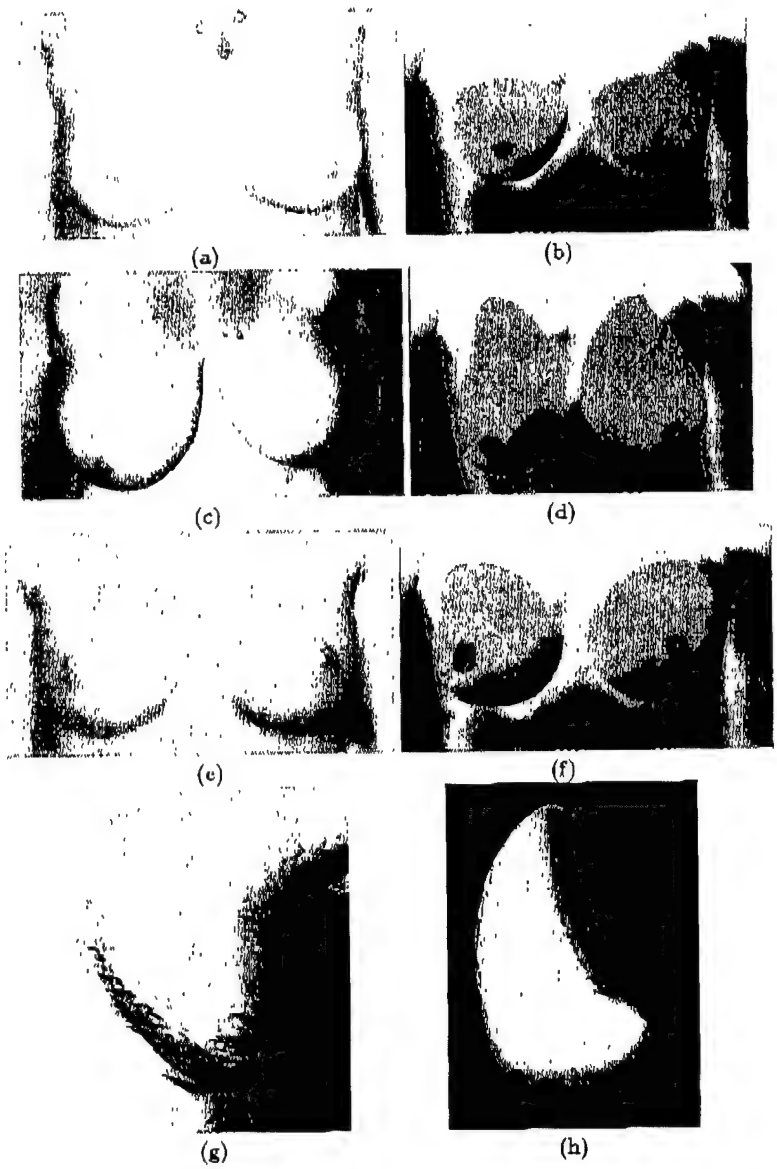

Fig. 6. (b,d,f) Examples of virtual breast models developed by a surgeon to model the female breasts depicted in (a,c,e). (g,h) Range data from a patient's breast and the estimated deformable model.

Seminars in Surgical Oncology 2000; 19:302–311

Adipose Tissue Engineering: The Future of Breast and Soft Tissue Reconstruction Following Tumor Resection

CHARLES W. PATRICK, JR., PhD*
Laboratory of Reparative Biology and Bioengineering, Department of Plastic Surgery, University of Texas M.D. Anderson Cancer Center, Houston, Texas

Reconstructive surgeons have always been at the forefront of medical technology. The history of reconstructive surgery began with ablative surgery, which was followed by tissue and organ transplantation, leading to contemporary tissue reconstruction. The field of reconstructive surgery is poised at the next stage of its evolution, namely tissue regeneration. The field of tissue engineering has largely defined this evolutionary leap. One active area of investigation is the development of tissue engineering strategies for adipose tissue. Bioengineers, life scientists, and reconstructive surgeons are synergistically coupling expertise in areas such as cell culture technology, tissue transfer, cell differentiation, angiogenesis, computer modeling, and polymer chemistry to regenerate adipose tissue de novo for breast replacement and soft-tissue augmentation following tumor resection. This work presents the current state of the art in adipose tissue engineering, as well the clinically translatable strategies currently under development. ***Semin. Surg. Oncol. 19:302–311, 2000.*** © 2000 Wiley-Liss, Inc.

KEY WORDS: **adipose tissue; biomedical engineering; breast implantation; capillaries; mastectomy; reconstructive surgical procedures**

INTRODUCTION

A mastectomy results in the loss of the breast mound that is largely composed of adipose tissue. Ideally, a surgeon prefers to refill the breast envelope with a patient's own adipose tissue. The contemporary standard of care for breast reconstruction includes utilizing implants or tissue transfer, both of which possess limitations [1]. Resection of tumors in the head and neck, and upper and lower extremities often results in contour defects due to loss of soft tissue, which is largely composed of subcutaneous adipose tissue. Again, a surgeon prefers to use a patient's own adipose tissue to sculpt contour deformities. As illustrated in Table I, there are numerous reconstructive, cosmetic, and correctional indications for the development of a clinically translatable strategy with which to restore a volume of adipose tissue.

Tissue engineering, coupled with knowledge gleaned from obesity and diabetes research as well as the amassed clinical experience with fat grafting, possesses the potential to provide surgeons with a source of patient-specific adipose tissue of a predefined volume. This work explores the current state of the art in adipose tissue engineering. The three fundamental components of a tissue construct—cells, scaffold, and microenvironment—are discussed first. Readers desiring a comprehensive perspective of tissue engineering should refer to the texts by Patrick et al. [2] and Lanza et al. [3]. Finally, strategies proposed for adipose tissue engineering germane to oncologic reconstructive surgery are presented.

CELLS

Fat Cells

Adipose tissue is ubiquitous in the human body; it is the largest tissue in the body, and is uniquely expendable in that most patients possess excess that can be harvested without creating contour deformities. However, autologous fat transplantation yields poor results, with 40–60% reduction in graft volume [1,4]. The reduction in adipose volume is postulated to be related to insufficient re-

Grant sponsor: Cancer Fighters of Houston; Grant sponsor: National Institutes of Health; Grant number: 2P30 CA1667; Grant sponsor: Plastic Surgery Educational Foundation; Grant sponsor: United States Army; Grant number: DAMD17-99-1-9268; Grant sponsor: University of Texas M.D. Anderson Cancer Center.

*Correspondence to: Charles W. Patrick, Jr., Ph.D., Director of Research, Department of Plastic Surgery, The University of Texas M.D. Anderson Cancer Center, 1515 Holcombe Blvd, Box 443, Houston, TX 77030. Fax: (713) 794-5492. E-mail: cpatrick@mdanderson.org

TABLE I. Indications for a Tissue Engineered Adipose Strategy

Category	Application	Specifics	Incidence or number of procedures/year
Reconstructive	Oncologic resection	Mastectomies	69,683 Breast reconstructions (3.1%)[a] [39]
		Parotidectomies	
	Complex trauma	Soft tissue deficits	
	Congenital abnormalities	Hemifacial microsomia	1 in 4,000 to 1 in 5,000 [40]
		Poland's syndrome	1 in 20,000 to 1 in 32,000 [41]
		Romberg's syndrome	
Cosmetic	Augmentation	Breast	132,378 Breast augmentations (augmentation mammoplasty) (6.0%)[a] [39]
			31,525 Breast lifts (mastoplexy) (1.4%)[a] [39]
		Cheek, chin, jaw	2,864 Cheek implants (malar augmentation) (0.1%)[a]
			4,795 Chin augmentations (mentoplasty) (0.2%)[a] [39]
		Lips	
		Buttocks	
	Rejuvenation	Wrinkles	1,246 Buttock lifts (0.1%)[a] [39]
			1,463 Fibril injections (0.1%)[a] [39]
	Nonspecific revision/resculpting	Various locations	45,851 Collagen injections (2.1%)[a] [39]
			25,437 Fat injections (1.1%)[a] [39]
Correctional	Implant removal	Breast	43,681 Removals (2.0%)[a]
	Bulking agent	Stress urinary incontinence	1,500,000
		Vocal cord insufficiency	
	Orthotic-related	Atrophied "cushion" in ball/heel of aged foot	
	Augmentation	Soft tissue deficits	

[a]Data represent 1998 statistics and (%) denotes the percentage of total plastic surgery procedures represented by the data.

vascularization. Some success has been achieved in transplanting small volumes of fat where diffusion can support cell survival [5,6]. The small volumes, however, are not clinically relevant for oncologic defects. The advent of liposuction led investigators to attempt the use of single-cell suspensions of mature adipocytes for soft-tissue augmentation. However, since they possess a cytoplasm composed of 80–90% lipid, aspirated adipocytes are easily traumatized by the mechanical forces of liposuction, resulting in ~90% damaged cells. The remaining 10% tend to form cysts or localized necrosis postinjection. Moreover, the terminal phenotype of mature adipocytes precludes taking advantage of ex vivo cell culture technology.

Recent progress has been made using preadipocytes—precursor cells that differentiate into mature adipocytes. Preadipocytes are fibroblast-like cells that uptake lipid during differentiation (Fig. 1). They grow easily with standard cell culture technologies and can be expanded ex vivo, and the molecular biology involved in preadipocyte differentiation has largely been elucidated through active research in the obesity and diabetes regimes [7–9]. However, much of the application-based biology of preadipocytes remains unknown (e.g., cell adhesion, cell motility, and response to various microenvironments). Human, rat, and swine preadipocytes have been routinely cultured [10–15]. Preadipocytes are typically isolated from enzyme-digested adipose tissue or liposuction aspirates. One can envision obtaining preadipocytes during a preoperative visit, for example, using current outpatient liposuction techniques. Alternatively, adipocyte stem cells may potentially allow one to develop cultures of preadipocytes. Researchers are predominantly focusing on using subcutaneous preadipocytes for tissue engineering strategies. It is known that fat depots at different anatomical locations behave differently [16–19]. Hence it remains to be seen if subcutaneous preadipocytes can adequately replace mammary adipose tissue. They should, however, suffice for soft-tissue augmentation strategies. The effects of patient age and menopausal status on preadipocyte biology within tissue-engineered constructs remain elusive. Moreover, many oncologic patients experience pre- or postoperative radiotherapy and/or chemotherapy. The effect of adjuvant therapies on adipose tissue engineering is presently unknown.

Vascular Cells

Any potential clinically translatable tissue engineering modality must consider the microvasculature. Clinical experience with tissue transfer alone proves this point. Adipose tissue is unique in that it possesses the capacity to continue to grow, and its vascular network grows in tandem (i.e., de novo angiogenesis) [20]. Adipose tissue is highly vascular. In fact, it is reported that each adipocyte is attached to at least one capillary. The capillary density of adipose is approximately one-third that of muscle. However, from a metabolic standpoint, normalizing for active protoplasm (since an adipocyte is largely lipid within its cytoplasm), the capillary bed of adipose is far richer (by ~2–3×) than that of muscle. Hence, it is paramount that adipose tissue

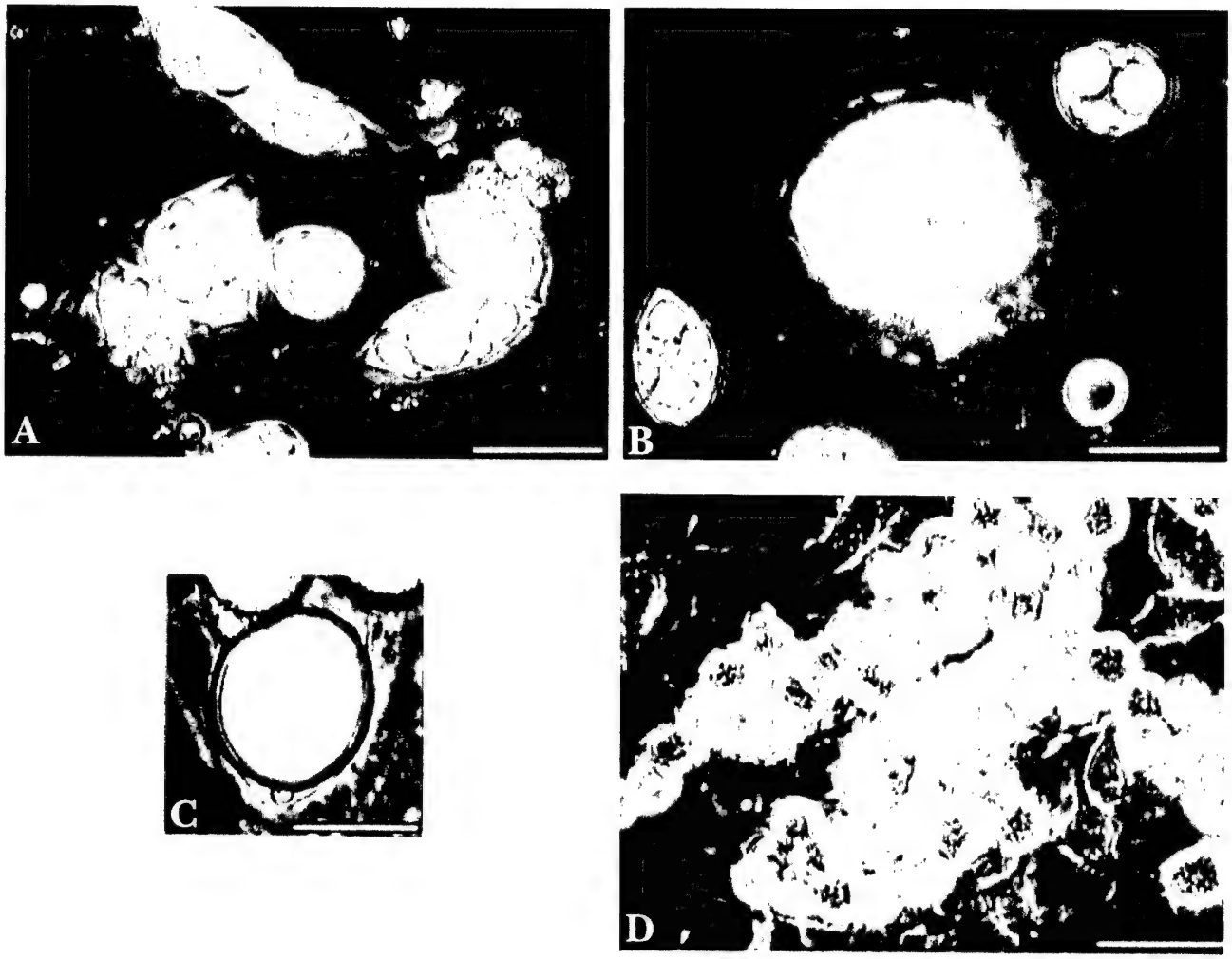

Fig. 1. Growth and differentiation of rat preadipocytes. Images **A** and **B** are phase contrast images of preadipocytes 7 days after initiation of differentiation. Note the accumulation and coalescence of lipid pools. **C:** Image of unilocular lipid pool within a single preadipocyte. **D:** Lobules of adipose tissue formed in vitro. Bars denote 50 μm.

constructs be well vascularized. In addition, adipose tissue is known to enhance angiogenesis through the secretion of growth factors and extracellular matrices (ECMs) [21–23].

Of the three biological mechanisms available to vascularize a tissue equivalent, only two are available to adults: revascularization and inosculation. Revascularization denotes the growth of capillaries from a host site into a tissue equivalent. Except for relatively thin constructs that can survive by diffusion, the slow kinetics (on the order of weeks) of this process abrogates its use for large constructs. It is hypothesized that strategies for soft-tissue augmentation will rely on revascularization since relatively thin layers of adipose will be required. In addition, wrapping a construct with highly vascular tissue may enhance revascularization. It has been proposed to use the highly vascular and adipocyte rich omentum to encase constructs [24,25]. Inosculation is the process of two capillaries or capillary networks fusing together. The kinetics of inosculation occur on the order of hours and are the predominant factor in reconstructive surgeons' ability to transfer tissue from a donor site to a recipient site. The use of inosculation in a tissue engineering strategy requires either the seeding of microvascular endothelial cells into a tissue equivalent followed by in situ development of a capillary network, or the ex vivo development and implantation of a capillary network. Strategies for breast reconstruction will no doubt require capillary networks as the large tissue mass required precludes relying solely on revascularization. Both modalities are actively being investigated but are hindered by the lack of understanding of the biological mechanisms that control inosculation, capillary formation, and cell culture technology of microvascular endothelial cells.

SCAFFOLDS

Numerous natural, synthetic, and hybrid materials have been utilized to act as adipose surrogates (Table II). These

TABLE II. Materials Used in Place of Adipose Tissue in Reconstructive Surgery

Material	Product (vendor)		Primary component(s)
ECM/Tissue Matrix	AlloDerm®	(LifeCell Corp)	Decellularized human dermal tissue
	Autologen®	(Collagenesis Inc)	Autologous human dermal collagen
	Cymetra™	(LifeCell Corp)	Micronized AlloDerm®
	Dermalogen™	(Collagenesis Inc)	Allogenous human dermal tissue matrix
	Fibrel®	(Mentor Corp)	Fibrin gel
	Hylaform®	(Biomatrix Corp)	Hyaluronic acid gel
	Restylane™	(Q-Med)	Viscoelastic hylan gel
	Tisseel®	(Baxter)	Human fibrin
	Zyderm® I	(Collagen Aesthetics)	Bovine dermal collagen (35 mg/mL)
	Zyderm® II	(Collagen Aesthetics)	Bovine dermal collagen (65 mg/mL)
	Zyplast®	(Collagen Aesthetics)	Zyderm® II with glutaraldehyde
Mineral/vegetable/oils			
Paraffin			
Polymers	Artecoll®	(Fofil Medical Int)	Polymethylmethacrylate microspheres
	Bioplastique®	(Bioplasty Inc)	Cross-inked polydimethylsiloxane
	Gortex®	(W.L. Gore & Associates)	Expanded polytetrafluoroethylene (ePTFE)
	Marlex®	(Davol Inc)	Porous/mesh-form polyethylene
	Softform™	(Collagen Aesthetics)	Expanded polytetrafluoroethylene (ePTFE)
Silicone	Various formulas	(Dow Corning)	

LifeCell Corporation, Branchburg, NJ; Collagenesis, Inc., Beverly, MA; Mentor Corp., Santa Barbara, CA; Biomatrix Corp., Ridgefield, NJ: Q-Med, Uppsala, Sweden; Collagen Aesthetics, Palo Alto, CA; Rofil Medical Int., Laguna Beach, CA; Bioplasty, Inc., Maastricht, The Netherlands; W.L. Gore & Associates, Flagstaff, AZ; Davol, Inc., Cranston, RI; Dow Corning, Midland, MI.

have predominantly been used to replace adipose volume and not function; that is, surgeons have largely focused on filling a defect site. Adipose tissue engineering possesses the potential to restore both volume and function. This depends, however, on preadipocytes adhering to appropriate support structures, or scaffolds. A support structure is required for anchorage-dependent cells to migrate and proliferate and to give a tissue equivalent the boundary conditions for final overall tissue shape. Scaffolds may either be implanted or injected.

Implantable materials utilized for adipose tissue engineering have predominantly been porous biodegradable polymer foams [1,4,26]. For instance, PLGA scaffolds preseeded with preadipocytes have demonstrated adipose tissue formation [26]. Polymer foams, however, will probably not be the optimum choice for breast scaffolds as they are too rigid for the breast envelope and would be uncomfortable for the patient. Nonbiodegradable scaffolds have also been investigated. Kral and Crandall [27] recently demonstrated the attachment and proliferation of preadipocytes on fluorotex monofilament-expanded polytetrafluoroethylene scaffolds coated with various ECMs.

Injectable materials, such as hydrogels, inherently possess optimum mechanical properties for use in the breast envelope, and for injection into soft-tissue defects. Both alginate and hyaluronic acid gels have been investigated [4,28,29]. In addition, preadipocytes proliferate and differentiate within fibrin gels (Fig. 2).

The optimum scaffold for breast tissue engineering remains elusive. Derivatizing polymers with adhesion molecules can potentially optimize scaffolds. However, this strategy is complicated by the fact that the constitution and distribution of the ECMs varies during adipocyte differentiation [30]. We have shown that preadipocytes readily adhere to laminin and fibronectin (Fig. 3). Hence, it would

Fig. 2. Rat preadipocytes seeded into and differentiating within a 2-mm-thick fibrin gel.

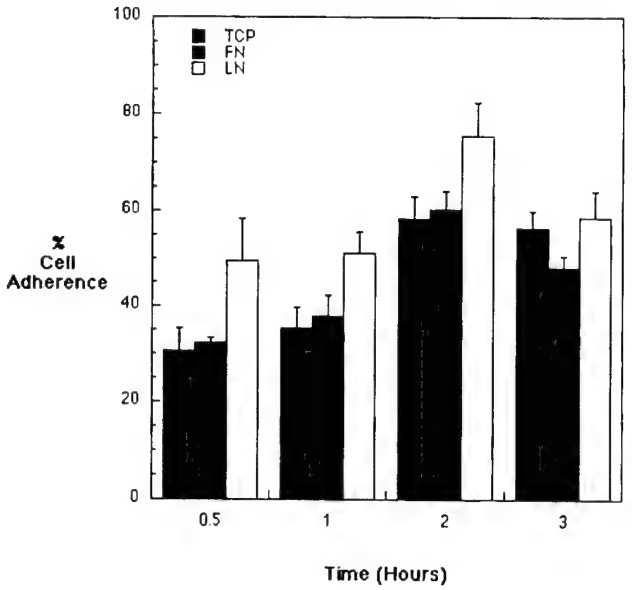

Fig. 3. Kinetics of preadipocyte adherence to tissue culture plastic (TCP), laminin (LN, 9–11 μg/cm^2), and fibronectin (FN, 5–7 μg/cm^2). Data denote mean ± SD.

seem conceivable to derivatize scaffolds with YGSIR and RGD, the cell-binding sequences of laminin and fibronectin, respectively. In fact, Mooney and colleagues [28] have derivatized alginate with RGD and observed increased adipogenesis when injected in a rat model. Although short-term studies have demonstrated adipose formation within biodegradable polymers [26], it remains to be determined whether the formed adipose tissue resorbs over the long term. We are currently involved in a year-long study to determine the sustainability of tissue-engineered adipose tissue (unpublished data).

TABLE III. Factors Positively (+) or Negatively (–) Affecting Adipose Differentiation

Factor	Effect
aFGF	+/–
bFGF	+/–
EGF	–
Glucocorticoid	+
Growth hormone	+
IGF-1	+
IL-11	–
Insulin	+
Interferon-γ	–
PDGF	+/–
Prostaglandins	+
TGF-α	–
TGF-β	–
Thyroid hormone	+
TNF-α	–

MICROENVIRONMENT

The microenvironment surrounding a tissue construct affects its differentiation and rate of tissue formation. Adipogenesis can be affected, in part, by growth factors (endo- and exogenous), pO_2 (normoxia vs. hypoxia), pH, adhesion molecules on ECM and support cells, and micromotion. Table III illustrates chemical factors that are reported to affect preadipocyte differentiation into adipocytes. Some factors (e.g., aFGF, bFGF, and PDGF) elicit conflicting results due to the fact it has not been elucidated whether the factors affect preadipocyte differentiation directly or indirectly through angiogenesis. Kawaguchi et al. [31] demonstrated de novo adipogenesis following injection of Matrigel and bFGF in mice. Yuksel and colleagues [32,33] have used biodegradable microspheres loaded with insulin, bFGF, and IGF-1 to

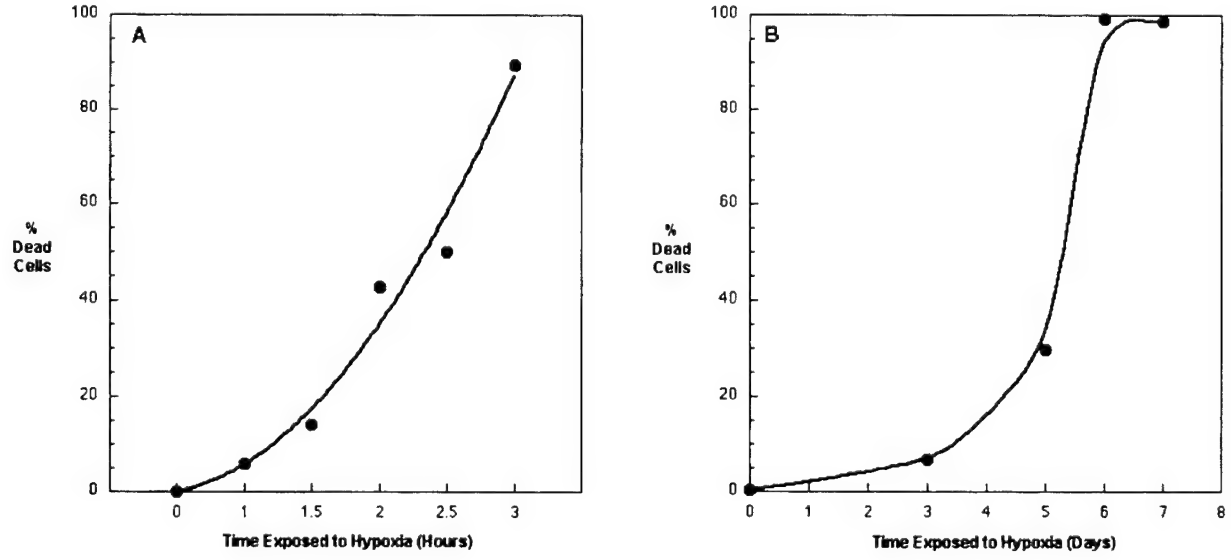

Fig. 4. Effect of hypoxia on the in vitro viability of (**A**) preadipocytes and (**B**) endothelial cells.

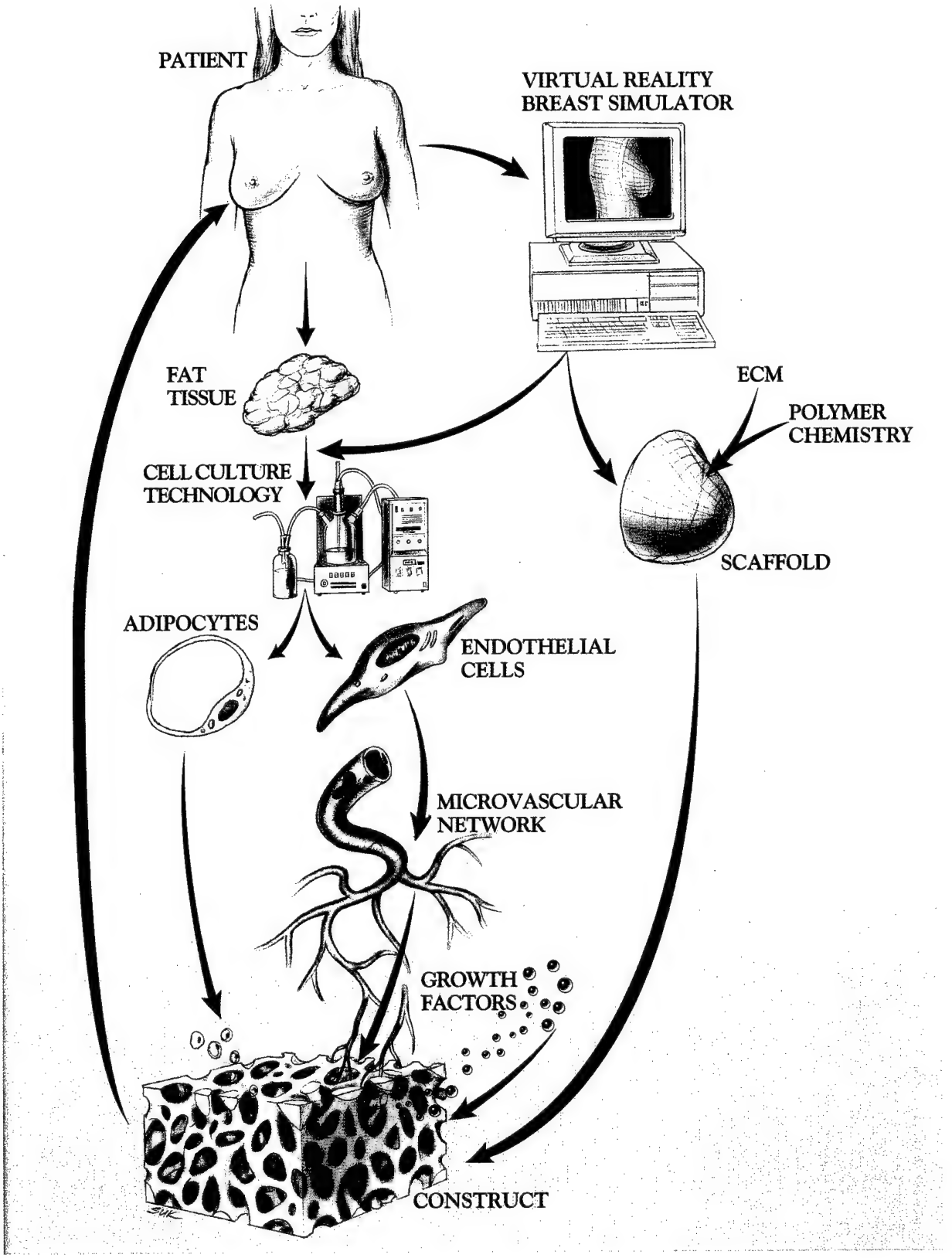

Fig. 5. Overview of proposed adipose tissue engineering strategy for developing a de novo breast mound.

differentiate preadipocytes to mature adipocytes in vivo. In addition, both EGF and TNF-α inhibit adipose differentiation [34,35]. Preadipocytes are extremely sensitive to hypoxic environments (Fig. 4). This is not surprising considering the historical results of free-fat grafting. However, this highlights a major design constraint as it limits the time preadipocytes can be implanted without an adequate microvascular network to supply nutrients. In contrast, microvascular endothelial cells have been shown to survive hypoxic conditions for 5–7 days (Fig. 4) [36,37].

PROPOSED STRATEGIES

Breast Reconstruction Strategies

One proposed strategy for breast tissue engineering is illustrated in Fig. 5. Adipose tissue is obtained from the patient via liposuction or fat biopsy. From the tissue sample, preadipocytes and capillary endothelial cells are isolated via enzymatic digestion and expanded ex vivo. The capillary endothelial cells are finessed to form microvascular networks. The preadipocytes and microvascular network are later placed, along with appropriate angiogenic and adipogenic growth factors, within a biodegradable polymer scaffold. The patient-specific scaffold shape, volume, and the number of cells required are obtained from a virtual breast simulator.

A breast tissue engineering strategy must be patient-specific to be truly clinically translatable. Unlike strategies for organs that can, for the most part, be grown as "one size fits all," breast shape and volume vary widely among the patient population. Breast implants, for instance, range from 100 mL to 2 L. Hence, methods must exist to predetermine design parameters preoperatively such that the final outcome is known a priori. To accomplish this goal, bioengineers, physicians, and computer scientists have combined skill sets to develop a first-generation virtual reality breast simulator (Fig. 6). The current system uses a global parametric deformable model of an ideal breast, and allows the surgeon to manipulate the shape of the breast by varying five key shape variables, analogous to the aesthetic and structural elements surgeons inherently vary during breast reconstruction. The variables include ptosis (sagging of the breast), top-shape (the breast's upper concavity/convexity), turn-top (orientation of the top half of the breast with respect to the shoulders), flatten-side (the side's concavity/convexity), and turn (deflection of nipple orientation from a perpendicular axis originating at the chest wall). The second generation of the virtual reality model is being developed to be truly patient-specific by importing three-dimensional measurements of the surface of the patient's breast obtained via surface scanning (Fig. 6).

Once the cells and growth factors are placed within the scaffold, the entire construct is implanted within the breast envelope following mastectomy. Using microsurgery techniques, the host vascular system is anastomosed with the

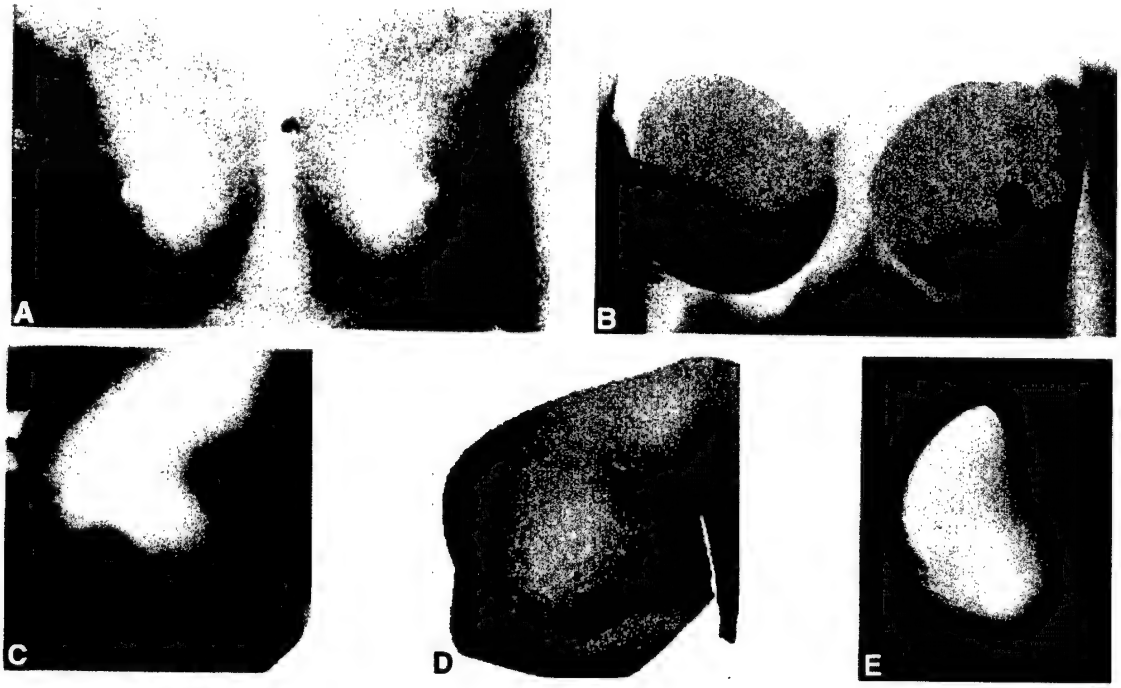

Fig. 6. Development of a virtual reality breast simulator. **A:** Image of patient. **B:** Virtual breast designed by the physician based on image A, using the first-generation simulator. **C:** Image of patient breast. **D:** 3D surface scan of breast in image C. **E:** Fitted virtual breast model of breast in C, resulting in a required volume of 987 mL and surface area of 453 cm^2. Images acquired in collaboration with Dr.M.J. Miller (M.D. Anderson Cancer Center) and Dr. I. Kakadiaris (University of Houston).

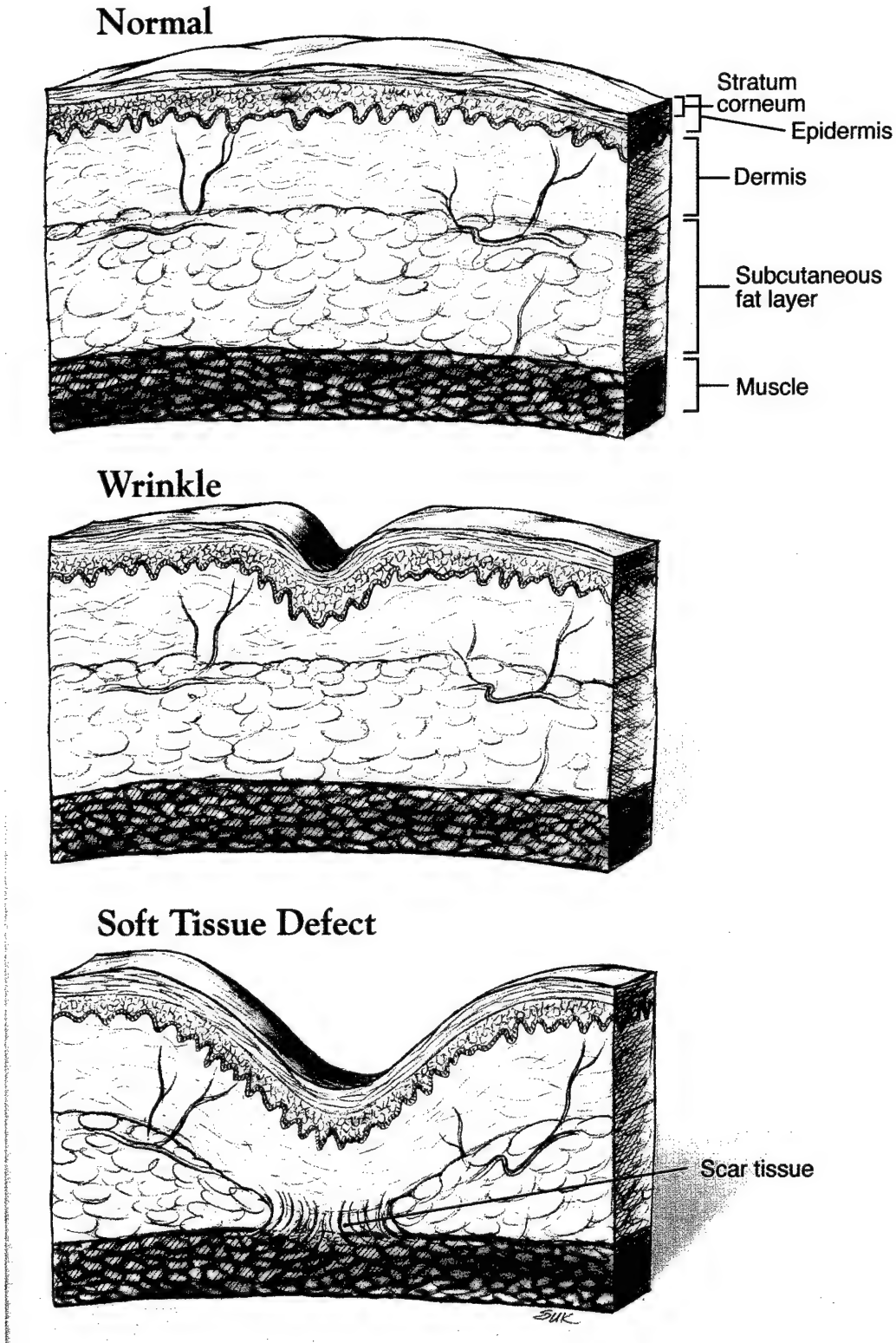

Fig. 7. Organizational differences between a normal cross-section of skin and that of a wrinkle and soft-tissue defect. In a wrinkle, a deficit in the dermis causes a contour defect that is translated to the epidermis and stratum corneum. In a soft-tissue defect, a tissue deficit occurs much deeper in the subcutaneous fat layer, causing a large contour defect that is translated to the dermis, epidermis, and stratum corneum. In addition, adhesion plaques form between the muscle and dermis.

construct's microvascular network. As the scaffold degrades, the preadipocytes proliferate and differentiate into adipose tissue. The microvascular system will reorganize accordingly. In essence, the patient becomes her own bioreactor for developing a new breast.

In addition to the above strategy, adjustable implants have been proposed. Vacanti and colleagues [38] have conceptualized serial injections of a cell-seeded hydrogel within a tissue expander device, with the tissue expander being decreased in size each time an injection is conducted.

Soft-Tissue Augmentation Strategies

Tissue engineering strategies for wrinkle and soft-tissue augmentation involve the restoration of localized contour defects. The restoration site for a wrinkle and soft-tissue defect differ in anatomical location (Fig. 7). In a wrinkle, a deficit in the dermis causes a contour defect that is translated to the epidermis and stratum corneum. Hence, an adipose product would be injected between the dermis and epidermis utilizing contemporary injection techniques. In a soft-tissue defect, a tissue deficit occurs much deeper in the subcutaneous fat layer, causing a large contour defect that is translated to the dermis, epidermis, and stratum corneum. In addition, adhesion plaques form between the muscle and dermis. Hence, an adipose product would be injected within the subcutaneous fat between the muscle and dermis. During the injection, the adhesion plaques would have to be cleaved. Obvious strategies include injecting hydrogels containing preadipocytes and adipogenic/angiogenic factors. Other strategies may involve developing a thin, flexible fabric composed of a biodegradable polymer or polymer blend that can be preseeded with preadipocytes.

CONCLUSIONS

The field of tissue engineering offers great potential in abrogating the current limitations of breast reconstruction and soft tissue augmentation following tumor resection. To be sure, great strides have already been achieved. However, the continued progress, and ultimately the clinical translation, of adipose tissue engineering applied to oncologic reconstructive surgery will require the active, synergistic collaboration of bioengineers, life scientists, and oncologic reconstructive surgeons. Only then will we truly be able to take advantage of technology and scientific knowledge to increase patient quality of life.

REFERENCES

1. Patrick Jr CW, Chauvin PB, Robb GL: Tissue engineered adipose. In Patrick Jr. CW, Mikos AG, McIntire LV (eds): "Frontiers in tissue engineering." Oxford: Elsevier Science; 1998; p. 369–382.
2. Patrick Jr CW, Mikos AG, McIntire LV: "Frontiers in tissue engineering." Oxford: Elsevier Science; 1998.
3. Lanza RP, Langer R, Vacanti J: "Principles of tissue engineering." San Diego: Academic Press; 2000.
4. Lee KY, Halberstadt CR, Holder WD, Mooney DJ: Breast reconstruction. In Lanza RP, Langer R, Vacanti J (eds): "Principles of tissue engineering." San Diego: Academic Press; 2000; p. 409–423.
5. Coleman SR: Long-term survival of fat transplants: controlled demonstrations. Aesth Plast Surg 1995;19:421–425.
6. Coleman SR: Facial recontouring with lipostructure. Clin Plast Surg 1997;24:347–367.
7. Mandrup S, Lane MD: Regulating adipogenesis. J Biol Chem 1997;272:5367–5370.
8. Loftus TM, Lane MD: Modulating the transcriptional control of adipogenesis. Curr Opin Genet Devel 1997;7:603–608.
9. MacDougald OA, Lane MD: Transcriptional regulation of gene expression during adipocyte differentiation. Ann Rev Biochem 1995;64:345–73.
10. Entenmann G, Hauner H: Relationship between replication and differentiation in cultured human adipocyte precursor cells. Am J Physiol 1996;270:C1011–C1016.
11. Hausman GJ, Richardson RL: Newly recruited and pre-existing preadipocytes in cultures of porcine stromal-vascular cells: morphology, expression of extracellular matrix components, and lipid accretion. Anim Sci 1998 1998;76:48–60.
12. Novakofski JE: Primary cell culture of adipose tissue. In Hausman GJ, Martin RJ (eds): "Biology of the adipocyte: research approaches." New York: Van Nostrand Reinhold; 1987; p. 160–197.
13. Shillabeer G, Forden JM, Lau DCW: Induction of preadipocyte differentiation by mature fat cells in the rat. J Clin Invest 1989;84: 381–387.
14. Strutt B, Khalil W, Killinger D: Growth and differentiation of human adipose stromal cells in culture. In Jones GE (ed): "Methods in molecular medicine: human cell culture protocols." Totowa, NJ: Human Press Inc.; 1996; p. 41–51.
15. Van RLR, Roncari DAK: Isolation of fat cell precursors from adult rat adipose tissue. Cell Tiss Res 1977;181:197–203.
16. Djian P, Roncari DAK, Hollenberg CH: Influence of anatomic site and age on the replication and differentiation of rat adipocyte precursors in culture. J Clin Invest 1983;72:1200–1208.
17. Hauner H, Entenmann G: Regional variation of adipose differentiation in cultured stromal-vascular cells from the abdominal and femoral adipose tissue of obese women. Int J Obesity 1991;15:121–126.
18. Kirkland JL, Hollenberg CH, Kindler S, Gillon WS: Effects of age and anatomic site on preadipocyte number in rat fat depots. J Gerontol 1994;49:B31–B35.
19. Kirkland JL, Hollenberg CH, Gillon WS: Effects of fat depot site on differentiation-dependent gene expression in rat preadipocytes. Int J Obes Rel Metabol Disord 1996;20 Suppl 3:S102–S107.
20. Crandall DL, Hausman GJ, Kral JG: A review of the microcirculation of adipose tissue: Anatomic, metabolic, and angiogenic perspectives. Microcirculation 1997;4:211–232.
21. Varzaneh FE, Shillabeer G, Wong KL, Lau DCW: Extracellular matrix components secreted by microvascular endothelia cells stimulate preadipocyte differentiation in vitro. Metabolism 1994;43(7): 906–912.
22. Silverman KJ, Lund DP, Zetter BR, et al: Angiogenic activity of adipose tissue. Biochem Biophys Res Commun 1988;153:347–352.
23. Zhang QX, Magovern CJ, Mack CA, et al: Vascular endothelial growth factor is the major angiogenic factor in omentum: mechanism of the omentum-mediated angiogenesis. J Surg Res 1997; 67:147–154.
24. Erol OO, Spira M: Reconstructing the breast mound employing a secondary island omental skin flap. Plast Reconstr Surg 1990;86: 510–518.
25. Sugawara Y, Harii K, Yamada A, et al: Reconstruction of skull defects with vascularized omentum transfer and split calvarial bone graft: two case reports. J Reconstr Microsurg 1998;14:101–108.
26. Patrick Jr CW, Chauvin PB, Reece GP: Preadipocyte seeded PLGA scaffolds for adipose tissue engineering. Tissue Eng 1999;5:139–151.
27. Kral JG, Crandall DL: Development of a human adipocyte synthetic polymer scaffold. Plast Reconstr Surg 1999;104:1732–1738.
28. Marler JJ, Guha A, Rowley J, et al: Soft-tissue augmentation with injectable alginate and syngeneic fibroblasts. Plast Reconstr Surg 2000;105:2049–2058.
29. Duranti F, Salti G, Bovani B, et al: Injectable hyaluronic acid gel for soft tissue augmentation. Dermatol Surg 1998;24:1317–1325.

30. Kubo Y, Kaidzu S, Nakajima I, et al: Organization of extracellular matrix components during differentiation of adipocytes in long-term culture. In Vitro Cell Dev Biol 2000;36:38–44.
31. Kawaguchi N, Toriyama K, Nicodemou-Lena E, et al: De novo adipogenesis in mice at the site of injection of basement membrane and basic fibroblast growth factor. Cell Biology 1998;95:1062–1066.
32. Yuksel E, Weinfeld AB, Cleek R, et al: Increased free fat-graft survival with the long-term, local delivery of insulin, insulin-like growth factor-I, and basic fibroblast growth factor by PLGA/PEG microspheres. Plast Reconstr Surg 2000;105:1712–1720.
33. Yuksel E, Weinfeld AB, Cleek R, et al: De novo adipose tissue generation through long-term, local delivery of insulin and insulin-like growth factor-1 by PLGA/PEG microspheres in an *in vivo* rat model: a novel concept and capability. Plast Reconstr Surg 2000; 105:1721–1729.
34. Serrero G: EGF inhibits the differentiation of adipocyte precursors in primary cultures. Biochem Biophys Res Commm 1987;146: 194–202.
35. Kras KM, Hausman DB, Martin RJ: Tumor necrosis factor-α stimulates cell proliferation in adipose tissue-derived stromal-vascular cell culture: promotion of adipose tissue expansion by paracrine growth factors. Obesity Res 2000;8:186–193.
36. Dore-Duffy P, Balabanov R, Beaumont T, et al: Endothelial activation following prolonged hypobaric hypoxia. Microvasc Res 1999;57:75–85.
37. Shweiki D, Itin A, Soffer D, Keshet E: Vascular endothelial cell growth factor induced by hypoxia may mediate hypoxia-initiated angiogenesis. Nature 1992;359:843–845.
38. Vacanti JP, Atala A, Mooney DJ, Langer RS: Breast tissue engineering. US Patent 5,716,404. USA, 1998.
39. American Society of Plastic Surgeons and Plastic Surgery Education Foundation; [1998; cited 00 Oct 17]. Available from: http://www.plasticsurgery.org/.
40. Kearns GJ, Padwa BL, Mulliken JB, Kaban LB: Progression of facial asymmetry in hemifacial microsomia. Plast Reconstr Surg 2000;105:492–498.
41. Havlik RJ, Sian KU, Wagner JD, et al: Breast cancer in Poland syndrome. Plast Reconstr Surg 1999;104:180–182.

THE ANATOMICAL RECORD 263:361–366 (2001)

Tissue Engineering Strategies for Adipose Tissue Repair

C.W. PATRICK, JR*

Laboratory of Reparative Biology & Bioengineering, Department of Plastic Surgery, The University of Texas M.D. Anderson Cancer Center and University of Texas Center for Biomedical Engineering, Houston, Texas

ABSTRACT

Tissue engineering is a relatively young field that combines engineering, clinical science, and life sciences to, in part, repair or regrow tissues. Adipose tissue has recently become a focus area for tissue engineering, encouraged by the large number of reconstructive, cosmetic, and correctional indications that could be addressed with clinically translatable adipose tissue engineering strategies. This review discusses the three aspects of an adipose construct, namely cell types, scaffold, and microenvironment, and presents current tissue engineering strategies under pursuit. Anat Rec 263:361–366, 2001. © 2001 Wiley-Liss, Inc.

Key words: adipose tissue; biomedical engineering; reconstructive surgical procedures; soft tissue augmentation; tissue engineering.

Resection of tumors in the head and neck and upper and lower extremities as well as trauma and congenital abnormalities often result in contour defects due to loss of soft tissue, largely composed of subcutaneous adipose tissue. The defects lead to abnormal cosmesis, affect the emotional well being of patients, and may impair function (e.g. range of motion). A surgeon would prefer to use a patient's own adipose tissue to sculpt contour deformities. Because mature adipose tissue does not transplant effectively, numerous natural, synthetic, and hybrid materials have been used to act as adipose surrogates. A nonexhaustive list of commercially available materials is provided in Table 1. Improved patient outcomes notwithstanding, many of these materials possess severe limitations such as unpredictable outcomes, fibrous capsule contraction, allergic reactions, suboptimum mechanical properties, distortion, migration, and long-term resorption. As illustrated in Table 2, there are numerous reconstructive, cosmetic, and correctional indications for the development of a clinically translatable strategy with which to restore a volume of adipose tissue.

Tissue engineering, coupled with knowledge gleaned from obesity and diabetes research, as well as the amassed clinical experience with fat grafting, possesses the potential to provide surgeons with a source of patient-specific adipose tissue. This manuscript explores the current state-of-the-art in adipose tissue engineering. The scope of this review will be limited to adipose tissue engineering applied to soft tissue defects. Adipose tissue engineering applied to breast reconstruction has been covered recently by this author (Patrick, 2000; Robb et al., in press). The three fundamental components of a tissue construct, namely cells, scaffold, and microenvironment, are discussed first, followed by proposed strategies for tissue augmentation. Readers desiring a comprehensive perspective of tissue engineering should refer to the texts by Patrick et al. (Patrick et al., 1998b) and Lanza et al. (Lanza et al., 2000).

FAT CELLS

Adipose tissue is ubiquitous, the largest tissue in the body, uniquely expendable, and most patients possess excess that can be harvested without creating contour deformities. However, autologous fat transplantation yields poor results, with 40–60% reduction in graft volume (Patrick et al., 1998a; Lee et al., 2000). The reduction in

Grant sponsor: Cancer Fighters of Houston; Grant sponsor: National Institutes of Health; Grant number: 2P30 CA1667; Grant sponsor: Plastic Surgery Educational Foundation; Grant sponsor: United States Army; Grant number: DAMD17-99-1-9268; Grant sponsor: The University of Texas M.D. Anderson Cancer Center.

*Correspondence to: Charles W. Patrick Jr., Ph.D., Department of Plastic Surgery, The University of Texas M.D. Anderson Cancer Center, 1515 Holcombe Blvd., Box 443, Houston, TX 77030. Fax: 713-794-5492; E-mail: cpatrick@mdanderson.org

Received 6 October 2000; Accepted 28 February 2001

Published online 12 July 2001; DOI 10.1002/ar.1113

TABLE 1. Materials used in place of adipose tissue in reconstructive surgery[a]

Material	Product (Vendor)	Primary component(s)
ECM/Tissue matrix	AlloDerm (LifeCell Corp)	Decellularized human dermal tissue
	Autologen (Collagenesis, Inc.)	Autologous human dermal collagen
	Cymetra (LifeCell Corp)	Micronized AlloDerm®
	Dermalogen (Collagenesis, Inc.)	Allogenous human dermal tissue matrix
	Fibrel (Mentor Corp)	Fibrin gel
	Hylaform (Biomatrix Corp)	Hyaluronic acid gel
	Restylane (Q-Med)	Viscoelastic hylan gel
	Tisseel (Baxter)	Human fibrin
	Zyderm I (Collagen Aesthetics)	Bovine dermal collagen (35 mg/mL)
	Zyderm II (Collagen Aesthetics)	Bovine dermal collagen (65 mg/mL)
	Zyplast (Collagen Aesthetics)	Zyderm® II with glutaraldehyde
Mineral/Vegetable Oils		
Paraffin		
Polymers	Artecoll (Rofil Medical Int)	Polymethylmethacrylate microspheres
	Bioplastique (Bioplasty, Inc.)	Cross-linked polydimethylsiloxane
	Gortex (W.L. Gore & Associates)	Expanded polytetrafluoroethylene (ePTFE)
	Marlex (Davol, Inc.)	Porous/mesh-form polyethylene
	Softform (Collagen Aesthetics)	Expanded polytetrafluoroethylene (ePTFE)
Silicone	Various formulas (Dow Corning)	

[a]ECM, extracellular matrix.

TABLE 2. Indications for a tissue engineered adipose strategy

Category[a]	Application	Specifics	Incidence or number of procedures/year
Reconstructive	Oncologic resection	Mastectomies	69,683 Breast reconstructions (3.1%)[b]
		Parotidectomies	
	Complex trauma	Soft tissue deficits	
	Congenital abnormalities	Hemifacial microsomia	1 in 4,000 to 1 in 5,600[c]
		Poland's syndrome	1 in 20,000 to 1 in 32,000[d]
		Romberg's syndrome	
Cosmetic	Augmentation	Breast	132,378 Breast augmentations (augmentation mammoplasty) (6.0%)[b]
			31,525 Breast lifts (mastoplexy) (1.4%)[b]
		Cheek, chin, jaw	2,864 Cheek implants (malar augmentation) (0.1%)[b]
			4,795 Chin augmentations (mentoplasty) (0.2%)[b]
		Lips	
		Buttocks	1,246 Buttock lifts (0.1%)[b]
	Rejuvenation	Wrinkles	1,463 Fibril injections (0.1%)[b]
			45,851 Collagen injections (2.1%)[b]
	Nonspecific revision/ resculpting	Various locations	25,437 Fat injections (1.1%)[b]
Correctional	Implant removal	Breast	43,681 Removals (2.0%)
	Bulking agent	Stress urinary incontinence	1,500,000
		Vocal cord insufficiency	
	Orthotic-related	Atrophied "cushion" in ball/ heel of aged foot	
	Augmentation	Soft tissue deficits	

[a]Adapted from Katz et al., 1999.
[b]American Society of Plastic Surgeons & Plastic Surgery Education Foundation, http://www.plasticsurgery.org/. Data represent 1998 statistics and (%) denotes the percentage of total plastic surgery procedures represented by the data.
[c]Kearns et al., 2000.
[d]Havlik et al., 1999.

adipose volume is postulated to be, in part, related to insufficient revascularization (Smahel, 1986; Nguyen et al., 1990). Some success has been achieved transplanting small volumes of fat where diffusion can support cell survival (Coleman, 1995, 1997). However, the small volumes are not clinically relevant for most soft tissue defects. The advent of liposuction led investigators to attempt using single cell suspensions of mature adipocytes for soft tissue

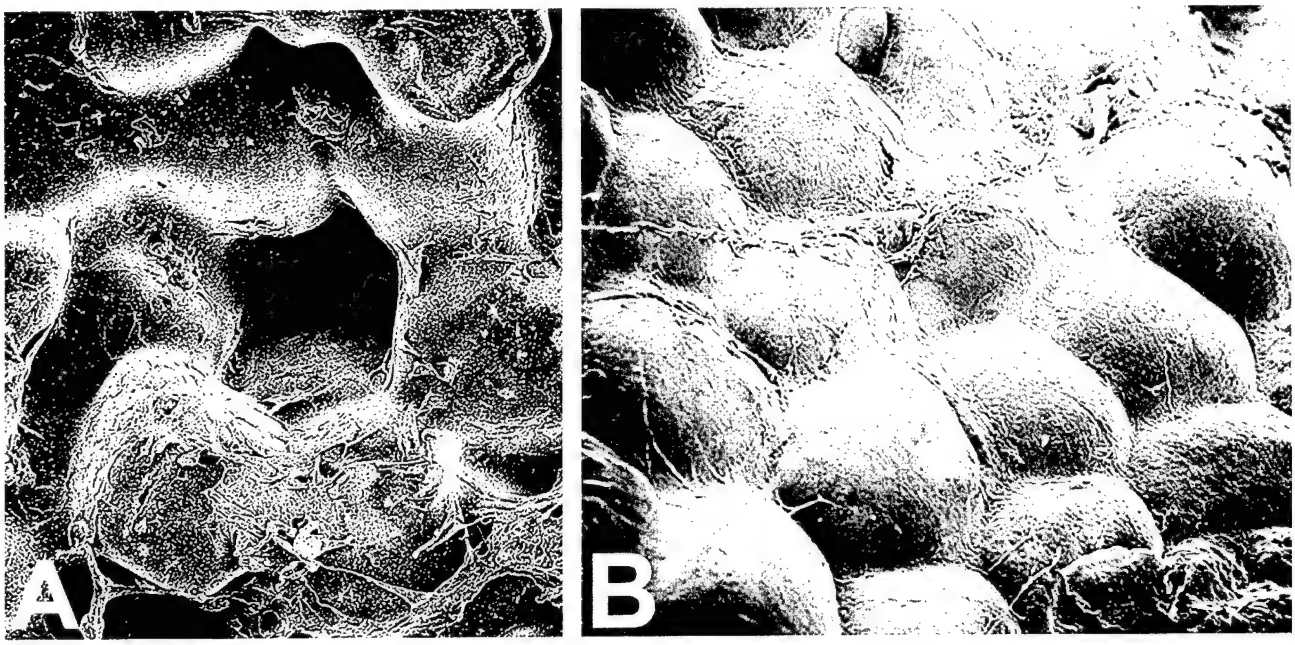

Fig. 1. Scanning electron photomicrographs. **A:** Adipose tissue formed within poly (L-lactic-co-glycolic) acid (PLGA) scaffolds preseeded with rat preadipocytes. **B:** Adipose tissue in vivo of rat epididymal fat pad. Note the similarity in morphology and extracellular matrix fibers.

augmentation. However, possessing a cytoplasm composed of 80–90% lipid, aspirated adipocytes are easily traumatized by the mechanical forces of liposuction, resulting in ~90% damaged cells. The remaining 10% tend to form cysts or localized necrosis postinjection. Moreover, the terminal phenotype of mature adipocytes precludes taking advantage of ex vivo cell culture technology.

Recent progress has been made using preadipocytes, precursor cells that differentiate into mature adipocytes. Preadipocytes are fibroblast-like cells that uptake lipid during differentiation (Patrick, 2000; Patrick et al., in press). They grow easily with standard cell culture technologies, can be expanded ex vivo, and the molecular biology involved in preadipocyte differentiation has largely been elucidated through active research in the obesity and diabetes regimens (MacDougald and Lane, 1995; Loftus and Lane, 1997; Mandrup and Lane, 1997). However, much of the application-based biology of preadipocytes remains unknown (e.g. cell adhesion, cell motility, and response to various microenvironments). Human, rat, and swine preadipocytes have been routinely cultured (Van and Roncari, 1977; Novakofski, 1987; Shillabeer et al., 1989; Entenmann and Hauner, 1996; Strutt et al., 1996; Hausman and Richardson, 1998). Preadipocytes are typically isolated from enzyme-digested adipose tissue or liposuction aspirates. One can envision obtaining preadipocytes during a preoperative visit, for example, by using current outpatient liposuction techniques. Alternatively, adipocyte stem cells may potentially allow one to develop cultures of preadipocytes. Researchers are predominantly focusing on using subcutaneous preadipocytes for tissue engineering strategies. It is known that fat depots at different anatomic locations behave differently (Djian et al., 1983; Hauner and Entenmann, 1991; Kirkland et al., 1994, 1996). Moreover, the affects of patient age and menopausal status on preadipocyte biology within tissue engineered constructs remain elusive. In addition, many oncologic patients experience preoperative or postoperative radiotherapy, chemotherapy, or both. The affect of adjuvant therapies on adipose tissue engineering is presently unknown.

TABLE 3. Factors positively (+) or negatively (−) affecting adipose differentiation

Factor	Affect
aFGF	+/−
bFGF	+/−
EGF	−
Glucocorticoid	+
Growth hormone	+
IGF-1	+
IL-11	−
Insulin	+
Interferon-γ	−
PDGF	+/−
Prostaglandins	+
TGF-α	−
TGF-β	−
Thyroid hormone	+
TNF-α	−

FGF, fibroblast growth factor; EGF, epidermal growth factor; IGF, insulin-like growth factor; IL, interleukin; PDGF, platelet-derived growth factor; TGF, transforming growth factor; TNF, tumor necrosis factor.

SCAFFOLDS

The materials listed in Table 1 have predominantly been used to replace adipose volume and not function. That is, surgeons have largely focused on filling a defect site. Adipose tissue engineering possesses the potential to

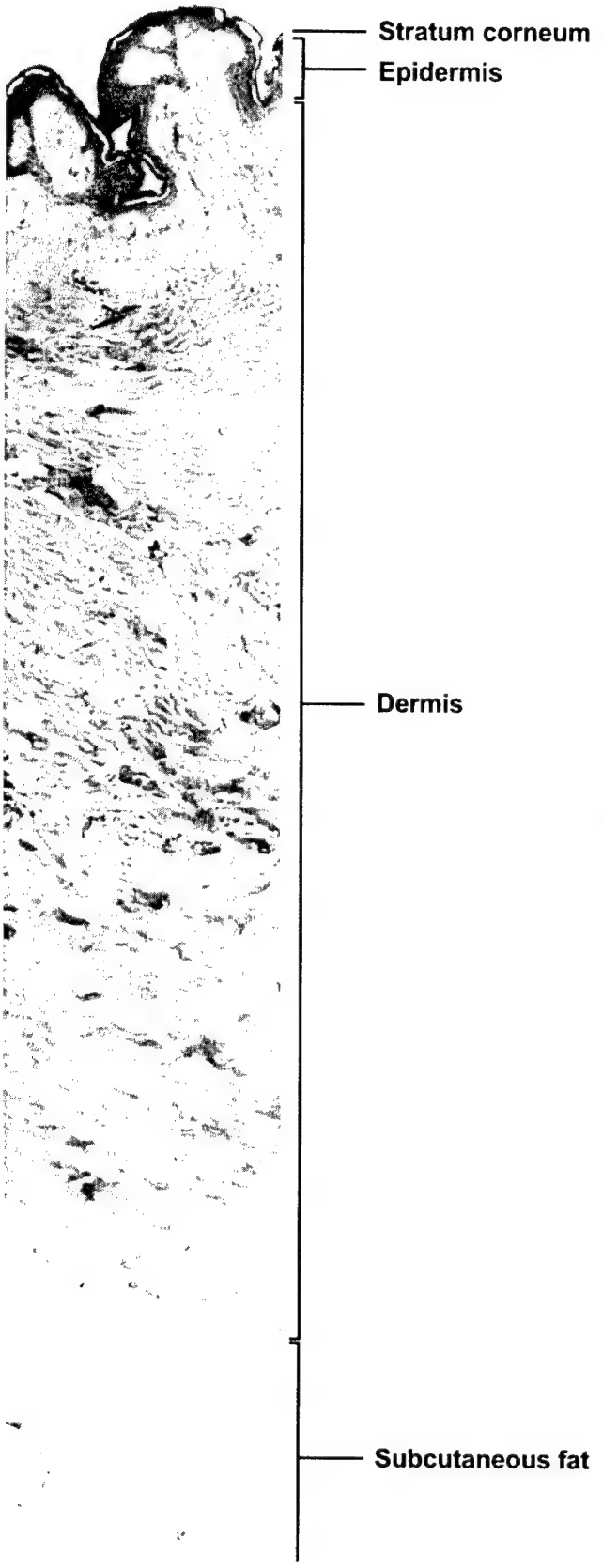

Fig. 2. Full-thickness histologic cross-section of human skin depicting the layers of interests in soft tissue augmentation. Hematoxylin and eosin stain.

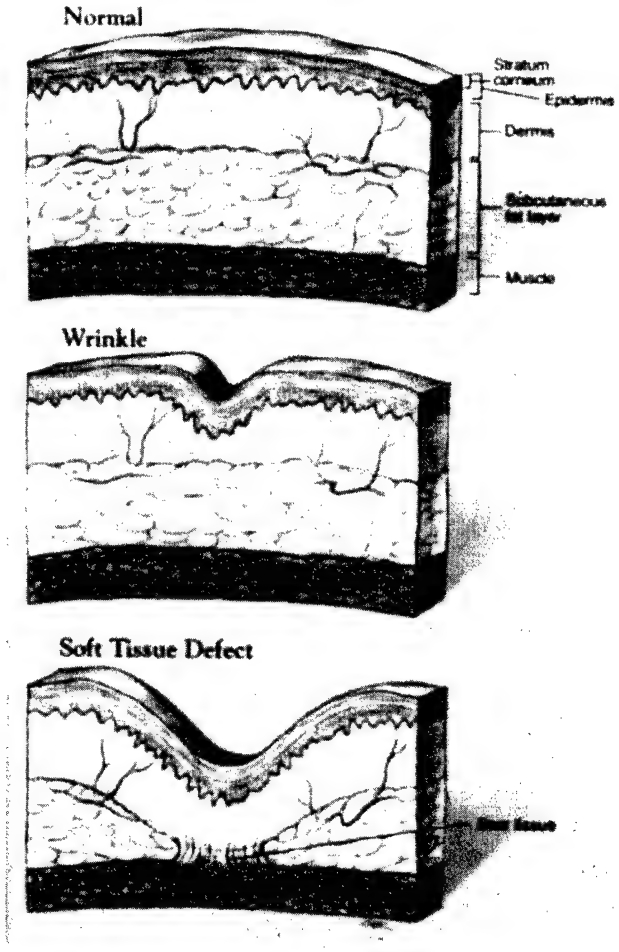

Fig. 3. Organizational differences between cross-section of normal skin and that of a wrinkle and a soft tissue defect. In a wrinkle, a deficit in the dermis causes a contour defect that is translated to the epidermis and stratum corneum. In a soft tissue defect, a tissue deficit occurs much deeper in the subcutaneous fat layer, causing a large contour defect that is translated to the dermis, epidermis, and stratum corneum. In addition, adhesion plaques form between the muscle and dermis.

restore both volume and function. However, this depends on preadipocytes adhering to appropriate support structures, or scaffolds. A support structure is required for anchorage-dependent cells to migrate and proliferate and to give a tissue equivalent the boundary conditions for final overall tissue shape. Scaffolds may either be implanted or injected.

Implantable materials used for adipose tissue engineering have predominantly been porous biodegradable polymer foams (Patrick et al., 1998a, 1999; Lee et al., 2000). For instance, poly (L-lactic-co-glycolic) acid (PLGA) scaffolds preseeded with preadipocytes have demonstrated adipose tissue formation (Patrick et al., 1999). Figure 1 demonstrates adipose tissue formation within PLGA scaffolds. However, polymer foams will probably not be the

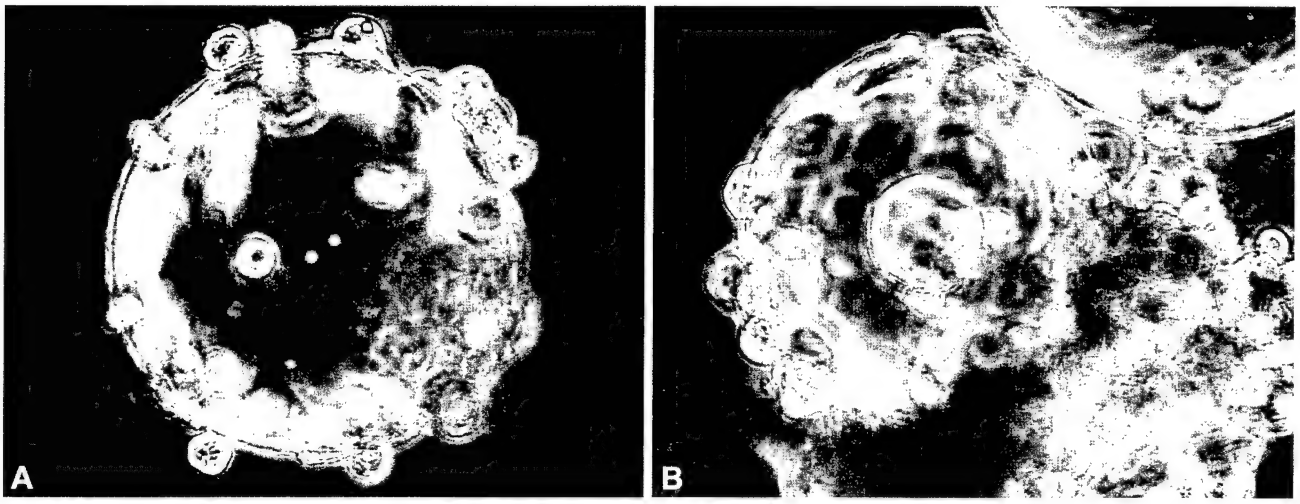

Fig. 4. **A:** Preadipocytes attached and differentiated on microcarrier beads within a stirred bioreactor. **B:** A lobule of adipose tissue is forming.

optimum choice for many applications as they are too rigid and would be uncomfortable for the patient. A more appropriate choice may be a biodegradable polymer felt that possesses draping qualities. Various polymer felts are currently being assessed in a joint venture between this author and Ethicon Endo-Surgery (data not shown). Nonbiodegradable scaffolds have also been investigated. For instance, Kral and Crandall recently demonstrated the attachment and proliferation of preadipocytes on fluorotex monofilament-expanded polytetrafluoroethylene scaffolds coated with various extracellular matrices (Kral and Crandall, 1999).

Injectable materials, such as hydrogels, inherently possess optimal mechanical properties for injection into soft tissue defects. In addition, injection techniques allow for the use of current medical technologies, abrogating the need to introduce new devices or retrain clinicians. Furthermore, hydrogel gelation can typically be controlled by means of temperature or chemical means. This allows cells to be homogeneously mixed in materials at a liquid state and then injected as a gel state. Both alginate and hyaluronic acid gels have been investigated (Duranti et al., 1998; Lee et al., 2000; Marler et al., 2000). In addition, we have shown that preadipocytes proliferate and differentiate within fibrin gels (data not shown).

The optimum scaffold for adipose tissue engineering remains elusive. Derivatizing polymers with adhesion molecules can potentially optimize scaffolds. In fact, Mooney and colleagues have derivatized alginate with RGD sequences and observed increased adipogenesis when injected in a rat model (Marler et al., 2000). Although short-term studies have demonstrated adipose formation within biodegradable polymers (Patrick et al., 1999), it remains to be determined whether the formed adipose tissue resorbs over long-term. We are currently involved in a year-long study to determine the sustainability of tissue engineered adipose tissue.

MICROENVIRONMENT

The microenvironment surrounding a tissue construct affects its differentiation and rate of tissue formation. Adipogenesis can be affected, in part, by growth factors (endo- and exogenous), pO_2 (normoxia vs. hypoxia), pH, adhesion molecules on extracellular matrices and support cells, and micromotion. Table 3 illustrates chemical factors that are reported to affect preadipocyte differentiation into adipocytes. Some factors (e.g. aFGF, bFGF, and PDGF) elicit conflicting actions because it has not been elucidated whether the factors affect preadipocyte differentiation directly or indirectly through angiogenesis. Kawaguchi et al. demonstrated de novo adipogenesis after injection of Matrigel and bFGF in mice (Kawaguchi et al., 1998). Yuksel and colleagues have used biodegradable microspheres loaded with insulin, bFGF, and IGF-1 to differentiate preadipocytes to mature adipocytes in vivo (Yuksel et al., 2000a,b). In addition, both EGF and TNF-α inhibit adipose differentiation (Serrero, 1987; Kras et al., 2000).

PROPOSED SOFT TISSUE AUGMENTATION STRATEGIES

Tissue engineering strategies for wrinkle and soft tissue augmentation involve restoration of localized subcutaneous defects that result in abnormal contour. Contour defects are primarily isolated to subcutaneous regions of the body and may occur in areas ranging from the epidermis to the adipose layer (Fig. 2). The restoration site for a wrinkle and soft tissue defect differ in anatomic location (Fig. 3). In a wrinkle, a deficit in the dermis causes a contour defect that is translated to the epidermis and stratum corneum. Hence, an adipose product would be injected or implanted between the dermis and epidermis by using contemporary injection techniques. In a soft tissue defect, a tissue deficit occurs much deeper in the subcutaneous fat layer, causing a large contour defect that is translated to the dermis, epidermis, and stratum corneum. In addition, adhesion plaques form between the muscle and dermis. Hence, an adipose product would be injected or implanted within the subcutaneous fat between the muscle and dermis. During the injection, the adhesion plaques would have to be cleaved. Obvious strategies include injecting hydrogels containing preadipocytes and adipogenic/angiogenic factors or implanting a thin, flexible fabric or felt composed of a biodegradable polymer

or polymer blend that can be preseeded with preadipocytes. The preadipocytes can be isolated from tissue harvested from a patient by means of liposuction or fat biopsy, followed by enzymatic digestion, and expansion ex vivo.

Another strategy being investigated involves injecting biodegradable polymer microspheres loaded with adipogenic/angiogenic factors and coated with preadipocytes. In essence, the microspheres will act as a cell carrier and drug delivery vehicle concomitantly. Figure 4 demonstrates preadipocytes cultured and differentiated on microcarrier beads within a continuously stirred bioreactor. The preadipocytes are able to attach to a spherical surface and withstand the low shear environment of the bioreactor. PLGA microspheres can be loaded with growth factors in diameters large enough for use as a cell carrier. We have demonstrated that the microspheres are able to provide a sustained release of vascular endothelial growth factor over a 21-day period (King and Patrick, 2000).

CONCLUSIONS

The field of tissue engineering offers great potential in abrogating limitations realized with standard of care for soft tissue augmentation after tumor resection and trauma. To be sure, great strides have already been achieved. However, the continued progress, and ultimately the clinical translation, of adipose tissue engineering will require the active, synergistic collaboration of bioengineers, life scientists, and clinicians. Only then will we truly be able to take advantage of technology and scientific knowledge to increase patient quality of life.

LITERATURE CITED

Coleman SR. 1995. Long-term survival of fat transplants: controlled demonstrations. Aesthetic Plast Surg 19:421–425.

Coleman SR. 1997. Facial recontouring with lipostructure. Clin Plast Surg 24:347–367.

Djian P, Roncari DAK, Hollenberg CH. 1983. Influence of anatomic site and age on the replication and differentiation of rat adipocyte precursors in culture. J Clin Invest 72:1200–1208.

Duranti F, Salti G, Bovani B, Calandra M, Rosati ML. 1998. Injectable hyaluronic acid gel for soft tissue augmentation. Dermatol Surg 24:1317–1325.

Entenmann G, Hauner H. 1996. Relationship between replication and differentiation in cultured human adipocyte precursor cells. Am J Physiol 270:C1011–C1016.

Hauner H, Entenmann G. 1991. Regional variation of adipose differentiation in cultured stromal-vascular cells from the abdominal and femoral adipose tissue of obese women. Int J Obes 15:121–126.

Hausman GJ, Richardson RL. 1998. Newly recruited and pre-existing preadipocytes in cultures of porcine stromal-vascular cells: morphology, expression of extracellular matrix components, and lipid accretion. Anim Sci 76:48–60.

Havlik RJ, Sian KU, Wagner JD, Binford R, Broadie TA. 1999. Breast cancer in Poland syndrome. Plast Reconstr Surg 104:180–182.

Katz AJ, Llull R, Hedrick MH, Futrell JW. 1999. Emerging approaches to engineering of fat. Clin Plast Surg 56:207–216.

Kawaguchi N, Toriyama K, Nicodemou-Lena E, Inou K, Torii S, Kitagawa Y. 1998. De novo adipogenesis in mice at the site of injection of basement membrane and basic fibroblast growth factor. Cell Biol 95:1062–1066.

Kearns CJ, Padwa BL, Mulliken JB, Kaban LB. 2000. Progression of facial assymetry in hemifacial microsomia. Plast Reconstr Surg 105:492–498.

King TW, Patrick CW Jr. 2000. Development and in vitro characterization of vascular endothelial growth factor (VEGF)-loaded poly(DL-lactic-co-glycolic acid)/poly(ethylene glycol) microspheres using a solid encapsulation/single emulsion/solvent extraction technique. J Biomed Mater Res 51:383–390.

Kirkland JL, Hollenberg CH, Kindler S, Gillon WS. 1994. Effects of age and anatomic site on preadipocyte number in rat fat depots. J Gerontol 49:B31–B35.

Kirkland JL, Hollenberg CH, Gillon WS. 1996. Effects of fat depot site on differentiation-dependent gene expression in rat preadipocytes. Int J Obes Relat Metabol Disord 20(Suppl 3):S102–S107.

Kral JG, Crandall DL. 1999. Development of a human adipocyte synthetic polymer scaffold. Plast Reconstr Surg 104:1732–1738.

Kras KM, Hausman DB, Martin RJ. 2000. Tumor necrosis factor-α stimulates cell proliferation in adipose tissue-derived stromal-vascular cell culture: promotion of adipose tissue expansion by paracrine growth factors. Obes Res 8:186–193.

Lanza RP, Langer R, Vacanti J. 2000. Principles of tissue engineering. San Diego: Academic Press.

Lee KY, Halberstadt CR, Holder WD, Mooney DJ. 2000. Breast reconstruction. In: Lanza RP, Langer R, Vacanti J, editors. Principles of tissue engineering. San Diego: Academic Press. p 409–423.

Loftus TM, Lane MD. 1997. Modulating the transcriptional control of adipogenesis. Curr Opin Genet Dev 7:603–608.

MacDougald OA, Lane MD. 1995. Transcriptional regulation of gene expression during adipocyte differentiation. Annu Rev Biochem 64:345–373.

Mandrup S, Lane MD. 1997. Regulating adipogenesis. J Biol Chem 272:5367–5370.

Marler JJ, Guha A, Rowley J, Koka R, Mooney D, Upton J, Vacanti JP. 2000. Soft-tissue augmentation with injectable alginate and syngeneic fibroblasts. Plast Reconstr Surg 105:2049–2058.

Nguyen A, Pasyk KA, Bouvier TN, Hassett CA, Argenta LC. 1990. Comparative study of survival of autologous adipose tissue taken and transplanted by different techniques. Plast Reconstr Surg 85: 378–386.

Novakofski JE. 1987. Primary cell culture of adipose tissue. In: Hausman GJ, Martin RJ, editors. Biology of the adipocyte: research approaches. New York: Van Nostrand Reinhold. p 160–197.

Patrick CW Jr. 2000. Adipose tissue engineering: the future of breast and soft tissue reconstruction following tumor resection. Surg Oncol 19:302–311.

Patrick CW Jr, Chauvin PB, Robb GL. 1998a. Tissue engineered adipose. In: Patrick CW Jr, Mikos AG, McIntire LV, editors. Frontiers in tissue engineering. Oxford: Elsevier Science. p 369–382.

Patrick CW Jr, Mikos AG, McIntire LV. 1998b. Frontiers in tissue engineering. Oxford: Elsevier Science.

Patrick CW Jr, Chauvin PB, Reece GP. 1999. Preadipocyte seeded PLGA scaffolds for adipose tissue engineering. Tissue Eng 5:139–151.

Patrick CW Jr, Wu X, Johnston C, Reece GP. Epithelial cell culture-breast. In: Atala A, Lanza R, editors. Methods in tissue engineering. San Diego: Academic Press (in press).

Robb GL, Miller MJ, Patrick CW. Breast tissue engineering. In: Atala A, Lanza R, editors. Methods in tissue engineering. San Diego: Academic Press (in press).

Serrero G. 1987. EGF inhibits the differentiation of adipocyte precursors in primary cultures. Biochem Biophys Res Commun 146:194–202.

Shillabeer G, Forden JM, Lau DCW. 1989. Induction of preadipocyte differentiation by mature fat cells in the rat. J Clin Invest 84:381–387.

Smahel J. 1986. Adipose tissue engineering in plastic surgery. Ann Plast Surg 16:444–452.

Strutt B, Khalil W, Killinger D. 1996. Growth and differentiation of human adipose stromal cells in culture. In: Jones GE, editor. Methods in molecular medicine: human cell culture protocols. Totowa, NJ: Human Press Inc. p 41–51.

Van RLR, Roncari DAK. 1977. Isolation of fat cell precursors from adult rat adipose tissue. Cell Tissue Res 181:197–203.

Yuksel E, Weinfeld AB, Cleek R, Wamsley S, Jensen J, Boutros S, Waugh JM, Shenaq SM, Spira M. 2000a. Increased free fat-graft survival with the long-term, local delivery of insulin, insulin-like growth factor-I, and basic fibroblast growth factor by PLGA/PEG microspheres. Plast Reconstr Surg 105:1712–1720.

Yuksel E, Weinfeld AB, Cleek R, Waugh JM, Jensen J, Boutros S, Shenaq SM, Spira M. 2000b. De novo adipose tissue generation through long-term, local delivery of insulin and insulin-like growth factor-1 by PLGA/PEG microspheres in an in vivo rat model: A novel concept and capability. Plast Reconstr Surg 105:1721–1729.

CHAPTER 10

EPITHELIAL CELL CULTURE: BREAST

Charles W. Patrick Jr., Xuemei Wu, Carol Johnston, and Greg P. Reece

INTRODUCTION

A breast is composed of many various tissue types, including blood vessels, adipose tissue, lymphatic vessels, connective tissue, and mammary glands. This chapter focuses on one tissue type, namely, adipose tissue. With advances in the molecular and cellular biology of adipose tissue, largely from the obesity and diabetes fields, and the maturation of tissue engineering, there has been a resurgence in the potential use of preadipocytes (adipogenic progenitor cells) in clinical strategies. Strategies under current investigation include soft tissue augmentation [1–4] and development of *de novo* breast [1,5] (also see Chapter 78 of this text). Preadipocytes are extremely attractive candidates for tissue engineering. Adipose tissue is uniquely expendable and abundant among most humans. Moreover, preadipocytes can easily be obtained from biopsied or excised fat and from minimally invasive liposuction aspirates. Unlike mature adipocytes, preadipocytes can withstand the mechanical trauma of aspiration and injection, as well as periods of ischemia. In addition, preadipocytes can be expanded into large numbers *ex vivo*, and the biological mechanisms dictating preadipocyte-to-adipocyte conversion are known and can be controlled [6–11].

This chapter describes the harvest, isolation, and *in vitro* culture of rat preadipocytes, as well as polymer seeding and histology of preadipocytes. Epididymal fat pads are utilized as the preadipocyte source, although other adipose tissue stores may be used. Implant integration, histogenesis, and the use of preadipocyte cell lines [12–19] are not discussed. Moreover, the influence of rat age and anatomic site on preadipocyte characteristics is not discussed [20–22]. All techniques can be scaled appropriately for other animal models and human tissue [23–31]. Moreover, the techniques utilize standard laboratory or easily obtainable equipment and supplies.

HARVEST AND ISOLATION OF PREADIPOCYTES

The following steps are required for harvest of epididymal fat pads from rats and isolation of preadipocytes from the fat pads. Steps 1–12 are conducted in an animal necroscopy facility, and steps 13–22 are conducted in a tissue culture facility. The presented procedures are in accordance with the guidelines of the American Association for Accreditation of Laboratory Animal Care (AAALAC) and the National Institutes of Health (NIH). Tables 10.1 and 10.2 list the materials, reagents, and solutions required.

1. Euthanize rat with CO_2.
2. Using electric clippers, shave the mid–lower abdomen.
3. Using Nair, a depilatory cream, completely remove the remaining hair per manufacturer's instructions.
4. Place the rat in supine position and stabilize the limbs (Fig. 10.1).
5. Scrub the harvest site with 70% ethanol.

Table 10.1. Preadipocyte Harvest and Isolation Reagents and Materials

Reagents	
Bovine serum albumin (BSA)	Sigma, St. Louis, MO
Ca^{2+}-, Mg^{2+}-free phosphate buffered saline (PBS)	
Collagenase, type IA	Sigma, St. Louis, MO
Dulbecco's Modified Eagle's Medium (DMEM)	
Fetal bovine serum (FBS)	Sigma, St. Louis, MO
Penicillin–streptomycin–glutamine (P/S/G), 100×	Gibco, Gaithersburg, MD
Materials	
0.22-μm Cellulose acetate syringe filter	Costar, Corning, NJ
250-μm Nylon mesh	Sigma, St. Louis, MO
40-μm Cell strainer	Falcon/Becton Dickinson, Franklin Lakes, NJ
50-ml Conical tube	Falcon/Becton Dickinson, Franklin Lakes, NJ
70% Ethanol wetted cotton balls	
Autoclaved, siliconized beaker	
Cell strainer	Sigma, St. Louis, MO
Electric clipper	
Iris scissors	ASSI, Westbury, NY
Mayo dissecting scissors	ASSI, Westbury, NY
Nair hair remover	
Tissue forceps (two required)	ASSI, Westbury, NY

6. Using dissecting scissors and tissue forceps, aseptically cut through the skin, muscle, and peritoneum along a midline Y-shaped incision, starting from the xiphoid cartilage of the sternum and down and along the inguinal regions of the lower body (Fig. 10.2).
7. Expose the abdominal cavity (Fig. 10.3).
8. Grasp and pull the epididymal adipose tissue (fat pad) with second pair of tissue forceps (Fig. 10.4).
9. Pull the epididymal fat pad until the testis is removed from scrotal sac (Fig. 10.5).
10. Using iris scissors, dissect the fat pad, taking care not to include the internal spermatic artery/vein and caput epididymis (Fig. 10.6).
11. Place harvested fat pad (Fig. 10.7) in a 50-ml conical tube filled with 4°C phosphate-buffered saline (PBS) supplemented with penicillin-streptomycin-glutamino (P/S/G) (Fig. 10.8).

Table 10.2. Preadipocyte Harvest and Isolation Solution Preparation

Complete DMEM (cDMEM) (per 500 ml)	350 ml DMEM 5 ml P/S/G 50 ml FBS
Digestion medium (per 2 fat pads)	4 ml 4°C PBS 3 mg/ml Collagenase 3 mg/ml BSA Sterilize through a 0.22-μm syringe filter
PBS with P/S/G	45 ml 4°C PBS 5 ml P/S/G

Fig. 10.1. Rat is in supine position, ventral view. Hair of the lower abdomen has been removed via shaving and depilatory cream. Posterior and anterior labels are included to denote rat's head-to-tail orientation.

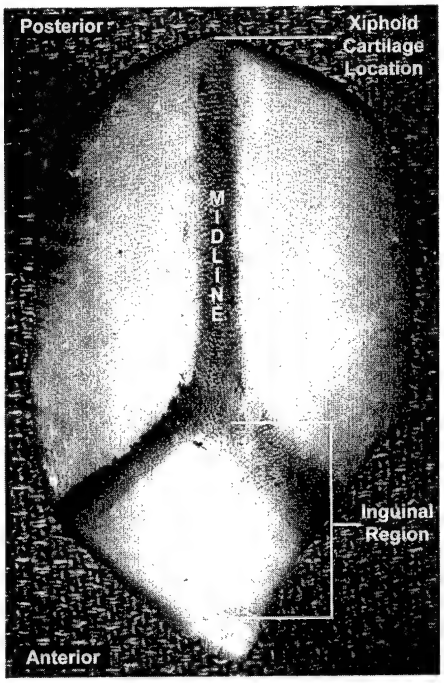

Fig. 10.2. Marking depicting incision to be made through skin, muscle, and peritoneum.

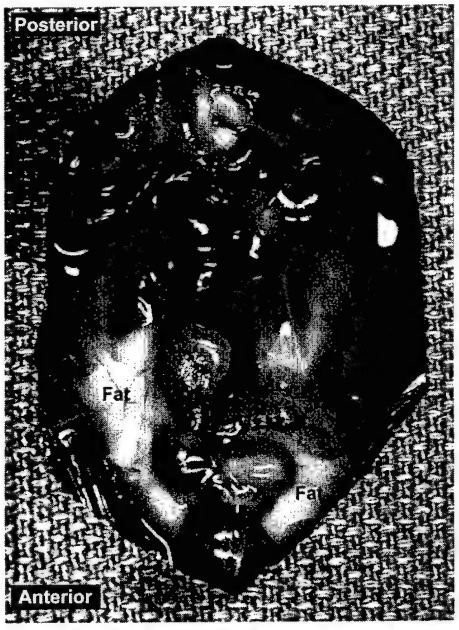

Fig. 10.3. Abdominal viscera in situ, ventral view.

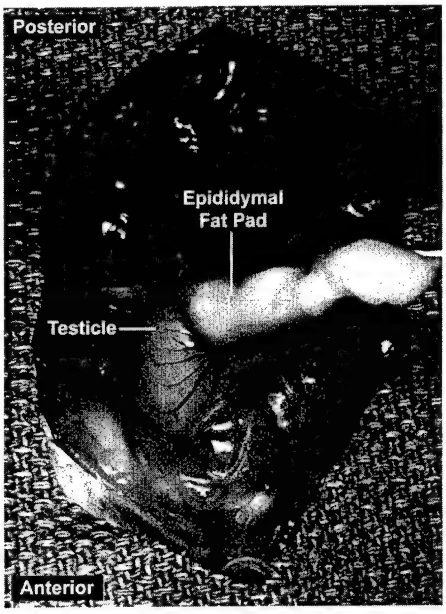

Fig. 10.4. Use of tissue forceps to remove epididymal fat pad.

12. Repeat steps 1–11 for the other epididymal fat pad.
13. Place the fat pads in a tissue culture dish in a biosafety cabinet and aseptically remove the large blood vessels (epididymal branch from internal spermatic artery/vein) and any hard tissue (portion of caput epididymis) with scissors and forceps. This minimizes fibroblast contamination of *ex vivo* cultures.
14. Finely mince the tissue with iris scissors.

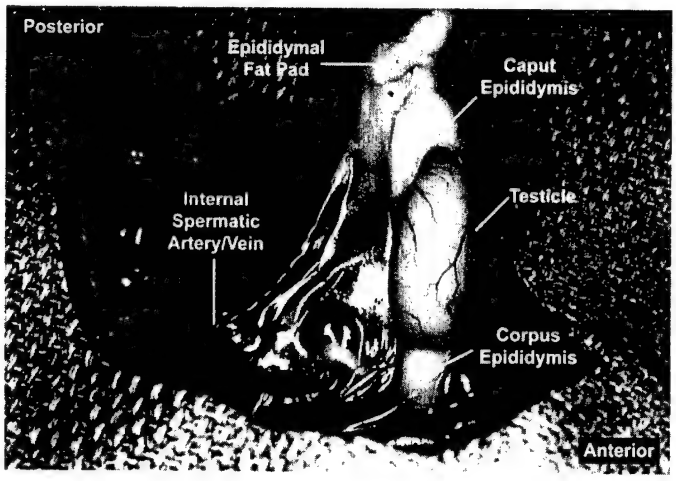

Fig. 10.5. View of epididymal fat pad and surrounding anatomy.

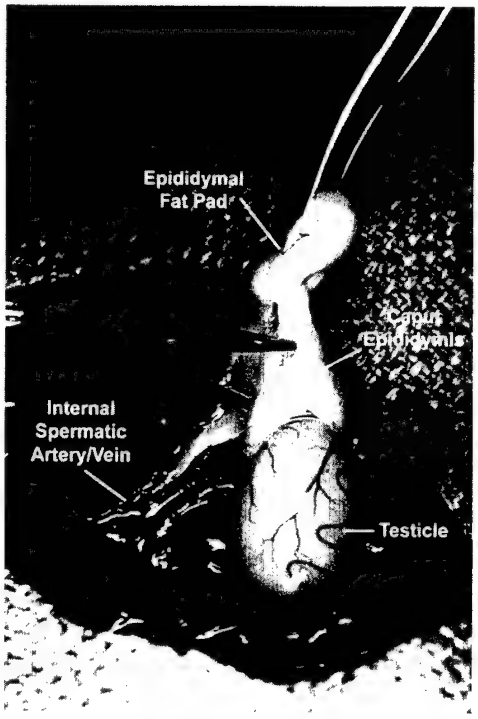

Fig. 10.6. Dissection of epididymal fat pad using iris scissors.

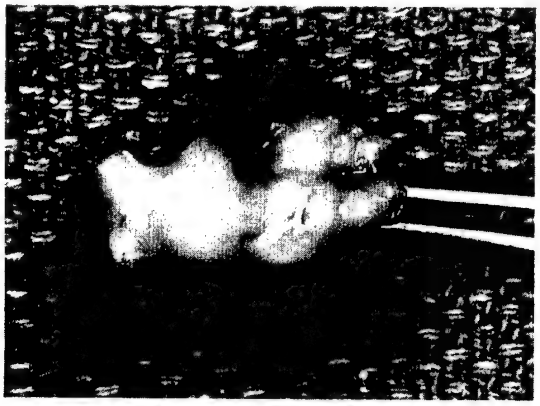

Fig. 10.7. Harvested epididymal fat pad.

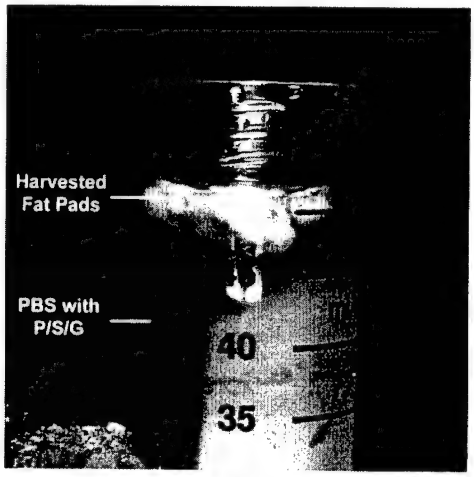

Fig. 10.8. Epididymal fat pads placed in PBS with antibiotics. The 50-ml conical tube is placed in an ice bath.

15. Place the minced tissue into a 50-ml conical tube with digestion medium and then on orbital shaker at a speed of 250 oscillations/min for 20 min at 37°C.
16. Filter the resulting slurry through a 250-μm nylon mesh into a siliconized beaker.
17. Filter the filtrate again through a 40-μm cell strainer into a 50-ml conical tube.
18. Centrifuge the final filtrate at 200*g* for 10 min at 4°C.
19. Aspirate the supernatant and resuspend the pellet (preadipocytes) in warm complete Dulbecco's Modified Eagle's Medium (cDMEM).
20. Seed the cells into a T75 tissue culture flask. The cell yield is approximately 10^6/ml.
21. Rinse and feed the cells with warm cDMEM after 24 h.
22. Feed the cells every 3 days.

CULTURE OF PREADIPOCYTES

Cells are passaged when the cell density is 90%. At this time, the cell number is approximately 10^7/ml. The preadipocytes are passed prior to confluency, since contact inhibition initiates adipocyte differentiation and ceases preadipocyte proliferation. Cells may be frozen, cold-stored, and thawed in accordance with routine cell culture procedures.

Preadipocytes initially possess a fibroblast-like morphology (Fig. 10.9A). Upon reaching confluency, preadipocytes begin to accumulate lipid pools within their cytoplasm (Fig. 10.9B). Lipid droplets continue to grow in volume and finally coalesce to form a unilocular lipid pool within the cell (Fig. 10.9C–F). At this point, a preadipocyte's cytoplasm is 80–90% lipid. Eventually, the lipid pools become buoyant enough to float mature adipocytes to the surface of the culture flask. The amount of lipid loading can be controlled in a dose-dependent manner by varying the amount of fetal bovine serum (FBS) in cDMEM. Ideally, preadipocytes are seeded into polymers prior to differentiation.

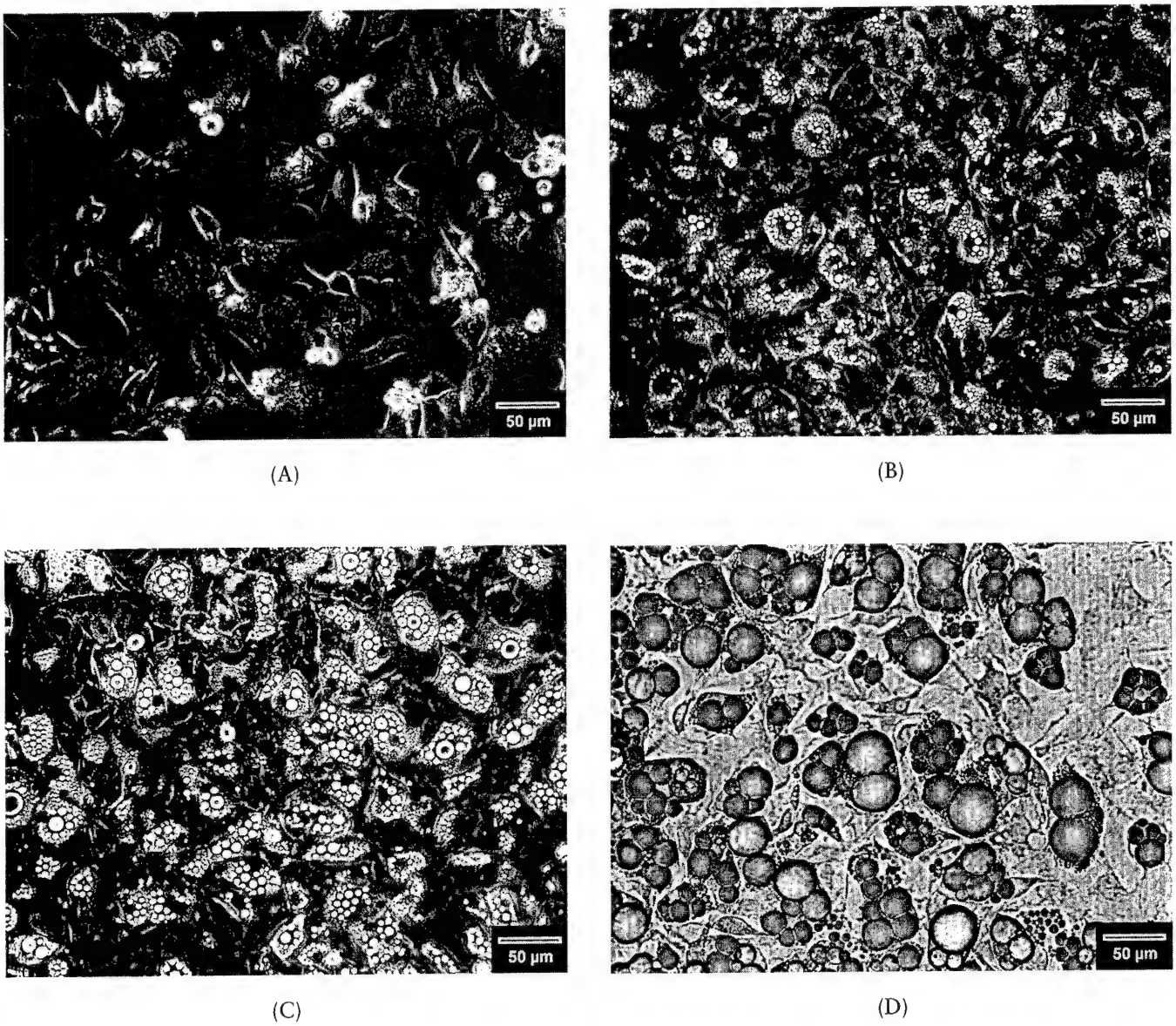

Fig. 10.9. Growth and differentiation of rat preadipocytes at five points postseeding: (A) 1 day, (B) 4 days, (C) 7 days, (D) 16 days, and (E) 22 days. Images (A)–(C) are phase contrast; images (D) and (E) are bright field. Note accumulation and coalescence of lipid pools as culture time progresses. (F) Image of unilocular lipid pool within a single preadipocyte. Bars denote 50 µm.

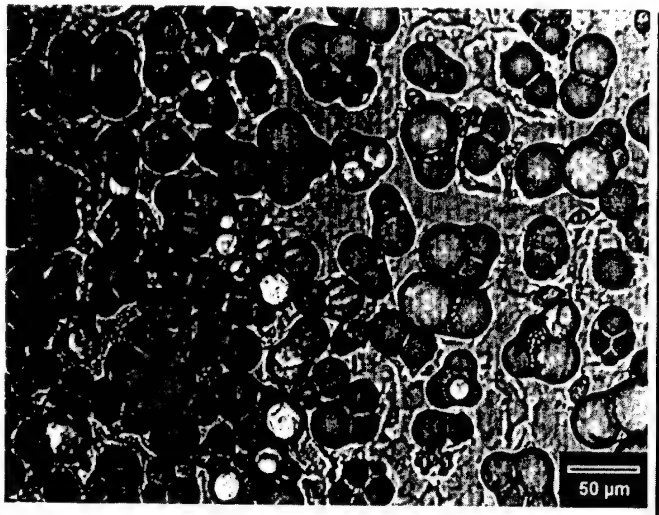

(E)

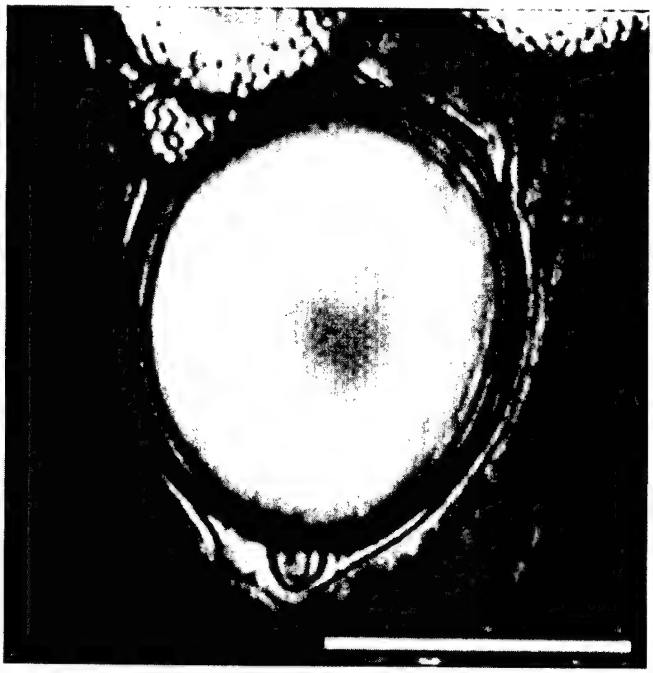

(F)

Fig. 10.9. (Continued).

POLYMER SEEDING

The following procedure for seeding poly(lactic-*co*-glycolic acid) (PLGA) polymer foams with preadipocytes [5] has proven successful with other biodegradable polymer foams and nonwoven fibers. Prior to seeding, foams are prewetted and sterilized with absolute ethanol for 30 min followed by two sterile saline washes at 20 min/wash and a DMEM wash for 20 min. A 20-µl suspension of preadipocytes (10^5 cells/mL) is injected onto each foam under sterile conditions. Prewetting permits the cell suspension to readily flow throughout the foam. Following 3 h for cell attachment, 24-well culture plates containing one foam/well are filled with 1.5 ml of medium per well. Foams are ready for implantation.

HISTOLOGY

Oil Red O

Adipocyte differentiation *in vitro* is routinely monitored by using oil red O staining for intracellular lipid pools [32] or phase contrast microscopy (lipid appears as phase bright, see Fig. 10.9A–C). The oil red O causes lipid pools to appear red under bright-field microscopy (labeled in Fig. 10.10). Tables 10.3 and 10.4 list the reagents and solutions required. Instructions are as follows.

1. Fix culture with 10% neutral buffer formalin.
2. Rinse with tap water.
3. Stain in oil red O for 10 min.
4. Wash with tap water.
5. Stain for 1 min in acidic Harris hematoxylin.
6. Wash with tap water.
7. Blue in ammonia water.
8. Wash with tap water.
9. Mount with an aqueous mounting medium or acquire pictures immediately. Results: fat, intense red; nuclei, blue.

Table 10.3. Oil Red O Reagents

Acetic acid	Fisher Scientific, Pittsburgh, PA
Ammonia hydroxide	Fisher Scientific, Pittsburgh, PA
Aqueous mounting media	Fisher Scientific, Pittsburgh, PA
Harris hematoxylin	Allegiance, McGaw Park, IL
2-Propanol, 98%	Fisher Scientific, Pittsburgh, PA
Neutral buffered formalin, 10%	Fisher Scientific, Pittsburgh, PA
Oil red O	Fisher Scientific, Pittsburgh, PA
Tap water	

Osmium Tetroxide

An osmium tetroxide (OsO_4) paraffin procedure is used to demonstrate fat within harvested *in vivo* polymer foams [33]. Routine staining outlines only "ghost" cells, since histological processing with organic solvents and alcohols extracts lipid from cells. The OsO_4 chemically combines with fat, blackening it in the process. Fat that combines OsO_4 is insoluble in alcohol and xylene, and the tissue can be processed for paraffin embedding and counterstained. Small fat droplets and individual cells are well demonstrated via this method, whereas gross amounts of fat are not fixed by this diffusion-dependent stain (Fig. 10.11). After staining with OsO_4, foams are processed for paraffin embedding using standard procedures, except that HistoSolve (Shandon Lipshaw), a xylene substitute, is used instead of xylene. Xylene dissolves many biodegradable polymers. Infiltrated foams are cut and oriented in embedding cassettes. Sections 6 μm thick are cut with a microtome (Leica, Wetzlar, Germany), placed on slides, stained with hematoxylin–eosin (H&E), and coverslipped. Sections are analyzed by means of bright-field microscopy (Fig. 10.11). Table 10.5 lists the materials and reagents required. Instructions are as follows.

1. Harvest polymer foams at the appropriate time from rats.
2. Place harvested foams directly in a vial containing 10 ml of 10% formalin and fix overnight at room temperature.
3. After 24 h, remove specimen from formalin and trim. If cross sections are desired, a small piece of the foam to be embedded in cross section is removed at this time.
4. Transfer specimens to individual embedding cassettes that have been appropriately labeled with a pencil.
5. Place all cassettes in a beaker under freely running tap water and wash for 1 h.
6. Wash for 1 h in freely running distilled water.

Table 10.4. Oil Red O Solution Preparation

Acidic Harris hematoxylin	48 ml Harris hematoxylin 2 ml Acetic acid
Ammonia water	3 ml Ammonia hydroxide 1000 ml water
Oil red O stock solution	2.5 g oil red O 500 ml 2-Propanol Mix well
Oil red O working solution	24 ml oil red O stock solution 16 ml Distilled water Mix well and let stand for 10 min. Filter. The filtrate can be used for several hours

CHAPTER 78

BREAST RECONSTRUCTION

Geoffrey L. Robb, Michael J. Miller, and Charles W. Patrick Jr.

INTRODUCTION

Breast cancer continues to be the most common cancer among women, other than cancers of the skin, with an incidence of nearly one of every three cancers occurring in American women. Approximately one in nine women in this country will develop breast cancer by 85 years of age. The United States has the highest incidence of breast cancer in the world, with 110.6 cases per 100,000 women. In the year 2000, roughly 182,800 new cases of invasive breast cancer were diagnosed.

From a surgical therapeutic perspective, 69,683 women underwent breast reconstruction in 1998, a 135% increase since 1992. This represents 3.1% of all plastic surgery procedures for that year. The majority of patients, 49%, were in the 35- to 50-year-old age group, while 36% were in the 51- to 64-year-old age group. Thirty-nine percent of the reconstructions were performed at the same time as the mastectomy, which represents the immediate use of both implants in 46% of patients as well as autogenous tissues in 37% of patients for breast reconstruction [1].

These statistics underscore the growing importance of cancer rehabilitation in the form of breast reconstruction for women affected by breast cancer in all age groups. As opposed to being an issue of mere vanity, restoration of the breast form and contour is valued for the necessary maintenance of self-esteem and body image. Even limited excisions of the breast for the eradication of cancer can produce permanent breast deformities and breast asymmetry. The relevant importance of this "woman's issue" was recently supported by the passage by both houses of Congress of the Omnibus Budget Bill. In this bill, insurance companies are required not only to underwrite reconstructive breast surgery following cancer treatment, but also to cover the additional procedures necessary to maintain symmetry with the opposite normal breast. There is a clear ethical and personal mandate to support the reconstruction of breast deformity, whether congenital, secondary to trauma, or, in particular, following cancer treatment.

TYPES OF BREAST RECONSTRUCTION

Plastic surgery for the breast may be broadly classified as either primarily reconstructive or aesthetic depending on the nature of the deformity. This distinction is primarily one of degree. Cosmetic procedures address deformities that are anatomically within normal limits but nevertheless present an appearance that is unsatisfactory to the patient. Aesthetic breast enlargement surgery, or augmentation mammaplasty, is one of the most common aesthetic procedures. Several hundred cubic centimeters of additional soft tissue or tissue equivalent may be required. Usually this is supplied by breast implants consisting of an envelope made of silicone elastomer filled with either saline solution or silicone gel. The ability to engineer additional fat would potentially eliminate the need for artificial breast implants. Reconstructive operations correct more extreme problems; however, they must still follow proper aesthetic principals. After all, the most sophisticated breast reconstruction that does not look like a normal breast will not be well accepted. Both reconstructive and aesthetic oper-

ations may require tissue replacement and therefore may be influenced by developments in tissue engineering.

Breast reconstruction is one of the most common reconstructive procedures. The usual indication is to restore the breast following complete removal (i.e., total mastectomy) performed for cancer treatment. It has been shown that women with breast cancer must deal with two separate emotional issues, the reality of a life-threatening disease and the possibility of losing a breast. Loss of the breast is not life-threatening, but many women find the deformity emotionally and psychologically disturbing [2]. A mastectomy causes a significant functional and cosmetic deformity, replacing the soft, projecting breast with a long, flat scar. The breast is a significant part of female body image and sense of femininity. The patient is reminded of her cancer experience every time she looks in a mirror. It can be difficult to find clothing. For some women, an external prosthesis may be satisfactory, but many find such devices cumbersome and unacceptable. Breast reconstruction is intended to overcome these problems and enhance the quality of life for women following mastectomy for breast cancer. The structure of the female breast consists of a container made of skin filled with soft glandular and fatty tissue.

Postmastectomy breast reconstruction involves replacing missing skin and soft-tissue volume to recreate the appearance of the breast. Current methods rely on breast implants [3], soft-tissue flaps [4], or a combination of these [5]. Each technique offers certain advantages depending on the patient. Reconstruction based primarily on artificial devices uses a process known as tissue expansion to create additional skin. This involves placing an inflatable silicone device called a tissue expander beneath the tissues. The expander is gradually inflated with physiological saline solution injected over several weeks. When the expansion is complete, the device is removed and the tissue is ready to use. This process has been shown to increase the amount of tissue and improve the blood supply. It requires up to 6 months to complete. The tissue expander is then replaced with a permanent implant to provide the necessary volume for the completed reconstruction.

Autologous tissue reconstruction is most often performed by means of skin and fat obtained from the lower anterior abdominal wall as a flap, called a transverse rectus abdominis musculocutaneous (TRAM) flap (Fig. 78.1). The tissue may be transferred by either keeping the rectus abdominis muscle attached superiorly or by performing a microvascular transfer [6]. The skin and fat may then be shaped to simulate the appearance of the breast. The tissue is a similar in consistency to breast tissue and provides a reconstructed breast that looks and feels the most natural. The transverse scar at the donor site, located midway between the umbilicus and the pubic area, is easily hidden by clothing. When there is inadequate tissue on the lower abdomen, the procedure can be combined with placement of a breast implant. In such cases, tissue may be harvested from either the back or the abdomen. If tissue is used, however, the results tend to be more natural and long-lasting. The disadvantages of these operations are that they are more time-consuming, have greater risks, and cause more scarring than other techniques.

There are advantages minimizing dependence on permanent breast implants for breast reconstruction. Implants can erode through the skin, become infected, and form deforming scars. They are more difficult to control during the shaping and contouring and can create unnatural surface contours over time. Breast implants are not a good option in patients who have been treated with radiation because of a tendency for firm scars to form around the implant. Reconstruction based entirely on tissue avoids these problems, but requires surgery other sites on the patient, resulting in alteration of normal areas. It is the opportunity to achieve a natural tissue reconstruction without donor site problems that provides the incentive to develop fat-tissue approaches to breast reconstruction. A tissue-engineered soft-tissue alternative would have wide application in postmastectomy breast reconstruction.

SURGICAL PRINCIPLES AND TISSUE ENGINEERING

To envision how tissue engineering methods might be applied to breast reconstruction, it is helpful to consider some surgical principles. The use of tissue in reconstructive surgery involves a two-step process of *transfer* from an uninjured location (donor site) and *modification* to replace or simulate the breast tissue that which has been lost (Fig. 78.1).

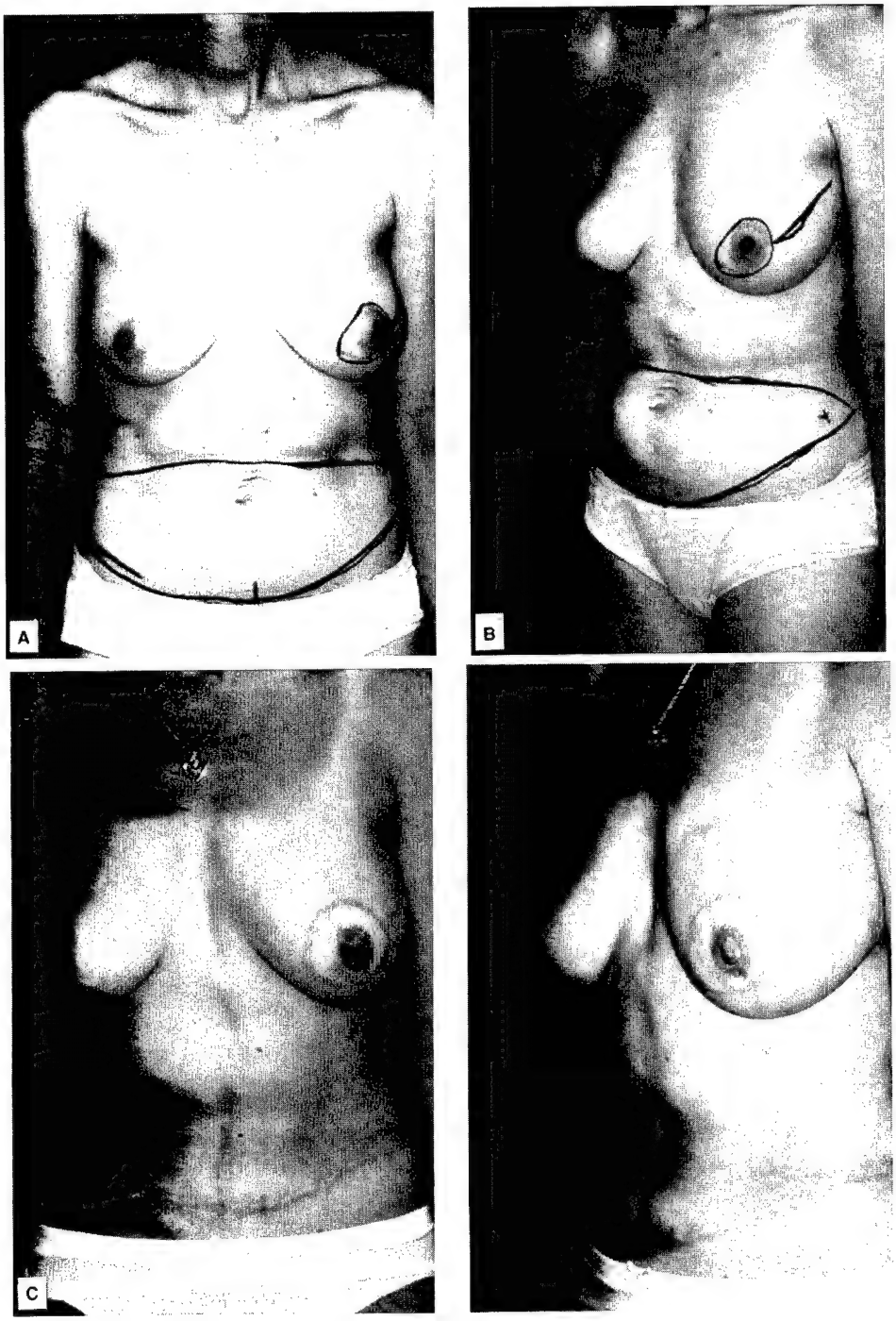

Fig. 78.1. (A) Preoperative skin-sparing mastectomy utilizing larger TRAM flap design owing to midline lower abdominal scar; (B) preoperative free TRAM reconstruction using skin-sparing mastectomy; (C) postoperative free TRAM reconstruction, nipple–areolar reconstruction completed; and (D) postoperative free TRAM reconstruction.

Tissue Transfer

Tissue transfer methods may be classified as either tissue grafts or flaps. A graft is any tissue transferred without its blood supply. Graft healing depends upon nutritive support passively available in the tissues surrounding the defect. Small amounts of skin, dermis, and fat may be transferred in this way. In breast reconstruction, these tissues are autologous, or obtained from an uninjured location on the same patient. The volume of tissue required for breast reconstruction is sufficiently large that it cannot survive transfer as a graft.

When a large amount of tissue is required, it must be transferred with a blood supply that originates from outside the zone of injury. This is the definition of a surgical "flap," the traditional term for a unit of tissue moved to another location with preservation of its blood supply. Tissue transferred as flaps may be moved into a compromised area because they will not depend on the ability of the surrounding tissues to supply nutritive support. A variety of surgical flaps have been described that provide skin and fat suitable for breast reconstruction. The most common, however, is located on the lower abdomen. The blood supply to this area passes through the rectus abdominis muscle. It is therefore possible to move the skin and fat of the lower abdomen to the chest for breast reconstruction, using the rectus muscle as a conduit for the blood supply. The most advanced transfer technique is a microvascular transfer. This method involves isolating the tissue unit on its primary vascular supply and temporarily dividing the blood vessels, cutting it "free" from the patient. Tissues transferred in this way are often called "free flaps." The vessels supplying the flap, usually 1–3 mm in diameter, are sewn with extremely fine suture materials to other vessels near the defect; the surgoon is aided by an operating microscope. Usually, two microvascular anastomoses are required, one for the artery and one for the vein. Skin and fat transferred in this way heal in the normal way with little contracture or loss of substance. Most of the history of plastic surgery consists of advances in techniques to transfer tissue.

Tissue Modification

Tissue modification is the second step of the reconstruction. After transfer, tissues must be reshaped to simulate missing structures. In contrast to tissue transfer techniques, tissue modification methods have changed little through the centuries. Surgeons still learn to manually alter tissues at the time of surgery, an often difficult and time-consuming process. The results are never exact. Original breast is approximated to a degree that varies depending on the nature of the tissues and the personal skill of the surgeon. The primary factor limiting these methods is the need to preserve adequate blood supply to all portions of the tissue. Efforts to overcome these limitations have focused improving the blood supply and "prefabricating" structures prior to transfer [7–14].

More elaborate methods of tissue modification leading up to tissue engineering have been described experimentally and used in selected patients. As early as 1963, attempts were made to revascularize tissues by direct transfer of blood vessels [15–17]. These techniques are based upon rearranging mature tissue elements into useful configurations prior to transfer. Even more advanced than simple rearrangement is direct modification of the tissue elements by using implants and induction factors to mold and transform. Hollow molding chambers made from inert titanium or silicone have been used in laboratory animals to create tissue flaps of different shapes [18,19]. Khouri *et al.* added a potent growth factor to control the differentiation of soft tissue inside molding chambers placed inside laboratory animals [20]. Despite these laboratory studies that demonstrate the feasibility of fabricating surgical flaps into different shapes, clinically useful techniques have yet to emerge. Only small amounts of tissue have been produced, and the proper shape has not been retained after removal of the mold.

The goal of tissue engineering is to improve our ability to modify tissues by shifting from working with whole tissues to more fundamental levels. From a surgeon's viewpoint, tissue engineering is modification of existing tissues at the cellular or molecular level to fabricate new tissues for reconstructive surgery.

TISSUE ENGINEERED BREAST EQUIVALENT

Preface

The application of tissue engineering to breast fabrication is a relatively new effort. The following sections give an overview of the state of the art and the preliminary attempts in this new venue of tissue engineering. The guiding concept is to develop a vascular construct to restore the breast mound and provide optimum cosmesis such that the limitations with tissue transfer and breast implants are abrogated. Strategies for developing tissue constructs within the breast envelope and *ex vivo* followed by subsequent implantation into the breast envelope are being investigated [21–24]. Restoring functional aspects of the breast, such

as lactation and tactile stimulation, are beyond the scope of current strategies. However, investigators have utilized tissue engineering strategies for nipple reconstruction [25].

To be sure, the development of a breast equivalent is particularly challenging. Unlike most other tissues and organs, breast tissue is highly variable among patients with respect to volume, composition, shape, soft-tissue biomechanics, ethnicity, age, and hormonal environment (i.e., pre-/postmenopause, pregnancy). Moreover, the final aesthetic outcome of a breast strongly affects the emotional well-being of a patient. In addition, breast aesthetics truly follow the platitude "beauty is in the eye of the beholder," and patient expectations often overrule a surgeon's concept of the individual's optimum breast.

Tissue engineering modalities can be segregated into four fundamental components, namely, cells, scaffold, microenvironment, and elucidation of patient-specific design parameters. Each is discussed here under the aegis of breast tissue engineering.

Cells for a Breast Equivalent

Adipose

A breast largely consists of adipose tissue setting in the skin envelope against the pectoral muscles of the chest wall. Naturally, the development of a tissue equivalent for breast restoration has focused on human adipose tissue. Adipose tissue is ubiquitous, the largest tissue in the body, uniquely expendable, and most patients possess excess that can be harvested without creating contour deformities. Autologous fat transplantation gives poor results, with 40–60% reduction in graft volume [22,26,27]. The reduction in adipose volume is postulated to be related to insufficient revascularization. The advent of liposuction led investigators to attempt using single-cell suspensions of mature adipocytes. However, since adipocytes possess a cytoplasm composed of 80–90% lipid, they readily tend, upon aspiration, to be traumatized by the mechanical forces of liposuction, resulting in about 90% damaged cells. The remaining 10% tend to form cysts or localized necrosis postinjection. Moreover, mature adipocytes cannot be expanded *ex vivo* because they are terminally differentiated.

Recent progress has been made by using preadipocytes, precursor cells that differentiate into mature adipocytes. Preadipocytes are fibroblast-like cells that uptake lipid during differentiation (see Chapter 10). They grow easily with standard cell culture technologies, they can be expanded *ex vivo*, and the molecular biology involved in differentiation has largely been elucidated through research in the obesity and diabetes areas [28,29]. However, much of the application-based biology of preadipocytes remains unknown (e.g., cell adhesion, cell motility, response to various microenvironments). Human, rat, and swine preadipocytes have been routinely cultured [30–35]. Preadipocytes are normally isolated from enzyme-digested adipose tissue or liposuction material [22]. Alternatively, adipocyte stem cells may potentially allow one to develop cultures of preadipocytes. Researchers are predominantly focusing on using subcutaneous preadipocytes for tissue engineering strategies. It is known that fat depots at different anatomical locations behave differently [36–39]. Hence, it remains to be seen if subcutaneous preadipocytes can adequately replace mammary adipose.

Microvascular Network

Any potential clinically translatable tissue engineering modality must consider the microvasculature. Adipose tissue is unique in that it has the capacity to continue to grow and its vascular network grows in tandem (i.e., *de novo* angiogenesis) [40]. Adipose tissue is highly vascular. The capillary density of adipose is approximately one-third that of muscle. However, from a metabolism standpoint and correcting for active protoplasm (i.e., since an adipocyte is largely lipid within its cytoplasm) the capillary bed of adipose is far richer (~ two or three times) than that of muscle. Adipose tissue is also known to enhance angiogenesis through the secretion of growth factors extracellular matrices (ECMs) [41–43].

Of the three biological mechanisms available to vascularize a tissue equivalent, only two are available to adults, namely, revascularization and inosculation. Revascularization denotes the growth of capillaries from a host site or tissue into a tissue equivalent. Except for relatively thin constructs, which can survive by diffusion, the slow kinetics (on the order of weeks) of this process typically abrogates it use for large constructs. It has

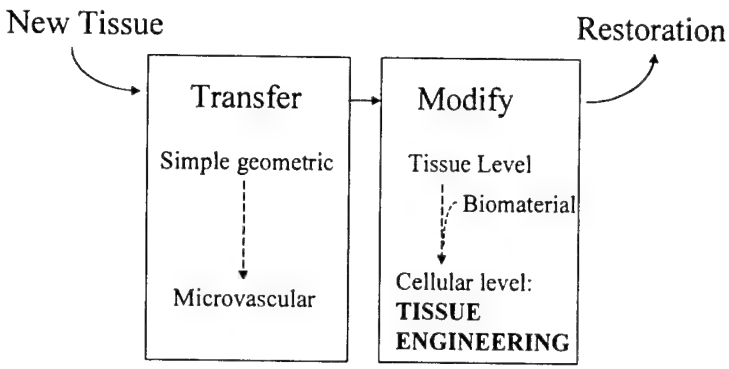

Fig. 78.2. Tissue engineering viewed in the context of the process of reconstructive surgery may be considered an advance in the step of tissue modification.

been proposed to use the highly vascular and adipocyte-rich omentum to encase constructs [44–46]. Inosculation is the process of two capillaries or capillary networks fusing together. The kinetics of inosculation occurs on the order of hours and is the predominant factor that allows plastic surgeons to transfer tissue from a donor site to a recipient site. The capillary networks of the recipient site and the graft fuse together, thus forming a patent vascular network throughout the graft. The use of inosculation in a tissue engineering strategy requires either the seeding of microvascular endothelial cells into or the *ex vivo* or *in situ* development of capillary networks within a tissue equivalent. Both modalities are being investigated but are currently hindered by the lack of understanding of the biological mechanisms that control inosculation and of understanding of capillary formation and cell culture technology of microvascular endothelial cells. Knowledge gained by using vein- or artery-derived endothelial cells cannot be directly translated to capillary endothelial cells.

Scaffolds

A support structure is required for anchorage-dependent cells to migrate and proliferate and to give a tissue equivalent the boundary conditions for final overall tissue shape. Implantable materials utilized have predominantly been porous biodegradable polymer foams [21–23]. For instance, poly(actic-*co*-glycolic acid) (PLGA) scaffolds preseeded with preadipocytes have demonstrated adipose tissue formation [21]. Polymer foams, however, will probably not be the optimum choice for breast scaffolds: they are too rigid for the breast envelope and would be uncomfortable for the patient. In 1999 Kral and Crandall used a non biodegradable scaffold to demonstrate the attachment and proliferation of preadipocytes on Fluorotex monofilament-expanded poly(tetrafluoroethylene) scaffolds coated with various ECMs [47]. Injectable materials, such as hydrogels, inherently possess optimum properties for use in the breast envelope. Both alginate and hyaluronic acid gels have been investigated [23,48,49]. In addition, preadipocytes successfully proliferated and differentiated within fibrin gels.

Finally, adjustable implants have been proposed. Vacanti and colleagues have conceptualized serial injections of a cell-seeded hydrogel within a tissue expander device, with the tissue expander being decreased in size each time an injection is conducted [50]. The optimum scaffold for breast tissue engineering remains elusive. Derivatizing polymers with adhesion molecules can potentially optimize scaffolds. However, this strategy is complicated by the variation of the constitution and distribution of the ECM during adipocyte differentiation [51]. Although short-term studies have demonstrated adipose formation within biodegradable polymers, it remains to be determined whether the formed adipose tissue resorbs over the long term. Investigators are involved in a year-long study to determine the sustainability of tissue engineered adipose [C. W. Patrick, Jr., unpublished data].

Adipose Microenvironment

The microenvironment surrounding a tissue construct affects its differentiation and rate of tissue formation. Adipogenesis can be affected, in part, by growth factors (endogenous and exogenous), pO_2 (normoxia vs hypoxia), pH, adhesion molecule on ECM and support cells, and micromotion. Kawaguchi *et al.* demonstrated *de novo* adipogenesis following in-

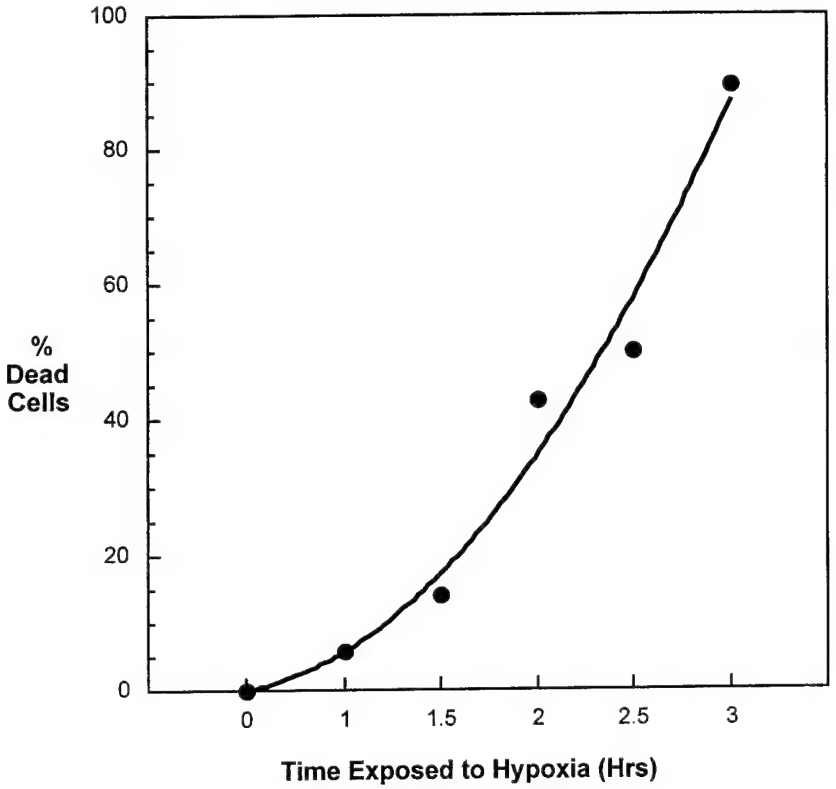

Fig. 78.3. Viability of rat preadipocytes exposed to a hypoxic environment (0% O_2).

jection of Matrigel and basic fibroblast-like growth factor (bFGF) in mice [52]. Yuksel and colleagues have used biodegradable microspheres loaded with insulin, bFGF, and insulin-like growth factor 1 to differentiate preadipocytes to mature adipocytes *in vivo* [53,54]. In addition, both epidermal growth factor and tumor necrosis factor α inhibit adipose differentiation [55,56]. Preadipocytes are extremely sensitive to hypoxic environments (Fig. 78.3). This is not surprising based on the historical results of free fat grafting. It is a major design constraint, however, insofar as it limits the time preadipocytes can be placed in a breast envelope without an adequate microvascular network. In contrast, microvascular endothelial cells have been shown to survive hypoxic conditions for 5–7 days.

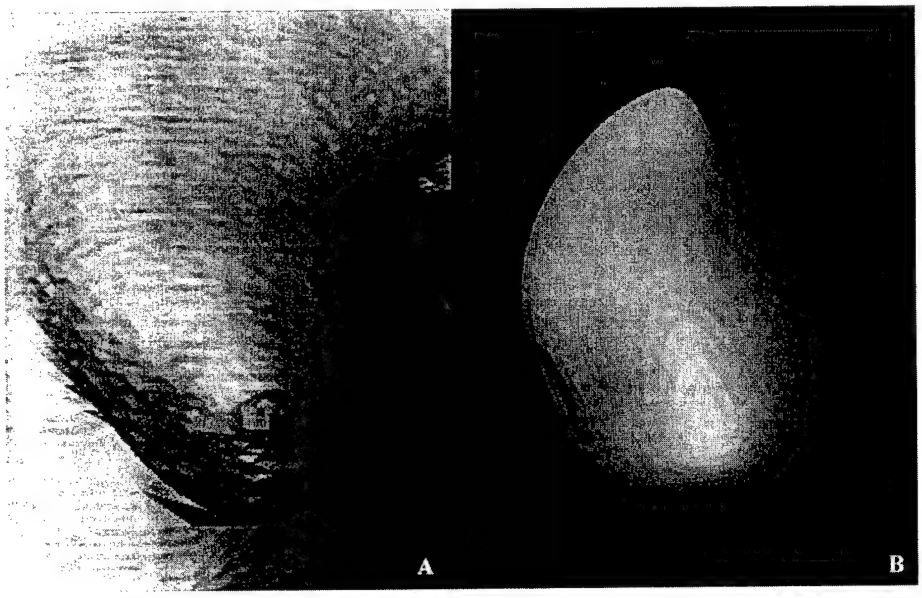

Fig. 78.4. Virtual reality breast simulator. (A) Range data of a patient's breast (three-dimensional surface scan). (B) Fitted virtual breast model, resulting in a volume of 987 ml and surface area of 453 cm^2.

Patient-Specific Design Parameters

To be truly clinically translatable a breast tissue engineering strategy must be patient specific. Unlike strategies for organs that can largely be grown as "one size fits all," breast shape and volume vary widely among the patient population. Breast implants, for instance, range from 100 ml to 2 liters. Hence, methods must exist to predetermine design parameters preoperatively such that the final outcome is known *a priori*. To accomplish this goal, bioengineers, physicians, and computer scientists have combined skill sets to develop a virtual reality breast simulator. A first-generation VR model of the female breast has been developed (Fig. 78.4) The system uses a global parametric deformable model of an ideal breast and allows the surgeon to manipulate the shape of the breast by varying five key shape variables, analogous to the aesthetic and structural elements surgeons inherently vary manually during breast reconstruction. The variables are ptosis (sagging of the breast), top-shape (top's concavity/convexity), turn-top (orientation of top half of the breast with respect to the shoulders), flatten-side (side's concavity/convexity), and turn (deflection of nipple orientation from a perpendicular axis originating at the chest wall). The second generation of the VR model is being developed to be patient specific by importing three-dimensional measurements of the surface of a patient's breast obtained via surface scanning.

References

1. Robb, G. L. (2000). Breast reconstruction. Internet Site: YourDoctor.com.
2. Gilboa, D., Borenstein, A., Floro, S., *et al.* (1990). Emotional and psychological adjustment of women to breast reconstruction and detection of subgroups at risk for psychological morbidity. *Ann. Plast. Surg.* **25**, 397–401.
3. Cohen, B. E., Casso, D., and Whetstone, M. (1992). Analysis of risks and aesthetics in a consecutive series of tissue expansion breast reconstructions. *Plast. Reconstr. Surg.* **89**, 840–843.
4. Bostwick, J., and Jones, G. (1994). Why I choose autogenous tissue in breast reconstruction. *Clin. Plast. Surg.* **21**, 165.
5. Fisher, J., and Hammond, D. (1994). The combination of expanders with autogenous tissue in breast reconstruction. *Clin. Plast. Surg.* **21**, 309.
6. Schusterman, M. A., Kroll, S. S., and Weldon, M. E. (1992). Immediate breast reconstruction: Why the free TRAM over the conventional TRAM? *Plast. Reconstr. Surg.* **90**, 255–261.
7. Özgenta, H. E., Shenaq, S., and Spira, M. (1995). Prefabrication of a secondary TRAM flap. *Plast. Reconstr. Surg.* **95**, 441–449.
8. Itoh, Y. (1992). An experimental study of prefabricated flaps using silicone sheets, with reference to the vascular patternization process. *Ann. Plast. Surg.* **28**, 140–146.
9. Mulliken, J. B., and Glowacki, J. (1980). Induced osteogenesis for repair and construction in the craniofacial region. *Plast. Reconstr. Surg.* **65**, 553–560.
10. Hirase, Y., Valauri, F. A., and Buncke, H. J. (1988). Prefabricated sensate myocutaneous and osteomyocutaneous free flaps: An experimental model. Preliminary report. *Plast. Reconstr. Surg.* **82**, 440–445.
11. Stark, G. B., Hong, C., and Futrell, J. W. (1987). Enhanced neovascularization of rat tubed pedicle flaps with low perfusion of the wound margin. *Plast. Reconstr. Surg.* **80**, 814–824.
12. Hussl, H., Russell, R. C., Zook, E. G., and Eriksson, E. (1986). Experimental evaluation of tissue Revascularization using a transferred muscular–vascular pedicle. *Ann. Plast. Surg.* **17**, 299–305.
13. Hyakusoku, H., Okubo, M., Umeda, T. A., and Fumiiri, M. (1987). A prefabricated hair-bearing island flap for lip reconstruction. *Br. J. Plast. Surg.* **40**, 37–39.
14. Khouri, R. K., Tark, K. C., and Shaw, W. W. (1992). Prefabrication of flaps using an arteriovenous bundle and angiogenesis factors. *Surg. Forum* pp. 597–599.
15. Dickerson, R. C., and Duthie, R. B. (1963). The diversion of arterial blood flow to bone. *J. Bone J. Surg. Am. Vol.* **45A**, 356.
16. Woodhouse, C. F. (1963). The transplantation of patent arteries into bone. *J. Int. Coll. Surg.* **39**, 437.
17. Orticochea, M. (1971). A new method for total reconstruction on the nose: The ears of donor areas. *Br. J. Plast. Surg.* **24**, 225.
18. Albrektsson, T., Branemark, P. A., Erikson, A., and Lindstrom, J. (1978). The preformed autologous bone graft. An experimental study in the rabbit. *Scand. J. Plast. Reconstr. Surg.* **12**, 215–223.
19. Fisher, J., and Yang, W. Y. (1988). Experimental tissue molding for soft tissue reconstruction: A preliminary report. *Plast. Reconstr. Surg.* **82**, 857–864.
20. Khouri, R. K., Koudsi, B., and Reddi, H. (1991). Tissue transformation into bone in vivo. *J. Am. Med. Assoc.* **266**, 1953–1955.
21. Patrick, C. W., Jr., Chauvin, P. B., *et al.* (1999). Preadipocyte seeded PLGA scaffolds for adipose tissue engineering. *Tissue Eng.* **5**, 139–151.
22. Patrick, C. W., Jr., Chauvin, P. B., *et al.* (1998). Tissue engineered adipose. *In* "Frontiers in Tissue Engineering" (C. W., Patrick, Jr., A. G. Mikos and L. V. McIntire, eds.), pp. 369–382. Elsevier, Oxford, UK.
23. Lee, K. Y., Halberstadt, C. R., *et al.* (2000). Breast reconstruction. *In* "Principles of Tissue Engineering" (R. P. Lanza, R. Langer and J. Vacanti, eds.), pp. 409–423. Academic Press, San Diego, CA.
24. Katz, A. J., Llull, R., *et al.* (1999). Emerging approaches to the tissue engineering of fat. *Clin. Plast. Surg.* **26**, 587–603.

25. Cao, Y. L., Lach, E., *et al.* (1998). Tissue engineered nipple reconstruction. *Plast. Reconstr. Surg.* **102**, 2293–2298.
26. Billings, E., Jr., and May, J. W., Jr. (1989). Historical review and present status of free fat graft autotransplantation in plastic and reconstructive surgery. *Plast. Reconstr. Surg.* **83**, 368–381.
27. Ersek, R. A. (1991). Transplantation of purified autologous fat: A 3-year follow-up disappointing. *Plast. Reconstr. Surg.* 87, 219–227.
28. Mandrup, S., and Lane, D. (1997). Regulating adipogenesis. *J. Biol. Chem.* **272**, 5367–5370.
29. Loftus, T. M., and Lane, M. D. (1997). Modulating the transcriptional control of adipogenesis. *Curr. Opin. Genet. Dev.* **7**, 603–608.
30. Entenmann, G., and Hauner, H. (1996). Relationship between replication and differentiation in cultured human adipocyte precursor cells. *Am. J. Physiol.* **270**, C1011–C1016.
31. Novakofski, J. E. (1987). Primary cell culture of adipose tissue. *In* "Biology of the Adipocyte: Research Approaches" (G. J. Hausman and R. J. Martin, eds.), pp. 160–197. Van Nostrand-Reinhold, New York.
32. Strutt, B., Khalil, W., *et al.* (1996). Growth and differentiation of human adipose stromal cells in culture. *In* "Methods in Molecular Medicine: Human Cell Culture Protocols" (G. E. Jones, ed.), pp. 41–51. Humanaa Press, Totowa, NJ.
33. Hausman, G. J., and Richardson, R. L. (1998). Newly recruited and pre-existing preadipocytes in cultures of porcine stromal–vascular cells: Morphology, expression of extracellular matrix components, and lip accretion. *Anim. Sci.* **76**, 48–60.
34. Shillabeer, G. Z., Li, Z.-H., *et al.* (1996). A novel method for studying preadipocyte differentiation in vitro. *Int. J. Obes.* **20**(3), S77–S83.
35. Van, R. L. R., and Roncari, D. A. K. (1977). Isolation of fat cell precursors from adult rat adipose tissue. *Cell Tissue Res.* **181**, 197–203.
36. Dijan, P., Roncari, D. A. K., *et al.* (1983). Influence of anatomic site and age on the replication and differentiation of rate adipocyte precursors in culture. *J. Clin. Invest.* **72**, 1200–1208.
37. Kirkland, J. L., Hollenberg, C. H., *et al.* (1996). Effects of fat depot site on differentiation-dependent gene expression in rate preadipocytes. *Int. J. Obes. Relat. Metab. Disord.* **20**(Suppl 3), S102–S107.
38. Kirkland, J. L., Hollenberg, C. H., *et al.* (1994). Effects of age and anatomic site on preadipocyte number in rat fat depots. *J. Gerontol.* 49, B31–35.
39. Hauner, H., and Entenmann, G. (1991). Regional variation of adipose differentiation in cultured stromal–vascular cells from the abdominal and femoral adipose tissue of obese women. *Int. J. Obes.* **15**, 121–126.
40. Crandall, D. L., Hausman, G. J., *et al.* (1997). A review of the microcirculation of adipose tissue: Anatomic, metabolic, and angiogenic perspectives. *Microcirculation* **4**, 211–232.
41. Silverman, K. J., Lund, D. P., *et al.* (1988). Angiogenic activity of adipose tissue. *Biochem. Biophys. Res. Commun.* **153**, 347–352.
42. Zhang, Q. X., Magovern, C. J., *et al.* (1997). Vascular endothelial growth factor is the major angiogenic factor in omentum: Mechanism of the omentum-mediated angiogenesis. *J. Surg. Res.* **67**, 147–154.
43. Varzaneh, F. E., Shillabeer, G., *et al.* (1994). Extracellular matrix components secreted by microvascular endothelia cells stimulate preadipocyte differentiation in vitro. *Metab. Clin. Exp.* **43**(7), 906–912.
44. Erol, O. O., and Spira, M. (1990). Reconstructing the breast mound employing a secondary island omental skin flap. *Plast. Reconstr. Surg.* **86**, 219–227.
45. Marschall, M. A., Gigas, E. G., *et al.* (1990). The omentum in reconstructive surgery. *In* "Mastery of Plastic & Reconstructive Surgery" (M. Cohn and R. M. Goldwyn, eds.), Vol. 1, pp. 95–101. Little, Brown, Boston.
46. Sugawara, Y., Harii, K., *et al.* (1998). Reconstruction of skull defects with vascularized omentum transfer and split calvarial bone graft: Two case reports. *J. Reconstr. Microsurg.* **13**, 101–108.
47. Kral, J. G., and Crandall, D. L. (1999). Development of a human adipocyte synthetic polymer scaffold. *Plast. Reconstr. Surg.* **104**, 1732–1738.
48. Marler, J. J., Guha, A., *et al.* (2000). Soft-tissue augmentation with injectable alginate and syngeneic fibroblasts. *Plast. Reconstr. Surg.* **105**, 2049–2058.
49. Duranti, F., Salti, G., *et al.* (1998). Injectable hyaluronic acid gel for soft tissue augmentation. *Dermatol. Surg.* **24**, 1317–1325.
50. Vacanti, J. P., Atala, A., *et al.* (1998). Breast tissue engineering. U.S. Pat. 5,716,404.
51. Kubo, Y., Kaidzu, S., *et al.* (2000). Organization of extracellular matrix components during differentiation of adipocytes in long-term culture. *In Vitro Cell. Dev. Biol.* **36**, 38–44.
52. Kawaguchi, N., Toriyama, K., *et al.* (1998). *De novo* adipogenesis in mice at the site of injection of basement membrane and basic fibroblast growth factor. *Cell Biol.* **95**, 1062–1066.
53. Yuksel, E., Weinfeld, B., *et al.* (2000). Increased free fat-graft survival with the long-term, local delivery of insulin, insulin-like growth factor-I, and basic fibroblast growth factor by PlGA/PEG microspheres. *Plast. Reconstr. Surg.* **105**, 1712–1720.
54. Yuksel, E., Weinfeld, A. B., *et al.* (2000). *De novo* adipose tissue generation through long-term, local delivery of insulin and insulin-like growth factor-1 by PLGA/PEG microspheres in an *in vivo* rat model: A novel concept and capability. *Plast. Reconstr. Surg.* **105**, 1721–1729.
55. Serrero, G. (1987). EGF inhibits the indifference of adipocyte precursors in primary cultures. *Biochem. Biophys. Res. Commun.* **146**, 194–202.
56. Kras, K. M., Hausman, D. B. *et al.* (2000). Tumor necrosis factor stimulates cell proliferation in adipose tissue-derived stromal–vascular cell culture: Promotion of adipose tissue expansion by paracrine growth factors. *Obes. Res* 8, 186–193.

TISSUE ENGINEERING
Volume 8, Number 2, 2002

Long-Term Implantation of Preadipocyte-Seeded PLGA Scaffolds

C.W. PATRICK, Jr., Ph.D., B. ZHENG, M.D., C. JOHNSTON, H.T. (ASCP), and G.P. REECE, M.D.

ABSTRACT

Studies were performed in a long-term effort to develop clinically translatable, tissue engineered adipose constructs for reconstructive, correctional, and cosmetic indications. Rat preadipocytes were harvested, isolated, expanded *ex vivo*, and seeded within PLGA scaffolds. Preadipocyte-seeded and acellular (control) scaffolds were implanted for 1–12 months. Explanted scaffolds were stained with osmium tetroxide, processed, and counterstained using H&E. Quantitative histomorphometric analysis was performed on all tissue sections to determine the amount of adipose tissue formed. Analyses revealed maximum adipose formation at 2 months, followed by a decrease at 3 months, and complete absence of adipose and PLGA at 5–12 months. These results extend a previous short-term study (*Tissue Engineering* 1999;5:134) and demonstrate that adipose tissue can be formed *in vivo* using tissue engineering strategies. However, the long-term maintenance of adipose tissue remains elusive.

INTRODUCTION

THE APPLICATION OF TISSUE ENGINEERING to the development of adipose tissue constructs has captured the interests of numerous investigators over the past two years.[1–8] This is due in part to the realization that there are many reconstructive, correctional, and cosmetic indications for patient-specific adipose constructs.[4] In a previous qualitative study, we demonstrated adipose tissue formation within preadipocyte (PA)–seeded PLGA scaffolds implanted for 2 and 5 weeks.[3] Many questions were raised at the conclusion of this initial study. One such question is whether adipose tissue that forms within PLGA scaffolds remains over long periods of time and whether it remains after its supporting polymer scaffold entirely degrades. This question merits consideration based on the longstanding observation that transplanted mature fat resorbs over time. This present study is a continuation and elaboration of the former. Specifically, PAs are seeded within PLGA scaffolds and implanted for 1–12 months. Adipose formation is quantitatively assessed by coupling histology with microscopy and image analysis.

University of Texas Center for Biomedical Engineering and Laboratory of Reparative Biology and Bioengineering, Department of Plastic Surgery, University of Texas M. D. Anderson Cancer Center, Houston, Texas.

MATERIALS AND METHODS

Adipose harvest and in vivo culture

The methods for harvesting and culturing the PAs were previously described.[3,9] Briefly, PAs were isolated from epididymal fat pads of male, 250 g, 70–80-day-old Lewis rats (Harlan) via enzymatic digestion. Rats were euthanized with CO_2 asphyxiation and the shaved harvest site was scrubbed with Betadyne followed by alcohol wash. Within 5 min of death, epididymal adipose tissue was aseptically harvested and placed in 4°C saline solution supplemented with 500 U/mL penicillin and 500 μg/mL streptomycin (Gibco). Using a dissecting microscope, connective tissues and tissue containing blood vessels were resected from the fat. This minimizes fibroblast contamination of *ex vivo* cultures. Harvested tissue was finely minced with a scalpel and enzymatically digested in Ca^{+2}/Mg^{+2}-free saline supplemented with 2% (w/v) type I collagenase (Sigma Chemical Co.) and 5% (w/v) bovine serum albumin (BSA) for 20 min at 37°C on a shaker. For four fat pads, 5 mL of dissociation medium is required. The digested tissue was filtered through a 250-μm mesh followed by a 90-μm nylon mesh to separate undigested debris and capillary fragments from PAs. The filtered cell suspension was centrifuged, and the resulting pellet of PAs was then plated at 10^4 cells/cm^2 onto plastic culture flasks. PAs were cultured in Dulbecco's Modified Eagle's Medium (DMEM) supplemented with 10% fetal bovine serum (FBS), 100 U/mL penicillin, and 100 μg/mL streptomycin. During cell expansion, the PAs were passed prior to confluency since contact inhibition initiates adipocyte differentiation and ceases PA proliferation.[10–15] The 1° passage yields approximately 1.5×10^6 PAs/fat pad.

Polymer fabrication and seeding

PLGA is employed as a model polymer. PLGA foam fabrication and seeding were conducted as previously described.[3] Fabrication of 2.5-mm-thick, 12-mm-diameter, and 90% porosity polymer disks were prepared by a particulate-leaching technique. Briefly, 5 g of solid 75:25 PLGA (Birmingham Polymers Inc.) polymer were dissolved in 80 mL of dichloromethane (Fisher Scientific) to form a solution. Sieved NaCl crystals (Fisher) at a NaCl:PLGA weight fraction of 1:9 were evenly dispersed over a 150-mm Pyrex petri dish (Fisher) with a Teflon lining (Cole-Parmer Instrument Co.). The PLGA/dichloromethane solution was then gently poured over the NaCl crystals. Sieved NaCl crystal size distribution was measured with quantitative microscopy and found to be 135–633 μm. Dichloromethane was evaporated under vacuum, leaving a polymer/NaCl composite 2.5-mm thick. The composite was removed from the Teflon-lined petri dish, and 12-mm-diameter disks were cut using a plug cutter and drill press. The NaCl crystals were then leached from the composite disks by immersion in 800 mL of DI water for 48 h (water changed every 8 h) to yield porous disks. Disks were lyophilized and stored in a vacuum dessicator until use.

FIG. 1. **(A)** Example of preadipocyte-seeded disk transplantation. **(B)** Example of disk harvest (1 month).

Prior to seeding, the test materials were prewetted and sterilized with absolute ethanol for 30 min followed by two sterile saline washes at 20 min/wash and a DMEM wash for 20 min. A 20-μL suspension of PAs (10^5 cells/mL) was injected onto each disk under sterile conditions. Prewetting permits the cell suspension to readily flow throughout the materials. Following 3 h for cell attachment, 24-well culture plates containing one disk/well were filled with 1.5 mL of medium/well. Before transporting the cell-seeded constructs to the operating room, DMEM media was removed and replaced with complete L-15 media, and the constructs were placed in a mobile 37°C warmer. The use of L-15 precludes the need for 5% CO_2 for pH control.

In vivo implantation

Seeded disks were implanted on the back musculature of Lewis rats under anesthesia (0.2 mL/100 gbw intramuscular injection of premixed solution composed of 64 mg/mL ketamine HCl, 3.6 mg/mL xylazine, and 0.07 mg/mL atropine sulfate).[3,9] An isogenic strain is required to avoid an immune response to seeded PAs. The University of Texas M.D. Anderson Cancer Center Animal Care and Use Committee has approved the implantation of PA seeded disks. After shaving the back, two longitudinal incisions (~2 cm each) were made through the skin of the dorsal midline. Individual "pockets" for each disk were prepared between the cutaneous trunci and back muscles of both flanks by careful dissection. Disks were inserted

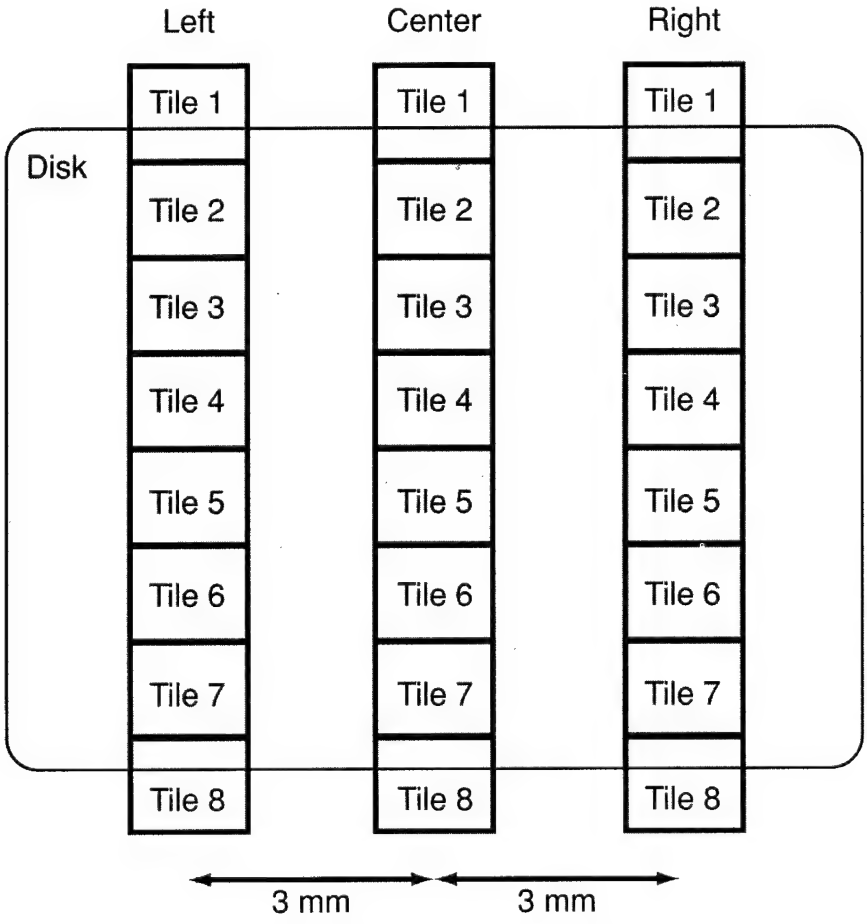

FIG. 2. Illustration depicting image analysis strategy. Three full-thickness images were acquired for each histological section of seeded/control PLGA disks—a center image and left/right images 3 mm from the center. Each full-thickness image was constructed by tiling eight individual 640 × 480 pixel images.

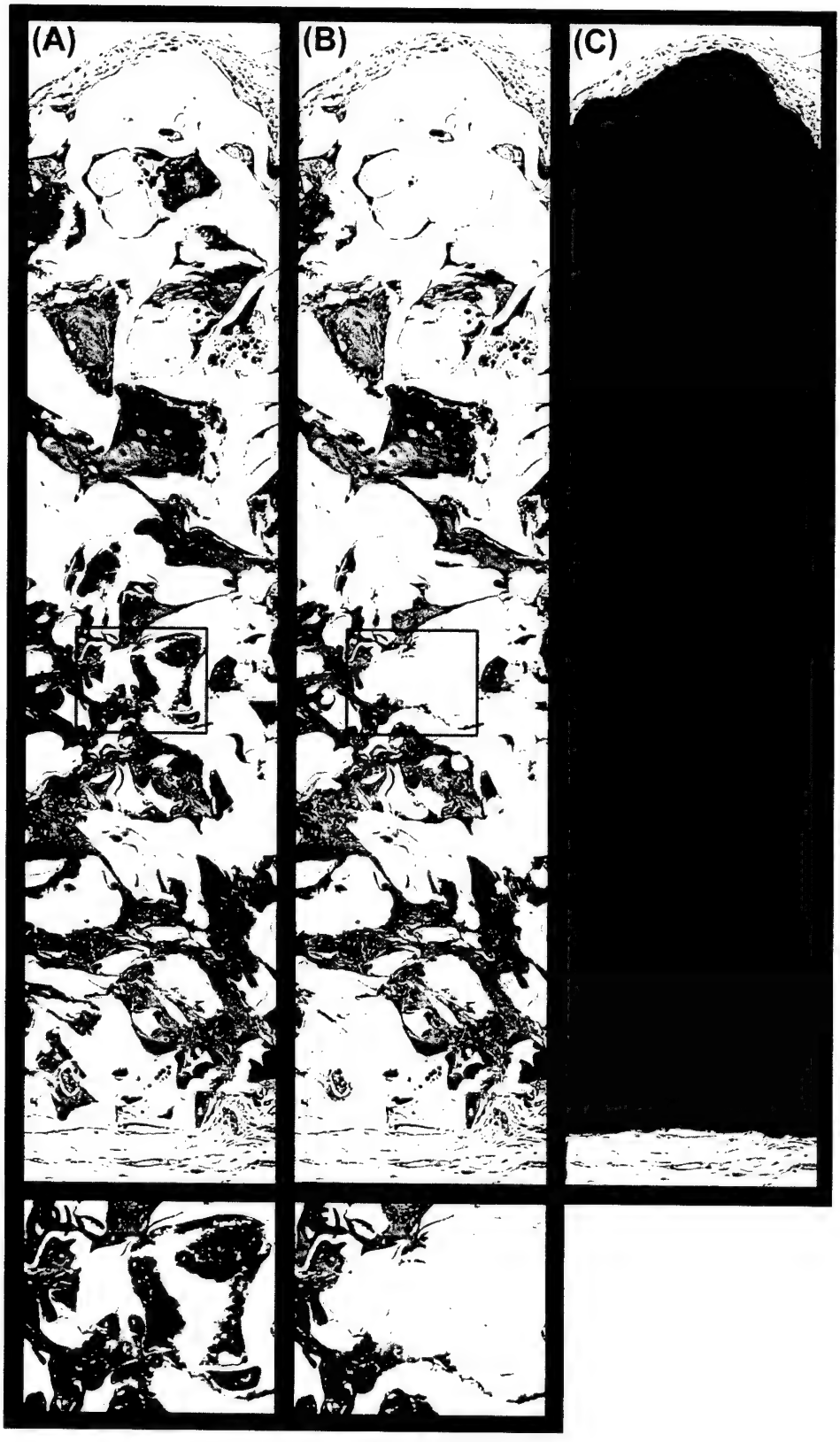
(A)
(B)
(C)

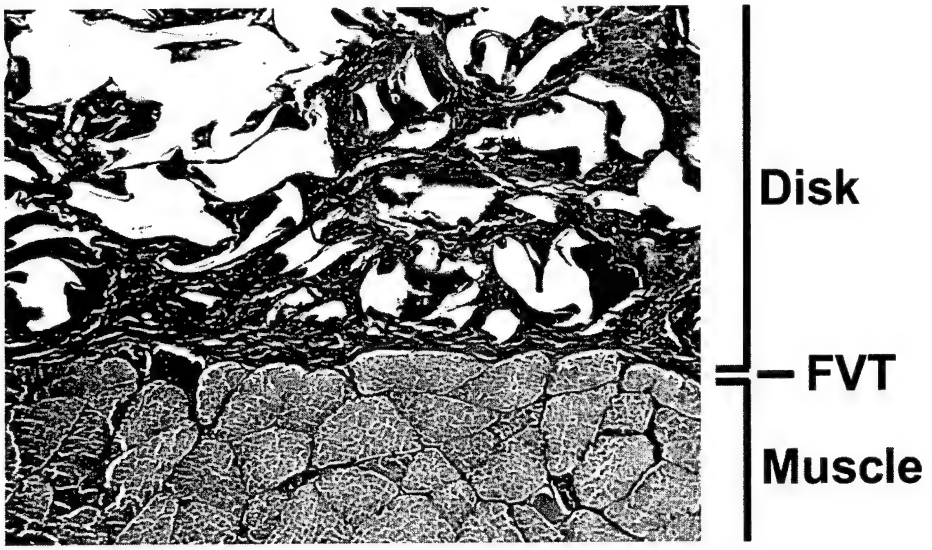

FIG. 4. Representative histology (H&E) depicting the interface between PLGA disks and skeletal muscle beds of the rat. There is no void space or fascia present at the interface, only a thin layer of fibrovascular tissue (FVT). The entire PLGA disk thickness is not shown. Original magnification, ×100.

into each pocket and sutured in place with 5-0 suture (Ethicon), as shown in Figure 1A. Two disks were placed on each side of the incision (four disks per rat) and the incisions closed with 4-0 suture (Ethicon) (Fig. 1B). Animals were housed individually and fed standard rat chow. The disks were left *in vivo* 1, 2, 3, 5, 7, 9, and 12 months. After the elapsed time, the rats were euthanized with CO_2 and the disks harvested. Immediately after harvest, the disks were placed in 10% neutral buffered formalin (Fisher) for future histology.

For this study, a total of 42 rats were used at 6 rats/time period. Each rat was implanted with four disks. Two disks were seeded with PAs, and two disks were implanted without seeding to serve as acellular controls. A total of 84 seeded and 84 acellular disks were used in this study.

Histology

An osmium tetroxide (OsO_4) paraffin procedure was used to demonstrate fat within half of the harvested *in vivo* disks.[3] The remaining half of the disks were frozen for storage and future analyses. Routine staining outlines only "ghost" cells since histological processing with organic solvents and alcohols extract lipid from cells. OsO_4 chemically combines with fat, blackening it in the process. Fat that combines OsO_4 is insoluble in alcohol and xylene, and the tissue can be processed for paraffin embedding and counterstained. After staining with OsO_4, disks were processed for paraffin embedding using standard procedures, except that Histosolve (Shandon) was substituted for xylene. Sections 4 μm thick were cut on a microtome (Leica), placed on slides, counterstained with H&E, and coverslipped to view fibrovascular tissue. Sections were analyzed using brightfield microscopy.

Determination of adipose tissue

High magnification images of histology slides were acquired using an inverted microscope (Olympus), color CCD camera (Olympus), computer-controlled XYZ stage (Ludl Electronic Products), IPLab software

FIG. 3. Illustration depicting routing of full-thickness image tiling and segmentation. (**A,D**) Osmium tetroxide–labeled adipose tissue. (**B,E**) Segmented adipose tissue area (light gray) of A and E, respectively. (**C**) Segmented disk area (dark gray) of A. D and E are higher magnification images of areas denoted by box in A and B, respectively.

(Scanalytics), and a PowerPC (Apple). Images were acquired at a resolution of 0.61 pixels/μm using a 20×, 0.40 NA objective (Olympus). A depiction of the image analysis strategy is shown in Figure 2. Three full-thickness images were acquired automatically from each slide: at the center, ~3 mm right of the center, and ~3 mm left of the center. Image acquisition consisted of digitally tiling eight 640 × 480 pixel images for each full thickness image. Hence, each image was 640 × 3,840 pixels or 390 μm × 2,342 μm (Fig. 3A,D). Next, using image segmentation, the user selected areas of adipose tissue formation (i.e., OsO_4-stained regions) consisting of mature adipocytes or lipid-filled differentiating PAs (Fig. 3B,E). The total scaffold area was determined (Fig. 3C). Data are presented as percent of adipose tissue, defined as follows:

$$\% \text{ Adipose Formation} = 100 \cdot \left(\frac{\Sigma \text{ Left, Center, Right Adipose Area}}{\Sigma \text{ Left, Center, Right Scaffold Area}} \right)$$

Data from center, left, and right full thickness images were pooled, resulting in one value for each slide rather than three.

RESULTS

There were no complications due to surgery or postoperative recovery from anesthesia. Scaffold harvest was unremarkable with no hematomas or seromas. Scaffolds remained intact and appeared to be well-vascularized based on gross inspection (Fig. 1B). As shown in Figure 4, the PLGA disks were sutured in di-

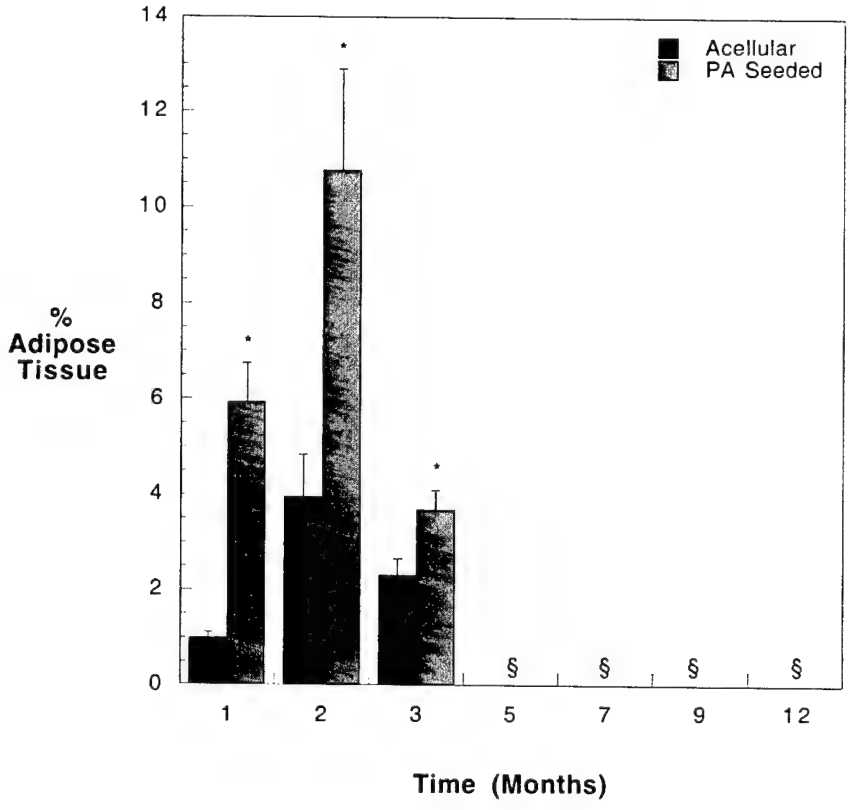

FIG. 5. Percent adipose tissue formation in acellular and preadipocyte (PA)–seeded scaffolds versus implantation time. Data are mean ± SEM of $n = 6$. *Statistical difference in adipose tissue presence between acellular and PA seeded scaffolds ($p \leq 0.05$). §Rats with entirely resorbed PLGA scaffolds and no adipose tissue.

rect apposition to muscle, with no void space or fascia present. Hence, barriers to scaffold revascularization were minimized.

Figure 5 demonstrates the percent adipose formation within the acellular and PA seeded PLGA scaffolds. For months 1–3, PA-seeded scaffolds demonstrated statistically more adipose tissue than their acellular controls. Adipose tissue formation appears to peak at 10.7% at 2 months followed by a decrease. PLGA scaffolds were entirely degraded by 5 months. No PLGA scaffold or fat tissue was present in rats harvested at 5–12 months. The absence of PLGA at $\geq$5 months is in keeping with the 75:25 copolymer's approximate degradation kinetics of 4–5 months. Exact degradation kinetics is dependent on scaffold geometry, porosity, and molecular weight.

A thin layer of adipose tissue was observed within the fibrovascular tissue (i.e., foreign body capsule) around, but outside both acellular and PA-seeded disks (Fig. 6). The thin layer of adipose tissue was highly vascular and is presumably formed from resident PAs recruited to the foreign body capsule. This observation was noted in the former short-term study[3] and with proprietary cell-seeded and acellular polymers from Johnson & Johnson Corporate Biomaterials Center (data not shown). There was no difference in the layer characteristics at implantation times of 1, 2, and 3 months or between acellular and PA-seeded disks.

Histologically, the amount of all tissue (fibrovascular and adipose combined) decreased between 1 and 3 months as the PLGA degraded (Fig. 7). Without polymer support, the tissue at 3 months formed threads of connecting tissue (Fig. 4C,D). The amount of macrophage infiltration qualitatively decreased with time as well as between 1 and 3 months (Fig. 8). Macrophage presence was localized to polymer–tissue interfaces.

DISCUSSION

This long-term study expanded the results observed with a previous short-term study that demonstrated adipose formation within PA-seeded PLGA scaffolds after 2 and 5 weeks of transplantation.[3] This study addresses the issue of long-term maintenance of adipose formation within a model polymer-cell system. Based on the animal model utilized, one concludes that PA-seeded PLGA scaffolds permit increasing adipose formation that peaks at approximately 2 months and decreases dramatically thereafter. It is encouraging to demonstrate viable adipose tissue formation within PA-seeded PLGA scaffolds for up to 2 months. However, the exact microenvironment required for long-term maintenance remains elusive.

There are several possible explanations for the resorption observed in this long-term study. One explanation may be related to the anatomical site of transplantation. Epididymal PAs were seeded within PLGA

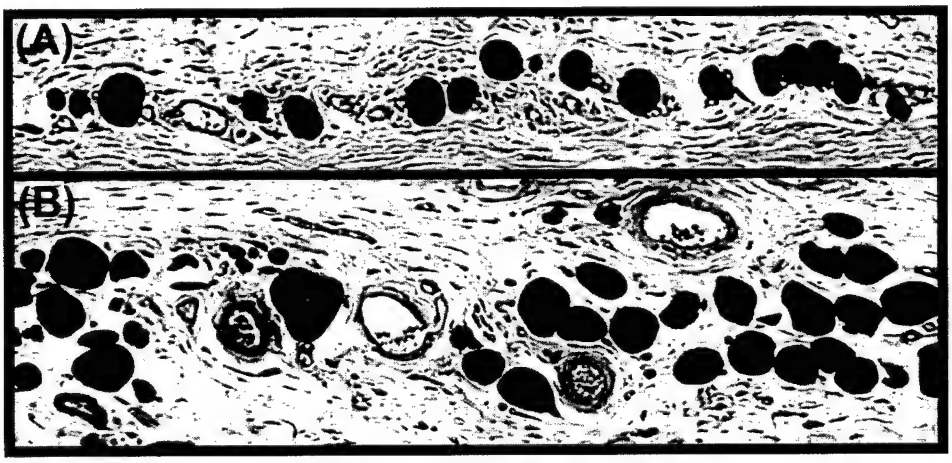

FIG. 6. Representative histology (OsO_4 and H&E) of thin layer of vascular adipose tissue observed outside acellular (**A**) and PA-seeded (**B**) disks. There were no differences in perivascular adipose formation between acellular and PA-seeded disks. Original magnification, $\times$100.

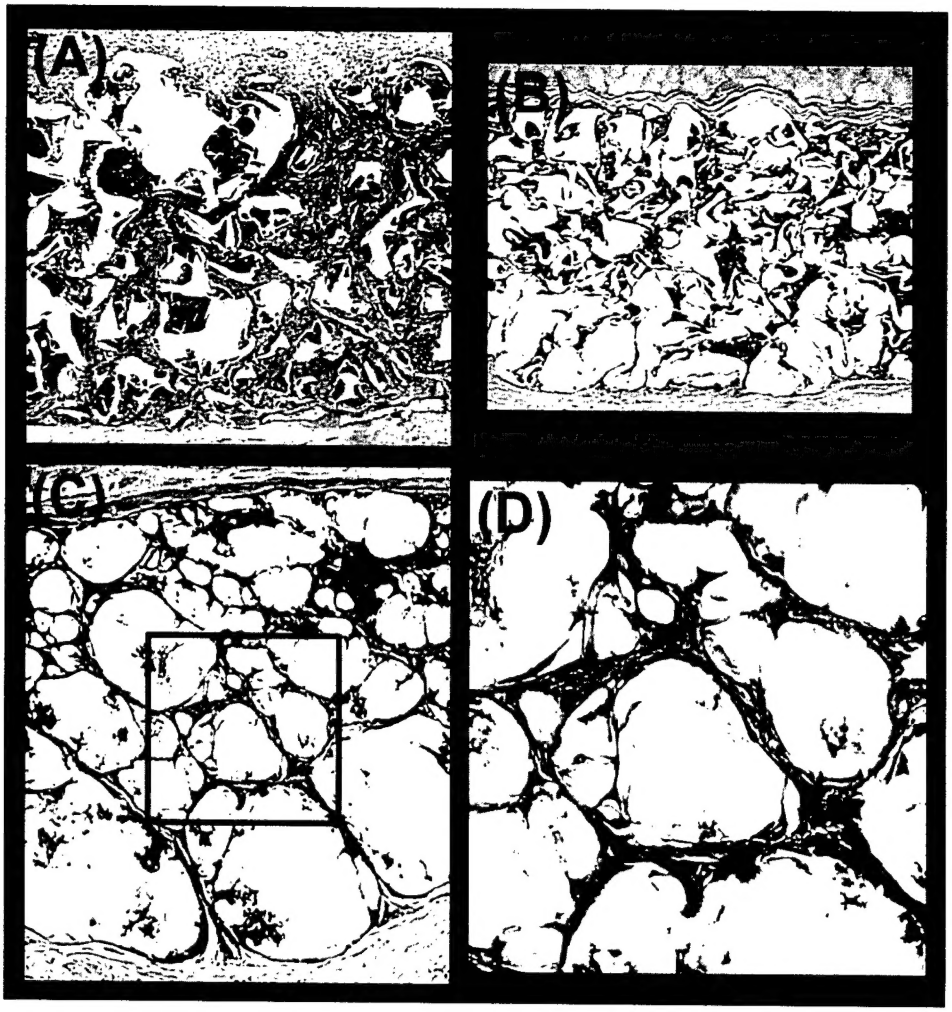

FIG. 7. Representative images (OsO_4 and H&E) depicting extent of tissue presence at 1 month (**A**), 2 months (**B**), and 3 months (**C,D**). D is higher magnification of area denoted in C. Original magnification, ×40 (A–C), ×200 (D).

scaffolds and transplanted to the dorsal subcutaneous region of the rat between two muscle beds, namely the panniculus carnosus (cutaneous trunci) muscle and skeletal muscles of the back. The thin layer of fascia separating the muscle beds was removed prior to construct implantation. Rats typically possess very little subcutaneous adipose tissue. Hence, the microenvironment present in the current model may not support long-term maintenance of adipose tissue. This may be a limitation of the animal model employed. Research is currently being conducted on characterizing a porcine model which has the potential of being a more amenable subcutaneous adipose model. Further, adipose tissue physiology (i.e., rate of replication, capacity for differentiation) is dependent on anatomical location.[16–19] That is, there are site-specific characteristics intrinsic to the PAs that result in regional variations in properties of adipose tissue. Thus, a subcutaneous microenvironment may not optimally support epididymal PAs.

Another explanation for the resorption observed may be the degree of vascularization. It has been known for decades that adequate vascular supply is essential for generation and maintenance of adipose tissue. ECM components secreted by microvascular endothelial cells have been shown to directly stimulate PA differentiation and replication.[20] When avascular constructs are transplanted *in vivo*, the angiogenesis response observed is that of a wound healing cascade. During the late stages of wound healing, there is significant vascular remodeling and involution. The regression of the neovascularization would intuitively re-

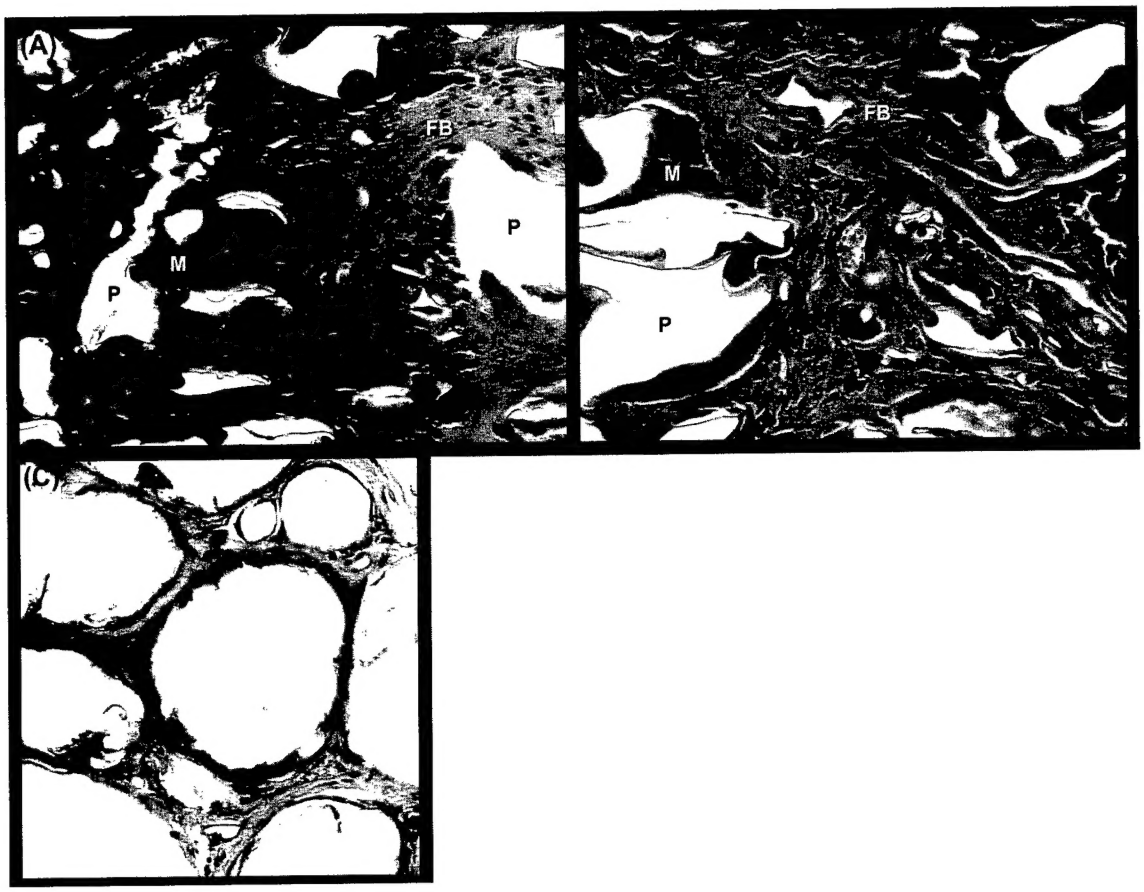

FIG. 8. Representative images (OsO_4 and H&E) depicting extent of macrophage infiltration at 1 month (**A**), 2 months (**B**), and 3 months (**C**). FB, fibroblasts; M, macrophages; P, polymer. Original magnification, ×400.

sult in a concomitant decrease in adipose volume. Moreover, as the amount of PLGA scaffold decreases with time, the influx of macrophages will decrease, as was observed in this study (Fig. 8). Likewise, the level of macrophage-secreted angiogenic factors will decrease resulting in regression of neovascularization. The exact level of vascularization was not determined in this study due to the fact that reagents required for CD31 staining of endothelial cells[21] dissolve the PLGA scaffold. However, gross examination of explants and qualitative examination of H&E-stained sections demonstrate numerous vessels at all time periods.

Long-term maintenance of adipose formation may require a specific, continued support structure. Anatomically, adipose tissue is held together by a network of ECMs (primarily collagen I) and is typically located in a defined anatomical space (e.g., the breast skin envelope for mammary adipose or between dermis and muscle for subcutaneous adipose). Although exact PLGA degradation was not assessed in this study, it is intriguing to note that the absence of adipose tissue corresponded to the absence of PLGA scaffold at time points $\geq$5 months. Further, at 3 months, the tissue within the disks formed thin interconnecting threads (Fig. 7C,D). One could speculate that the tissue was losing its support structure by 3 months. The use of 75:25 PLGA as a model polymer may limit the current model due to its relatively short degradation time. Using a biomaterial that degrades more slowly may allow adipose tissue to become more mature and maintain its presence longer than 2–3 months.

Finally, the resorption may be related to the lack of a continued, specific microenvironment. The microenvironment of PA regenerative proliferation and differentiation needs to be maintained at the site of transplantation. Several investigators have demonstrated the recruitment of endogenous PAs and *de novo*

adipose formation when the unique microenvironment consisting of Matrigel and bFGF are created in small animal models.[7,22,23] In this present study and others, we have observed formation of *de novo* adipose tissue within the fibrovascular capsule surrounding implanted acellular and PA-seeded biodegradable polymers (Fig. 6). The adipose tissue forms a thin layer parallel to the polymer surface and is surrounded by copious blood vessels (Fig. 6). Although speculative, endogenous PAs may recruit to the highly vascular regions and/or be attracted by factors released by early macrophage invasion.

The apparent resorption of adipose tissue with extended periods is not a new problem. Numerous strategies have been attempted to prevent adipose resorption following grafting, including using small diameter grafts and growth factors. The results of this study illustrate that the long-term maintenance of engineered adipose tissue is not a trivial task. In addition, results of this study suggest that a different combination of cell source, biomaterial, and animal model may lead to more mature adipose tissue for the study of long-term fat maintenance.

ACKNOWLEDGMENTS

We thank the following individuals from University of Texas' Laboratory of Reparative Biology and Bioengineering for their technical assistance with the *in vivo* study: Kristen Dempsey, Cynthia Frye, Gary Klaussen, Shannon Scott, and May Wu. This study was supported in part by a U.S. Army grant (DAMD17-99-1-9268), Cancer Fighter's of Houston grant, and a National Institutes of Health grant (CA16672).

REFERENCES

1. Lee, K.Y., Halberstadt, C.R., Holder, W.D., et al. Breast reconstruction. In: Lanza, R.P., Langer, R., Vacanti, J., eds. Principles of Tissue Engineering. San Diego: Academic Press, 2000, pp. 409–423.
2. Patrick, Jr., C.W., Chauvin, P.B., and Robb, G.L. Tissue engineered adipose. In: Patrick Jr., C.W., Mikos, A.G., McIntire, L.V., eds. Frontiers in Tissue Engineering. Oxford: Elsevier Science, 1998, pp. 369–382.
3. Patrick, Jr., C.W., Chauvin, P.B., and Reece, G.P. Preadipocyte seeded PLGA scaffolds for adipose tissue engineering. Tissue Eng. **5,** 139, 1999.
4. Patrick, Jr., C.W. Adipose tissue engineering: the future of breast and soft tissue reconstruction following tumor resection. Semin. Surg. Oncol. **19,** 302, 2000.
5. Kral, J.G., and Crandall, D.L. Development of a human adipocyte synthetic polymer scaffold. Plast. Reconstr. Surg. **104,** 1732, 1999.
6. Yuksel, E., Weinfeld, A.B., Cleek, R., et al. *De novo* adipose tissue generation through long-term, local delivery of insulin and insulin-like growth factor-1 by PLGA/PEG microspheres in an *in vivo* rat model: a novel concept and capability. Plast. Reconstr. Surg. **105,** 1721, 2000.
7. Beahm, E., Wu, L., and Walton, R.L. Lipogenesis in a vascularized engineered construct. Presented at the American Society of Reconstructive Microsurgeons, San Diego, 2000.
8. Patrick, Jr., C.W. Tissue engineering strategies for soft tissue repair. Anat. Rec. **263,** 361–366, 2001.
9. Patrick Jr., C.W., Wu, X., Johnston, C., et al. Epithelial cell culture—breast. In: Atala, A., and Lanza, R., eds. Methods in Tissue Engineering. San Diego: Academic Press, 2001, pp. 143–154.
10. Ailhaud, G., Amri, E.Z., Bardon, S., et al. The adipocyte: relationships between proliferation and adipose cell differentiation. Am. Rev. Respir. Dis. **142,** S57, 1990.
11. Butterwith, S.C. Molecular events in adipocyte development. Pharmac. Ther. **61,** 399, 1994.
12. Cornelius, P., MacDougald, O.A., and Lane, M.D. Regulation of adipocyte development. Annu. Rev. Nutr. **14,** 99, 1994.
13. MacDougald, O.A., and Lane, M.D. Transcriptional regulation of gene expression during adipocyte differentiation. Annu. Rev. Biochem. **64,** 345, 1995.
14. Ntambi, J.M., and Kim, Y.-C. Adipocyte differentiation and gene expression. J. Nutr. **130,** 3122S, 2000.
15. Smas, C.M., and SookSul, H.S. Control of adipocyte differentiation. Biochem. J. **309,** 697, 1995.
16. Djian, P., Roncari, D.A.K., and Hollenberg, C.H. Influence of anatomic site and age on the replication and differentiation of rat adipocyte precursors in culture. J. Clin. Invest. **72,** 1200, 1983.
17. Hauner, H., and Entenmann, G. Regional variation of adipose differentiation in cultured stromal-vascular cells from the abdominal and femoral adipose tissue of obese women. Int. J. Obesity **15,** 121, 1991.

18. Kirkland, J.L., Hollenberg, C.H., Kindler, S., et al. Effects of age and anatomic site on preadipocyte number in rat fat depots. J. Gerontol. **49,** B31, 1994.
19. Kirkland, J.L., Hollenberg, C.H., and Gillon, W.S. Effects of fat depot site on differentiation-dependent gene expression in rat preadipocytes. Int. J. Obesity Rel. Metab. Disord. **20,** Suppl 3, S102, 1996.
20. Varzaneh, F.E., Shillabeer, G., Wong, K.L., et al. Extracellular matrix components secreted by microvascular endothelial cells stimulate preadipocyte differentiation *in vitro*. Metabolism **43,** 906, 1994.
21. King, T.W., Johnston, C., and Patrick Jr., C.W. Quantification of vascular density using a semi-automated technique for immuno-stained specimens. Anal. Quant. Cytol. Histol. **24,** 39–48, 2002.
22. Kawaguchi, N., Toriyama, K., Nicodemou-Lena, E., et al. *De novo* adipogenesis in mice at the site of injection of basement membrane and basic fibroblast growth factor. Cell Biol. **95,** 1062, 1998.
23. Tabata, Y., Miyao, M., Inamoto, T., et al. *De novo* formation of adipose tissue by controlled release of basic fibroblast growth factor. Tissue Eng. **6,** 279, 2000.

Address reprint requests to:
Charles W. Patrick, Jr., Ph.D.
Department of Plastic Surgery
University of Texas M. D. Anderson Cancer Center
1515 Holcombe Blvd., Box 443
Houston, TX 77030

E-mail: cpatrick@mdanderson.org